Solar chromosphere in observations and simulations

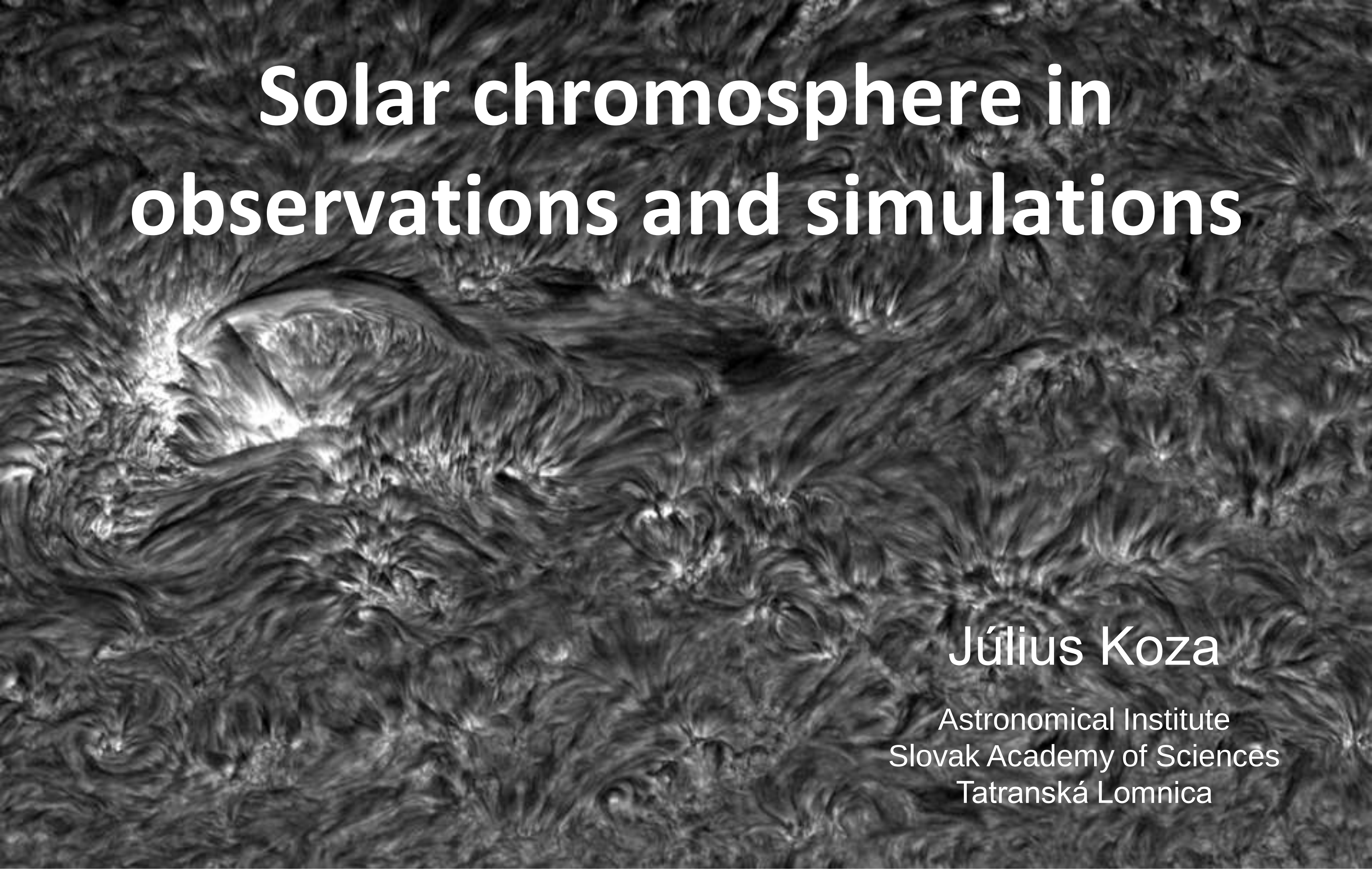

Július Koza

Astronomical Institute
Slovak Academy of Sciences
Tatranská Lomnica

Solis nuncius

PROGRAM CEZHRANIČNEJ SPOLUPRÁCE SLOVENSKÁ REPUBLIKA ČESKÁ REPUBLIKA 2007 2013

EURÓPSKA ÚNIA EURÓPSKY FOND REGIONÁLNEHO ROZVOJA

SPOLOČNE BEZ HRANÍC

FOND MIKROPROJEKTŮ

http://nicmosis.as.arizona.edu:8000/ECLIPSE_WEB/ECLIPSE_06/TSE2006_REPORT.html

The chromosphere: gateway to the corona ?

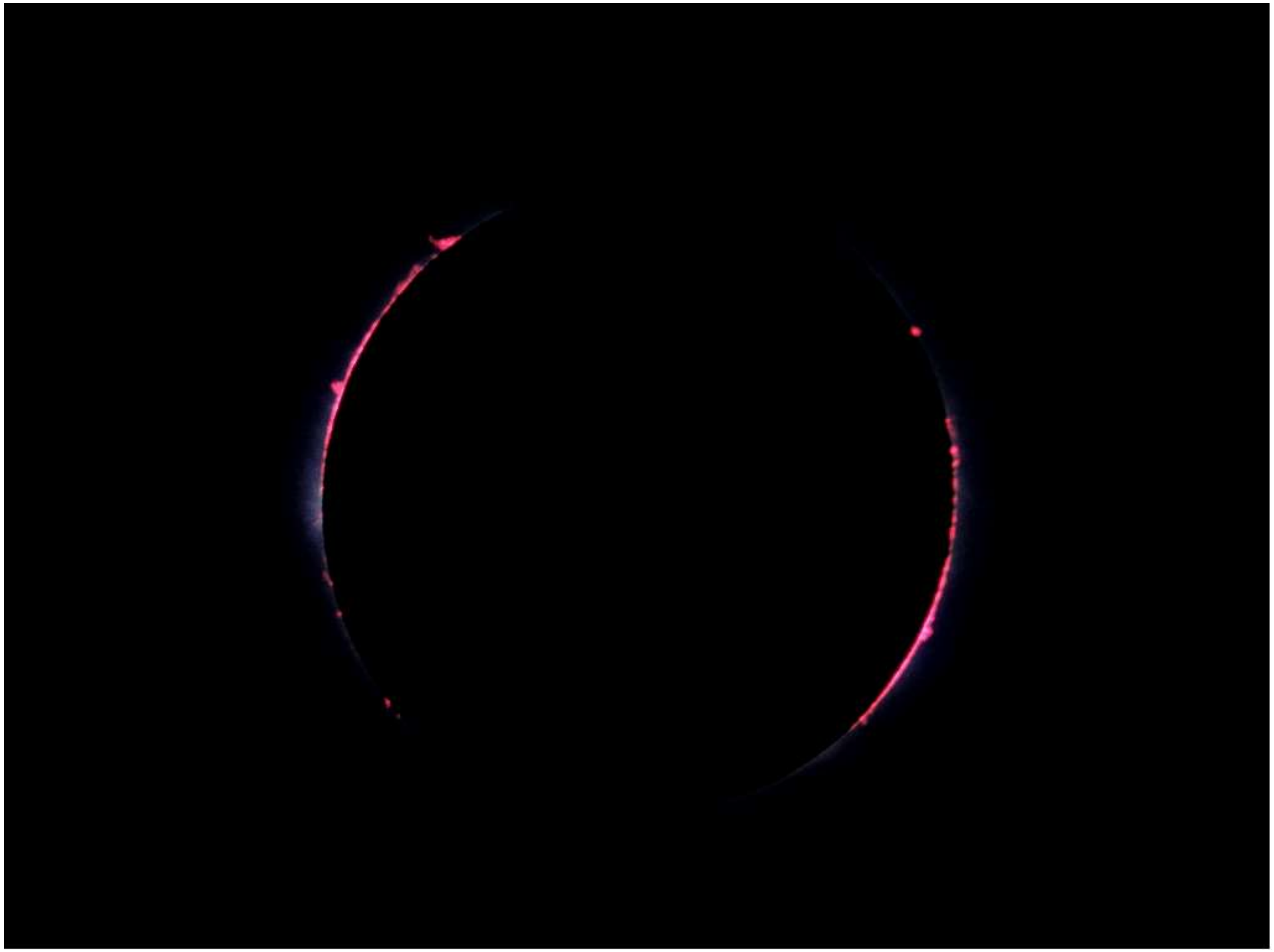

… Or the purgatory of solar physics ?

Judge (2010) ← clickable

A fiery purgatory in medieval

Purgatory is purification in which the souls are made ready for Heaven.

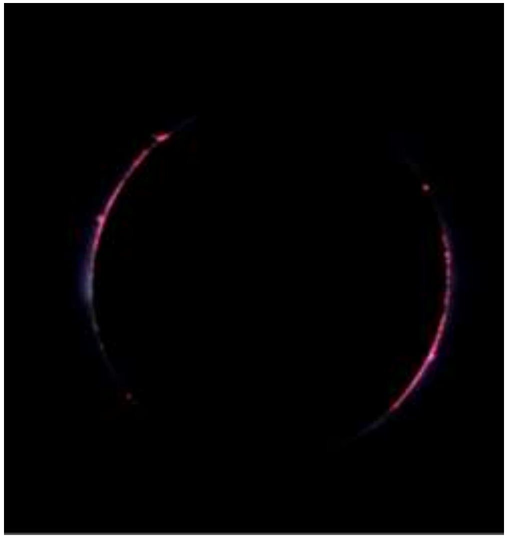

The Very Rich Hours of the Duke of Berry

The chromosphere: gateway to the corona ?

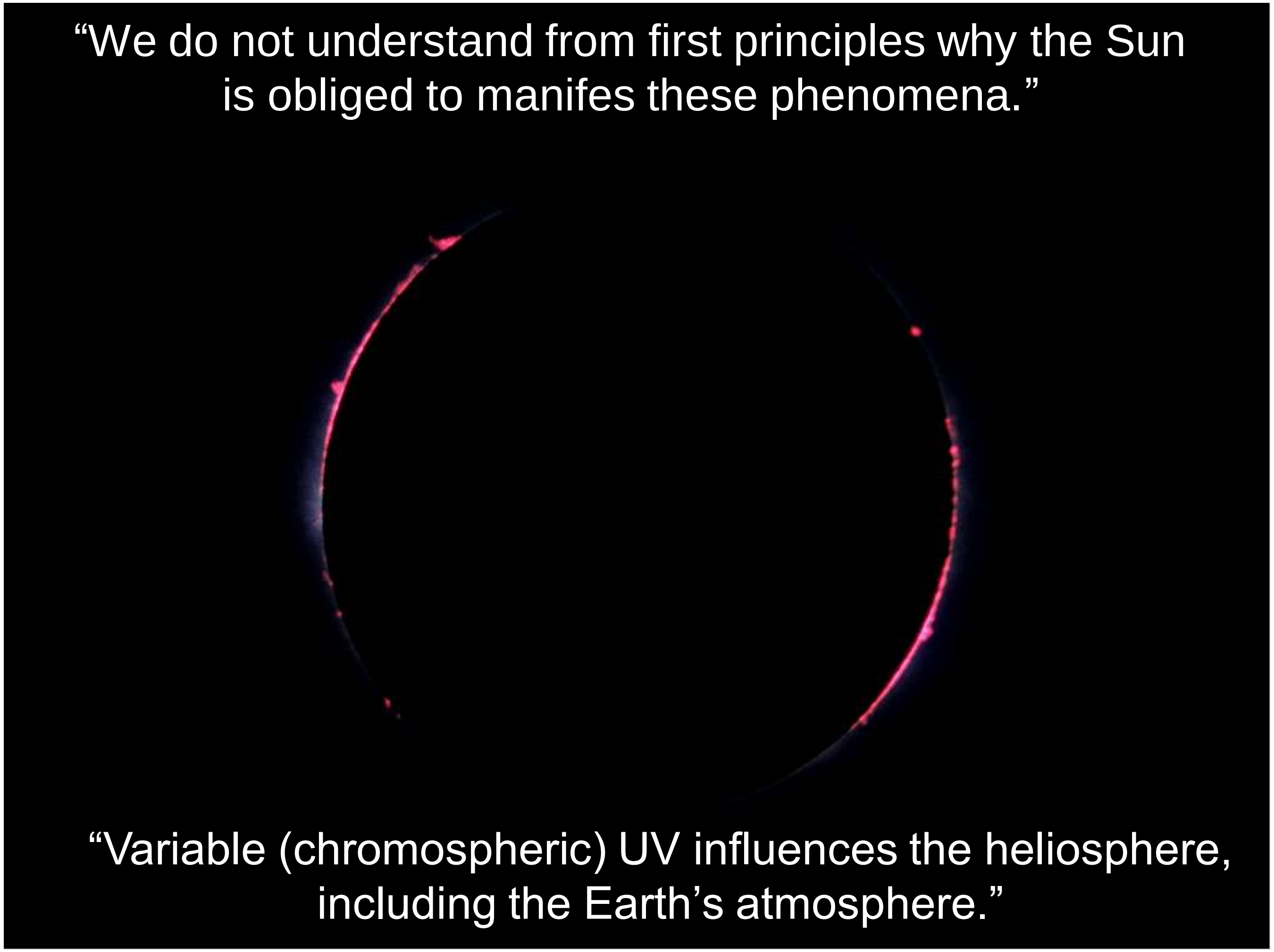

… Or the purgatory of solar physics ?

Judge (2010) ← clickable

Flash slitless spectrum

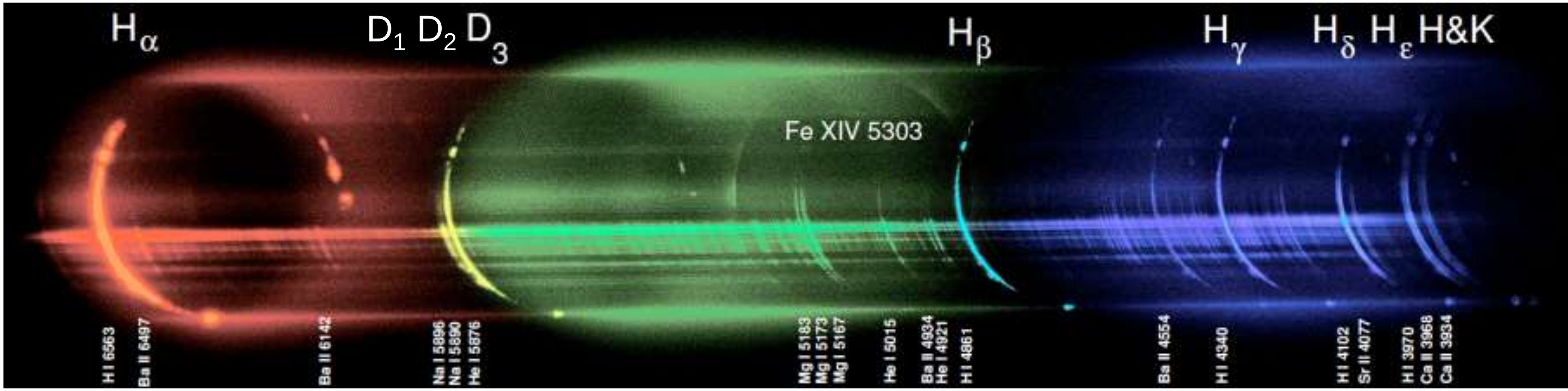

- reveals spectral lines formed in the chromosphere
- the chromosphere is optically thick (i.e., observable on the disk) in the lines seen in the flash spectrum

spectrum: EurAstro Team, Rutten (2010)

Flash slitless spectrum

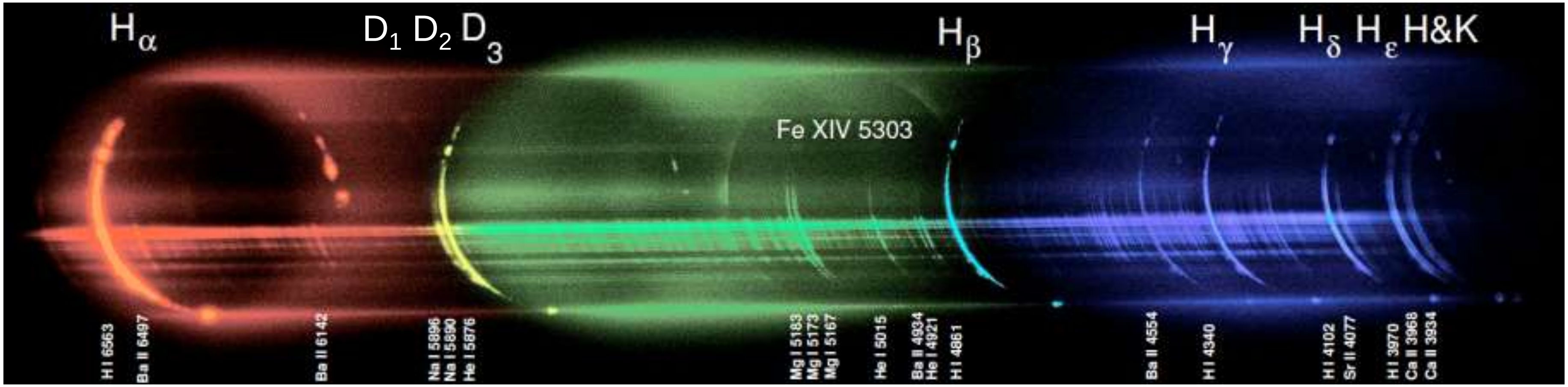

- reveals spectral lines formed in the chromosphere
- the chromosphere is optically thick (i.e., observable on the disk) in the lines seen in the flash spectrum

There are two exceptions. Which ?

spectrum: EurAstro Team, Rutten (2010)

Flash slitless spectrum

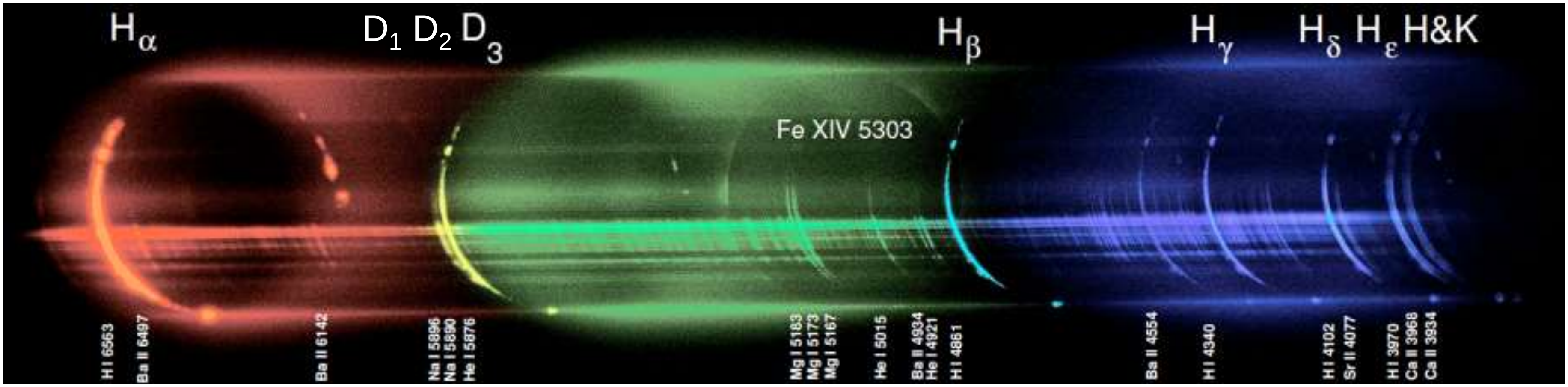

- reveals spectral lines formed in the chromosphere
- the chromosphere is optically thick (i.e., observable on the disk) in the lines seen in the flash spectrum

There are two exceptions. Which ?

- Na I D_1 & D_2 NOT chromospheric due to scattering source function (see Uitenbroek & Bruls, 1992)
- He I D_3 NOT seen in the disk spectrum

spectrum: EurAstro Team, Rutten (2010)

Principal chromosphere diagnostics

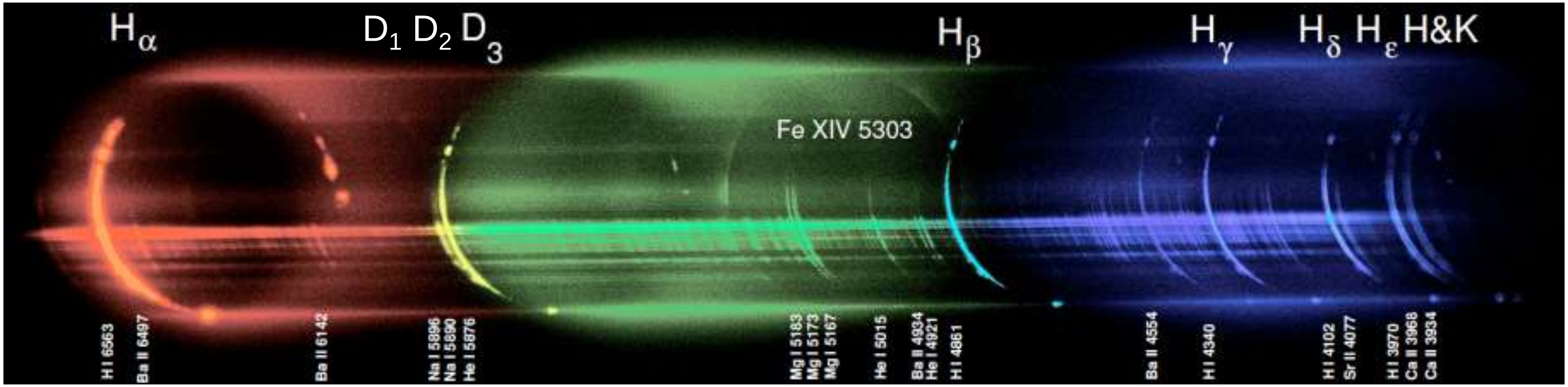

- visible: Hα, resonance lines Ca II H & K
- UV: Mg II k & h 2796 & 2803 Å (Mg II core-to-wing index)
  Ly α 1216 Å, He II 304 Å
- IR: triplet Ca II 8498, 8542, 8662 Å
  triplet He I 10 830 Å

spectrum: EurAstro Team

Chromosphere at high resolution

Spicules come at the stage

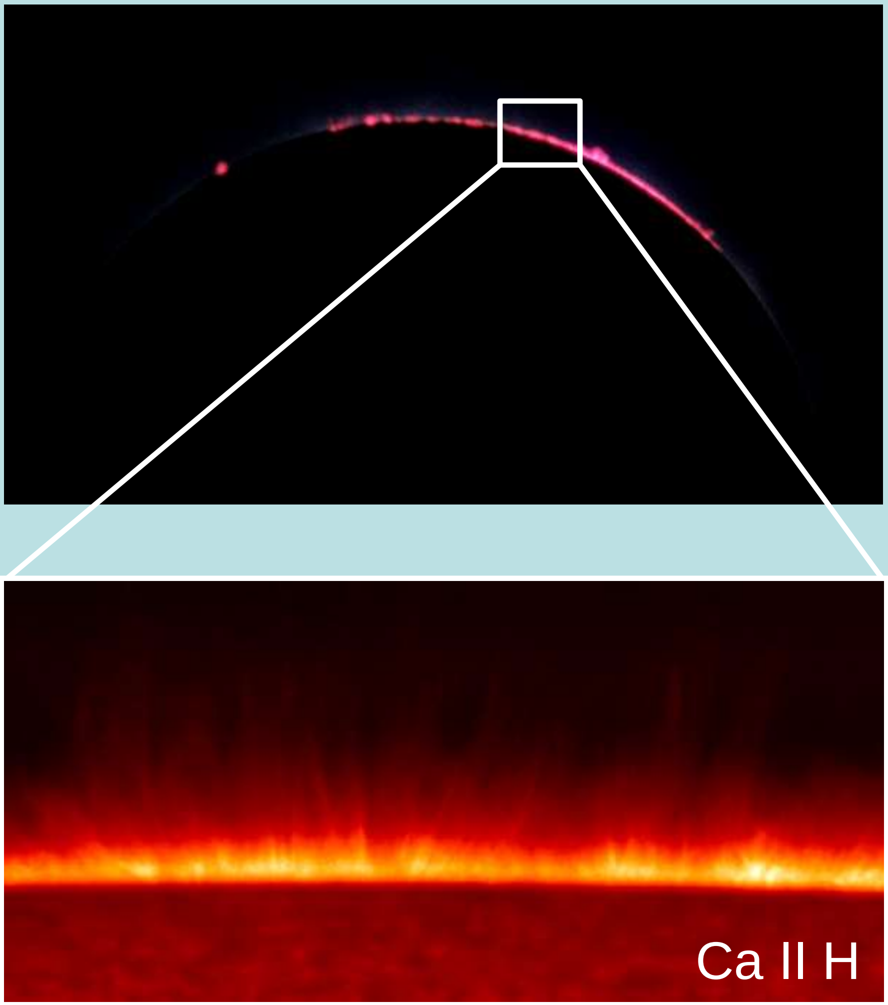

Centeno et al. (2008)

$$\beta = \frac{P_{gass}}{P_{mag}} = \frac{nkT}{B^2/8\pi}$$

lower chromosphere
bellow ≈ 1300 km: $\beta > 1$

spicules: $\beta << 1$

Spicules at very high resolution

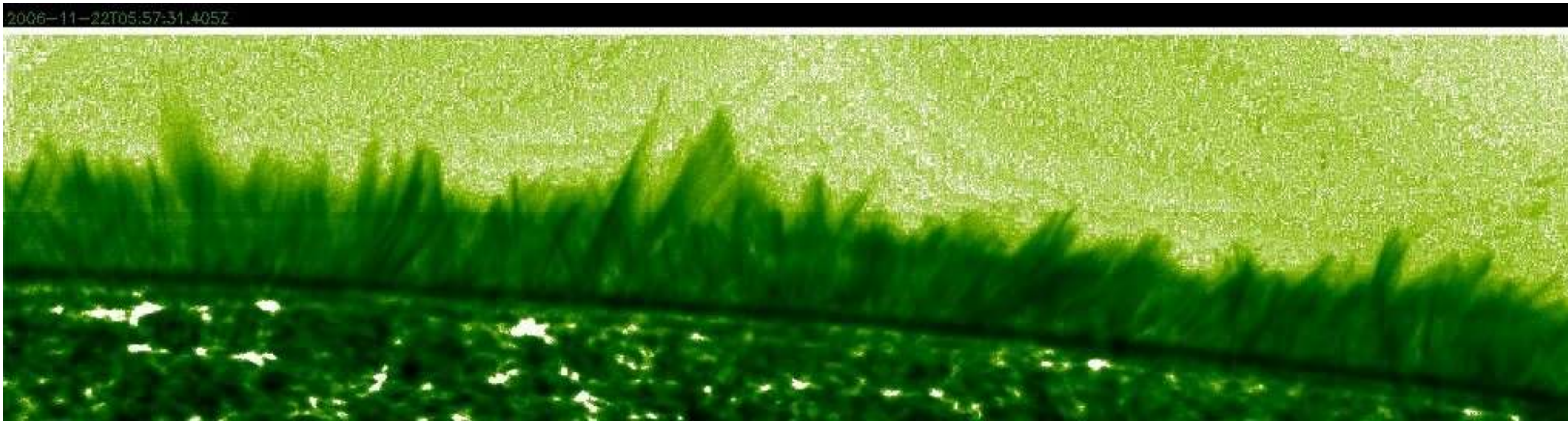

Hinode Ca II H

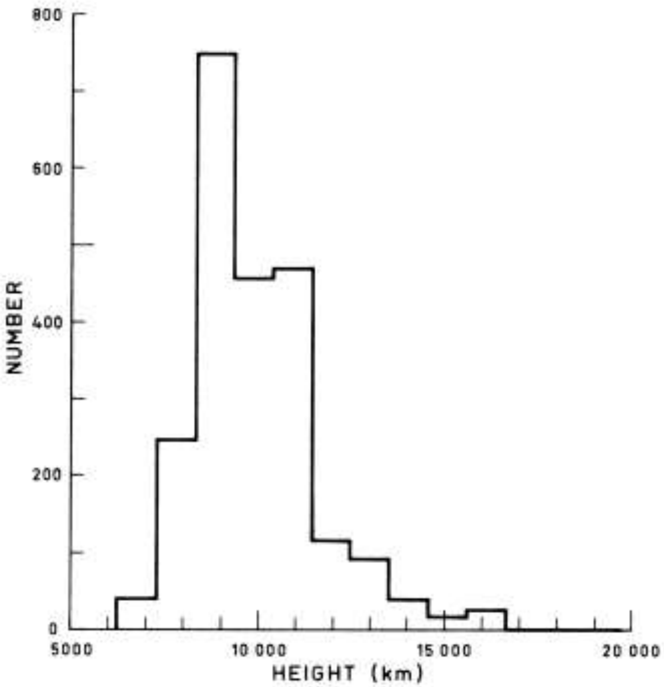

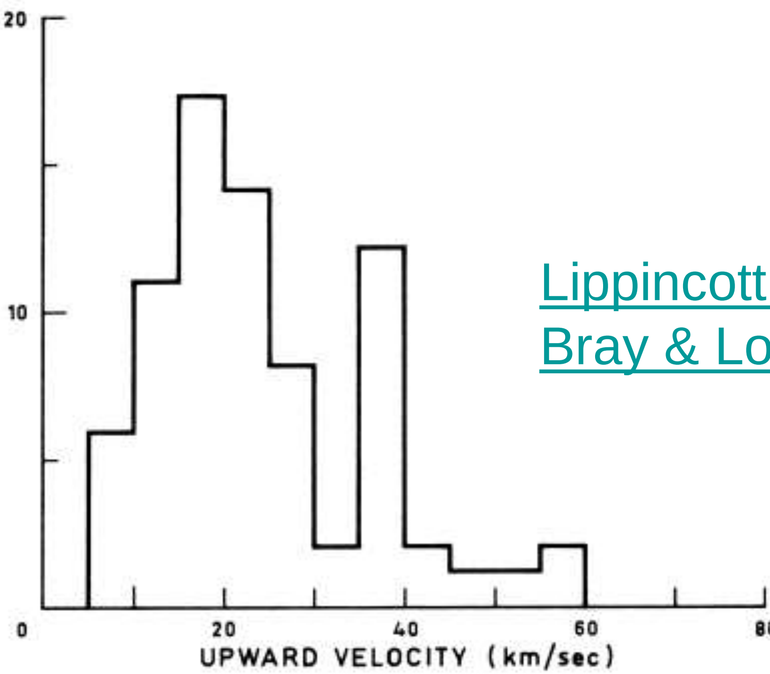

Lippincott (1957)
Bray & Loughhead (1974)

What drives spicules ?

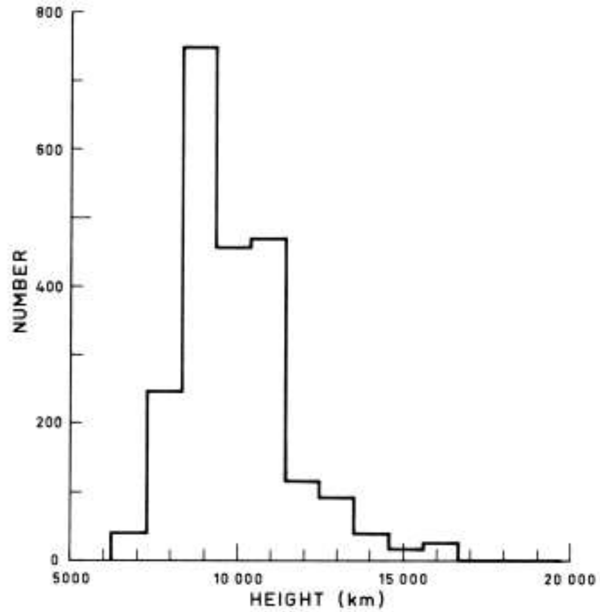

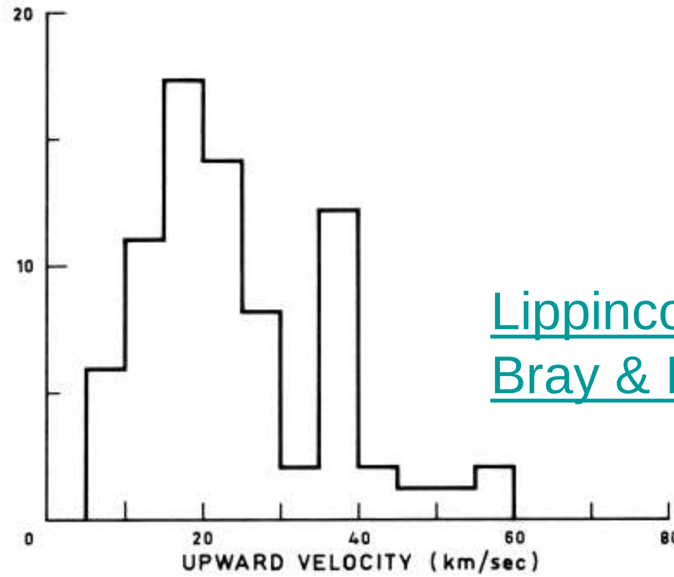

Lippincott (1957)
Bray & Loughhead (1974)

$\langle h_{max} \rangle \approx 9\,800$ km $\qquad \langle v_{max} \rangle \approx 24$ km s^{-1}

But : $\quad h_{max} = \dfrac{\langle v_{max} \rangle^2}{2g} = 1050\,\text{km} \qquad v_{max} = \sqrt{2g\langle h_{max} \rangle} = 73\,\text{km s}^{-1}$

g – solar gravity: 274 m s^{-2}

Unknown driver propels spicules along their trajectories.

Off-limb fine structures

Hinode Ca II H

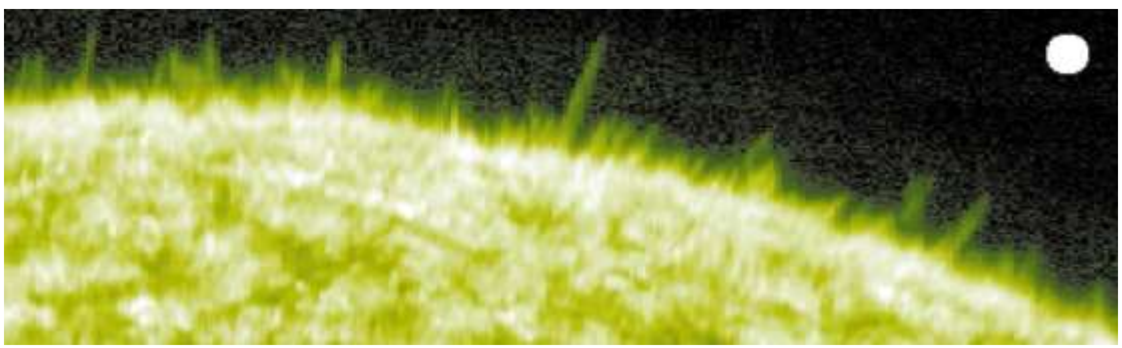

SoHO/SUMER O V

Wilhelm (2000)

spicules of type I and II
macrospicules
surges

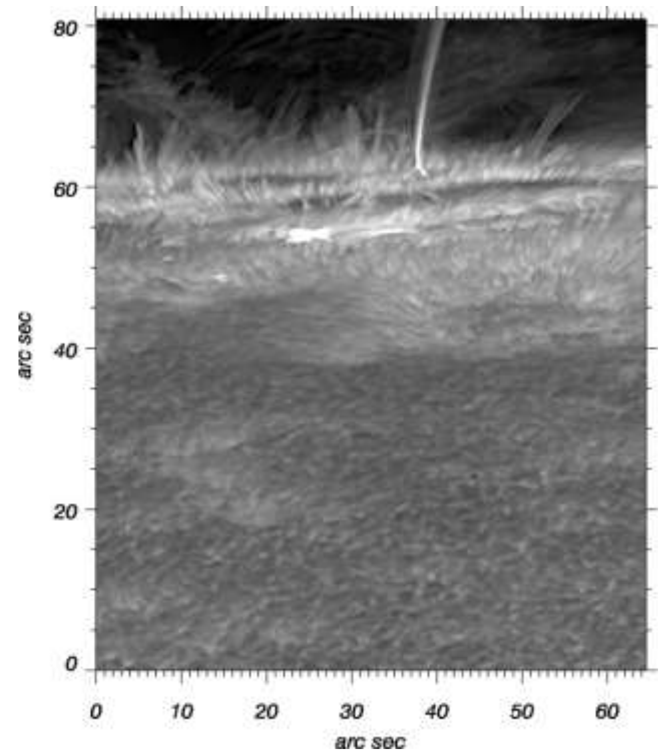

DOT Ca II H

Tziotziou et al. (2005)

On-disk fine structures

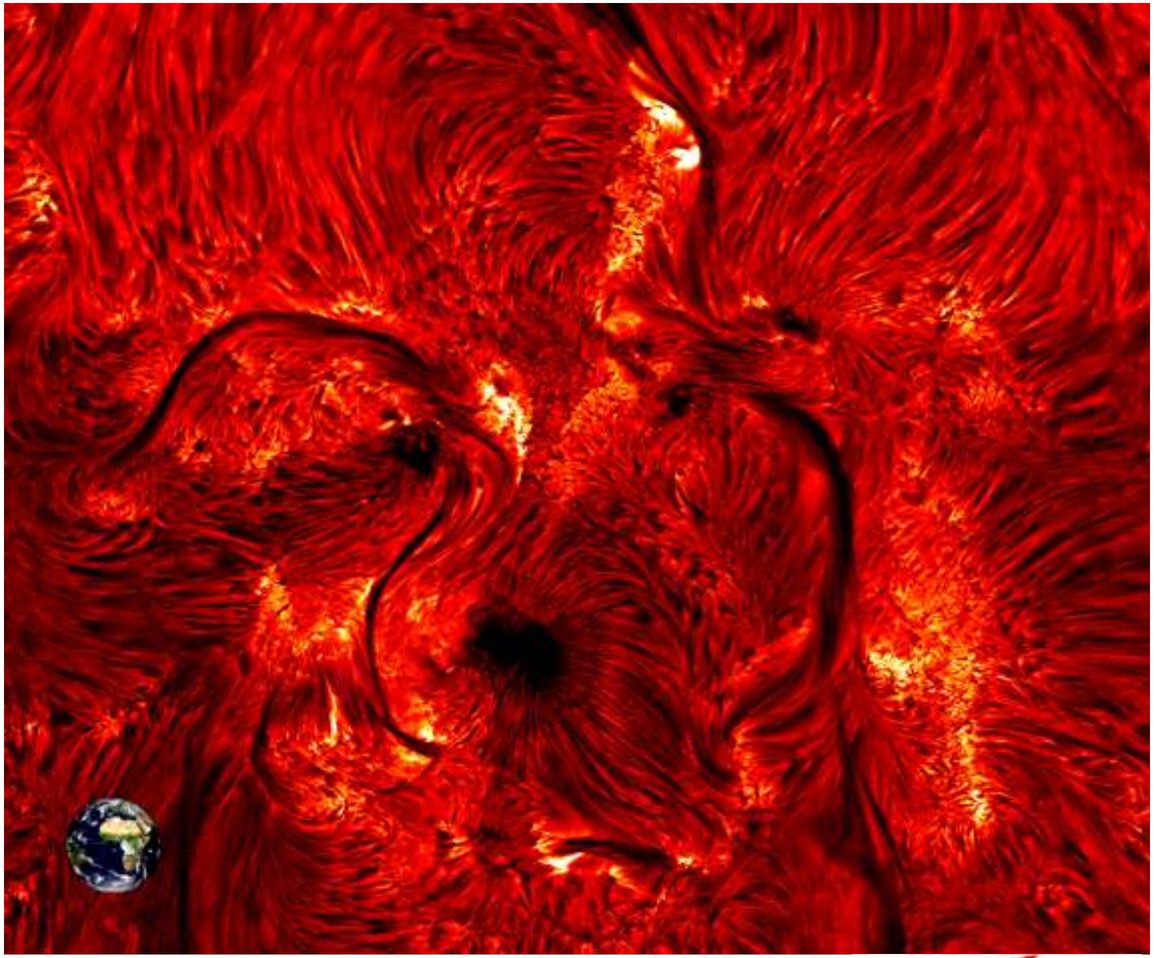

line center of Hα

Active regions:

- (dynamic, Hα) fibrils
- (bright, Ca II K) fibrils
- disk spicules
- grains
- (dynamic, Lyα, X-ray) jets
- (anemone, λ) jets

Quiet Sun:

- (dark, bright) mottles

Groups of mottles:

- rosettes
- bushes
- chains

The latest species:

- straws
- rapid blueshifted events
- black beads

Overview of the talk

1. **Observations**
   a) from the ground
      - imaging (SST, DST, DOT)
      - spectroscopy (SST)
      - spectropolarimetry (VTT)

   b) from space
      - Hinode

   c) simultaneous from the ground and space
      - DST + SDO

Overview of the talk

1. Observations

a) from the ground
- imaging (SST, DST, DOT)
- spectroscopy (SST)
- spectropolarimetry (VTT)

b) from space
- Hinode

c) simultaneous from the ground and space
- DST + SDO

2. Theory and simulations

- brief hindsight on 1-D simulations
- the latest 2-D simulations
- non-equilibrium time-dependent ionization of hydrogen
- solar atmosphere cartoons

Overview of the talk

1. Observations

a) from the ground
   - imaging (SST, DST, DOT)
   - spectroscopy (SST)
   - spectropolarimetry (VTT)

b) from space
   - Hinode

c) simultaneous from the ground and space
   - DST + SDO

2. Theory and simulations

- brief hindsight on 1-D simulations
- the latest 2-D simulations
- non-equilibrium time-dependent ionization of hydrogen
- solar atmosphere cartoons

3. The new window into the chromosphere

- Atacama Large Millimeter/submillimeter Array (ALMA)
- simulations of the solar chromosphere at millimeter and submillimeter wavelengths

State-of-the-art imaging of the chromosphere

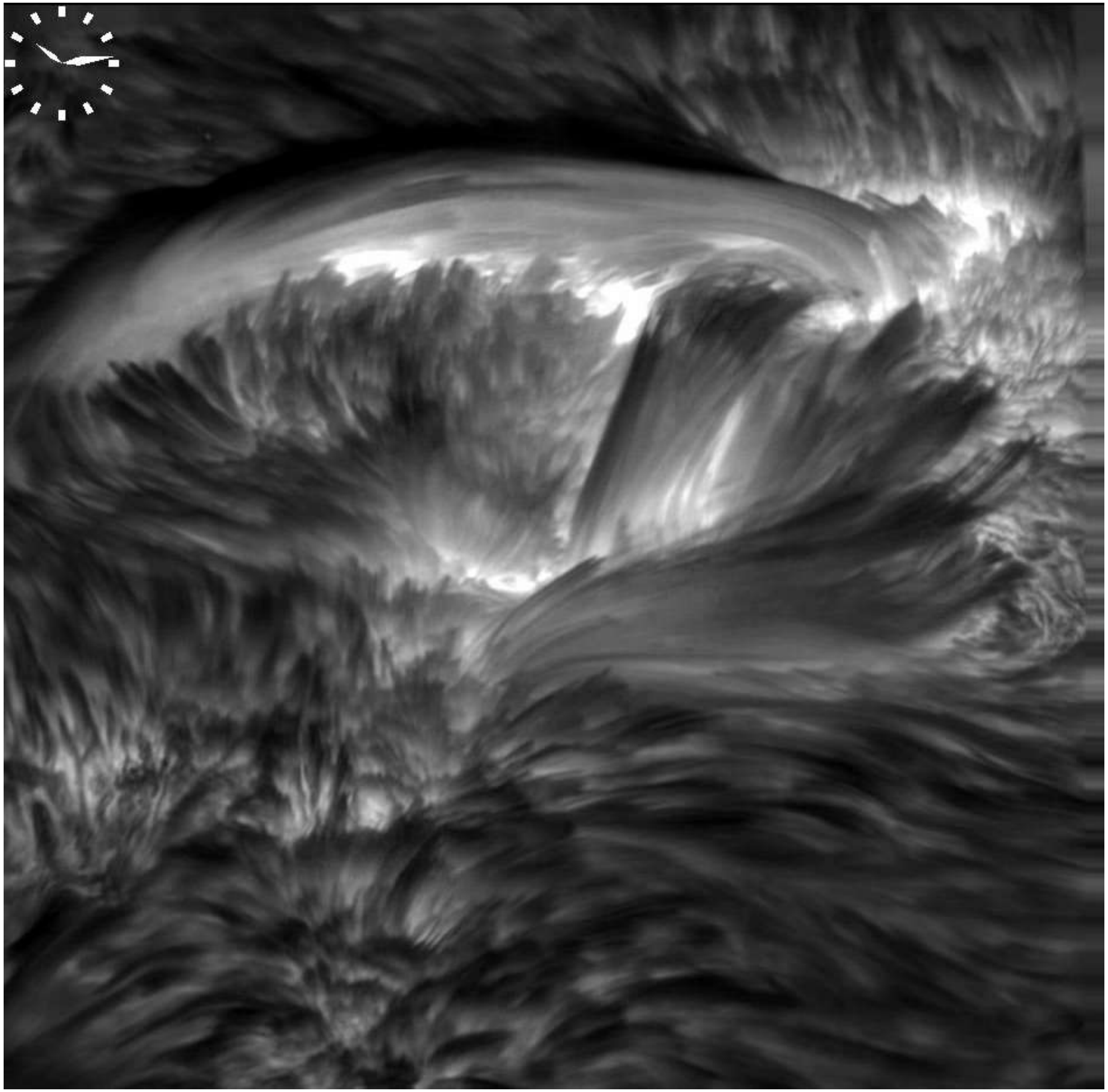

van Noort & Rouppe van der Voort (2006)

Swedish 1-m Solar Telescope
+ adaptive optics
+ image postprocessing

diagnostics: Hα line center
date: October 4, 2005
duration: 72 min

Resolutions
temporal: 3 frames per second
spatial: ~ 70 – 100 km

Field of view:
61 arcsec × 61 arcsec

Main result:
Hα image sequence with the highest resolution ever achieved.

Dynamic fibrils in Hα

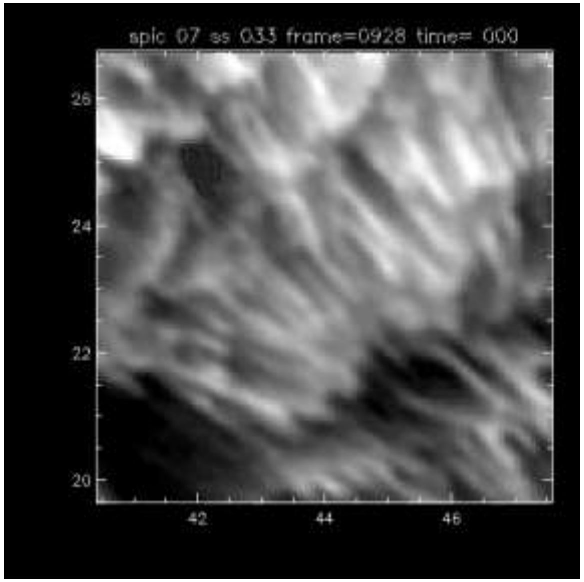

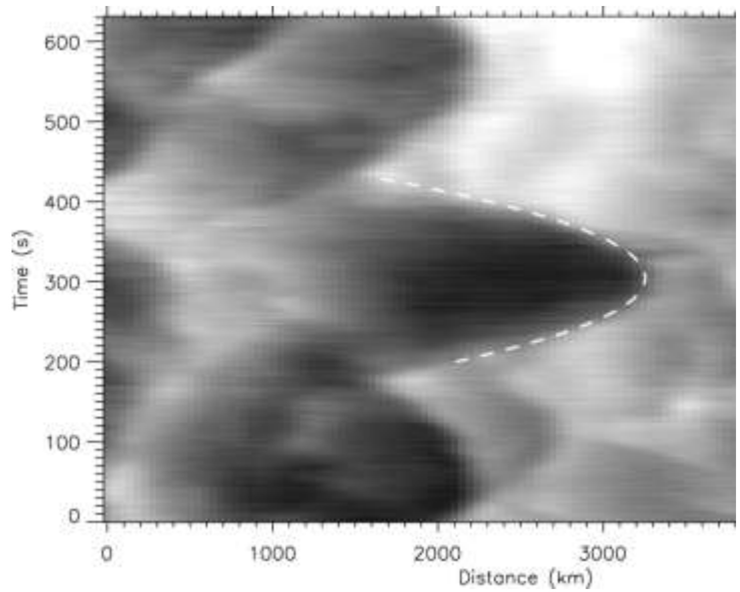

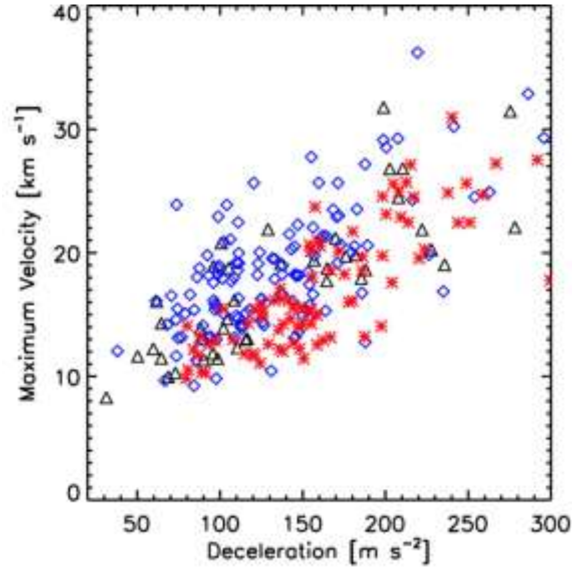

Hansteen et al. (2006)

De Pontieu et al. (2007)

Main results:

- confirmed extensions and retractions
- confirmed parabolic top trajectories
- linear relationship between maximum velocity and deceleration
- Hα dynamic fibrils in a plage co-spatial with areas of increased power of 5-min oscillations
- field-aligned magnetoacoustic shock excitation

Ca II 8542 Å - a new diagnostics of chromospheric fine structures

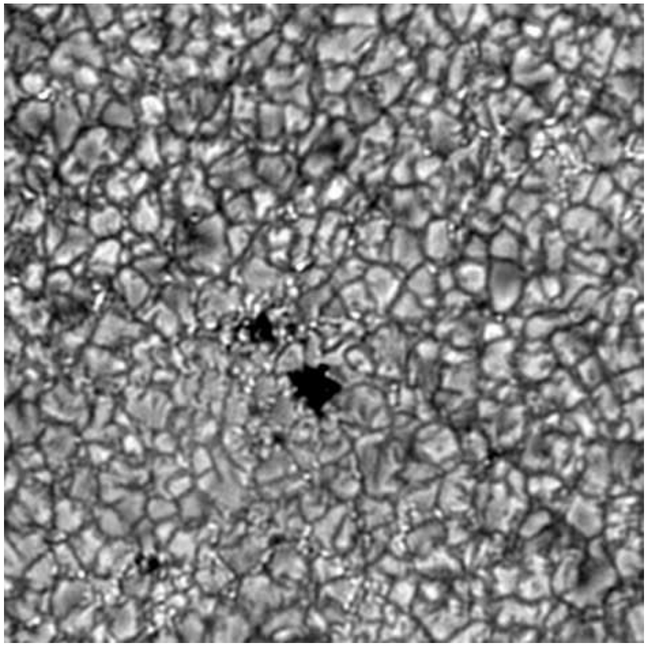

Dunn Solar Telescope
+ IBIS (Interferometric BImodal Spectrometer)
1 October 2005

Main results:
- discovery of fibrils in Ca II IR lines
- close similarity of Hα and Ca II IR fibrils

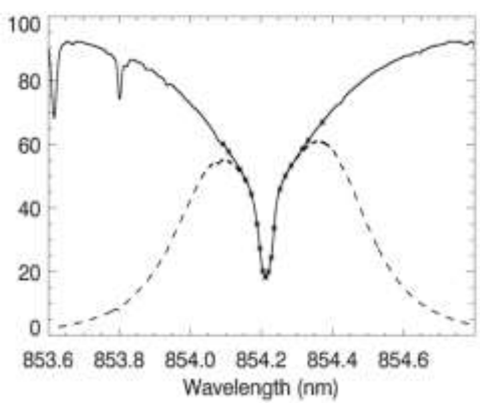

Cauzzi et al. (2008)

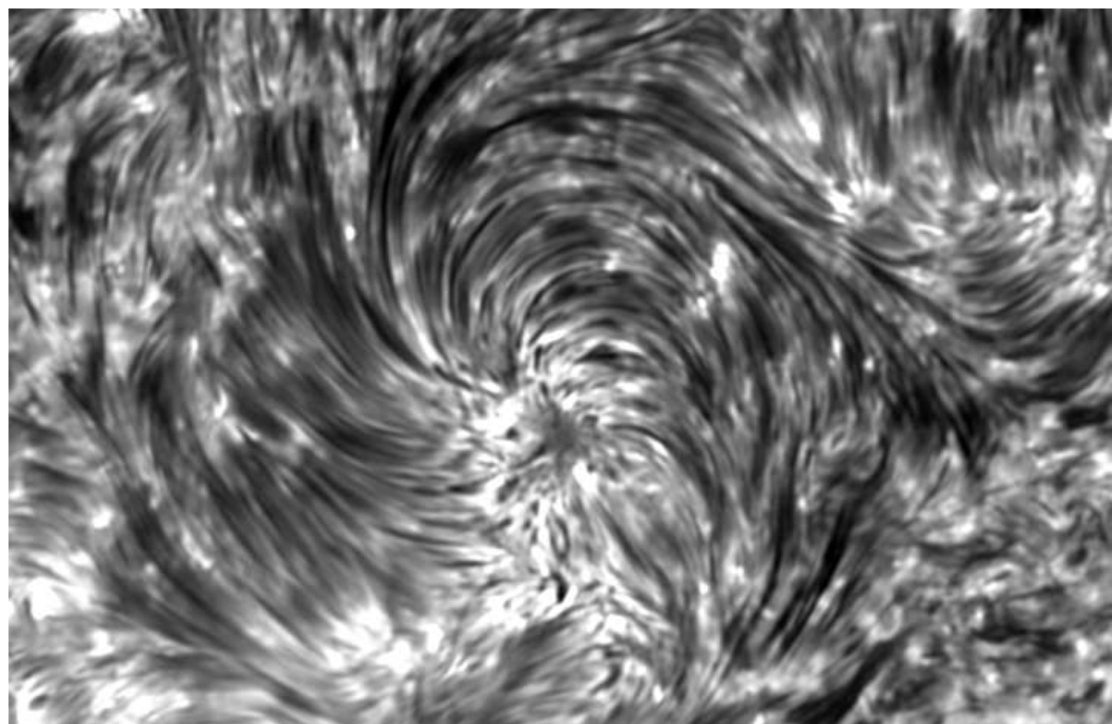

Multispectral tomographic observations

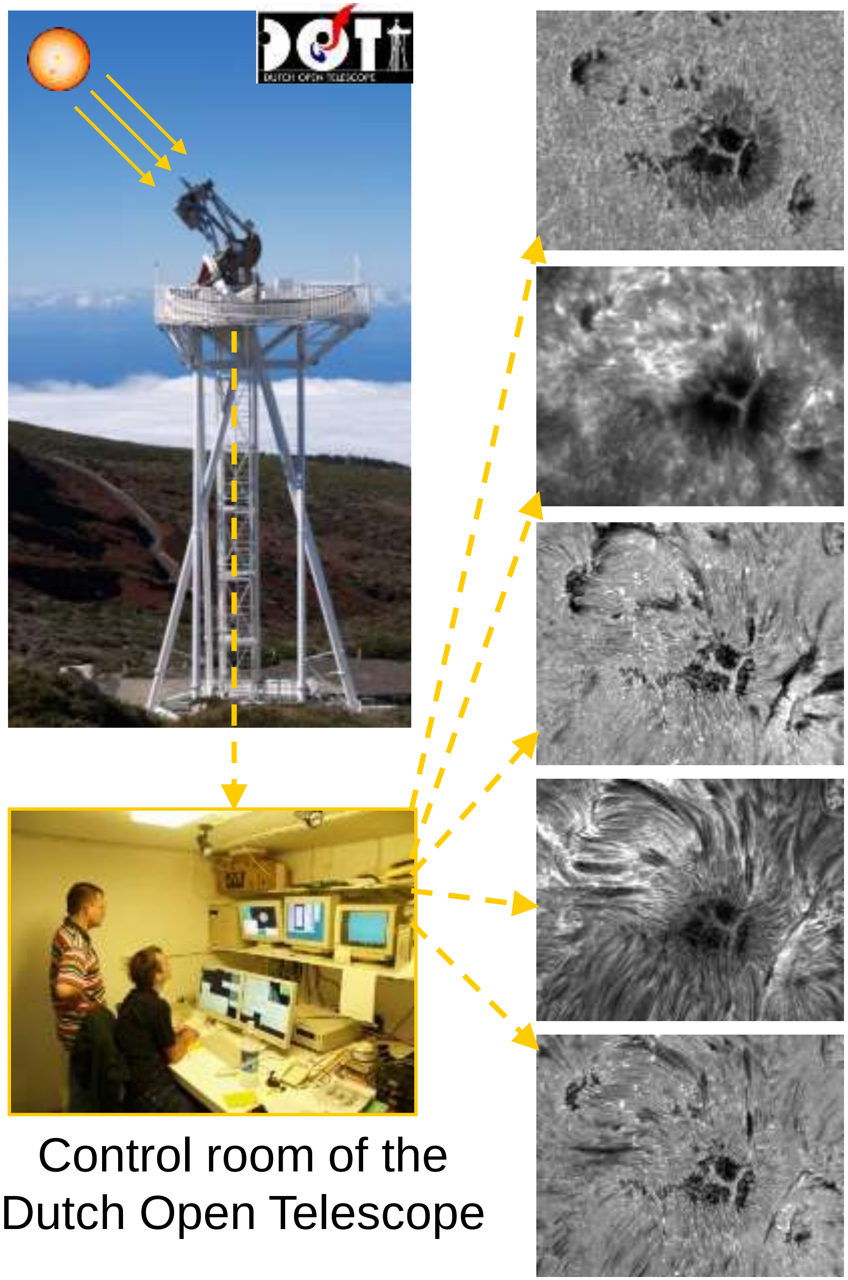

Control room of the
Dutch Open Telescope

Multispectral tomographic observations

Control room of the Dutch Open Telescope

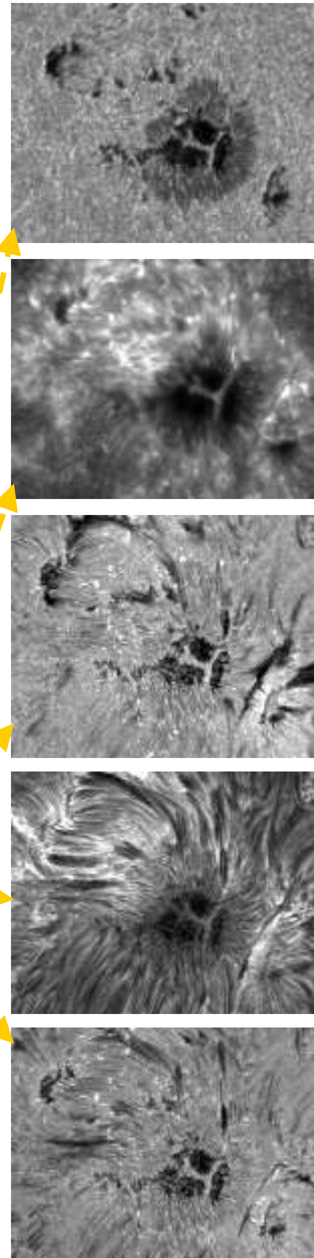

Speckle image reconstruction

$$F(x_1, y_1) = A \iint f(x, y) \times \exp\left\{ \mathrm{i} \frac{k}{2L} \left[(x - x_1)^2 + (y - y_1)^2 \right] \right\} \mathrm{d}x\mathrm{d}y,$$

Speckle code

Computer cluster for fast image reconstruction

Demo of speckle reconstruction

Hα – line center

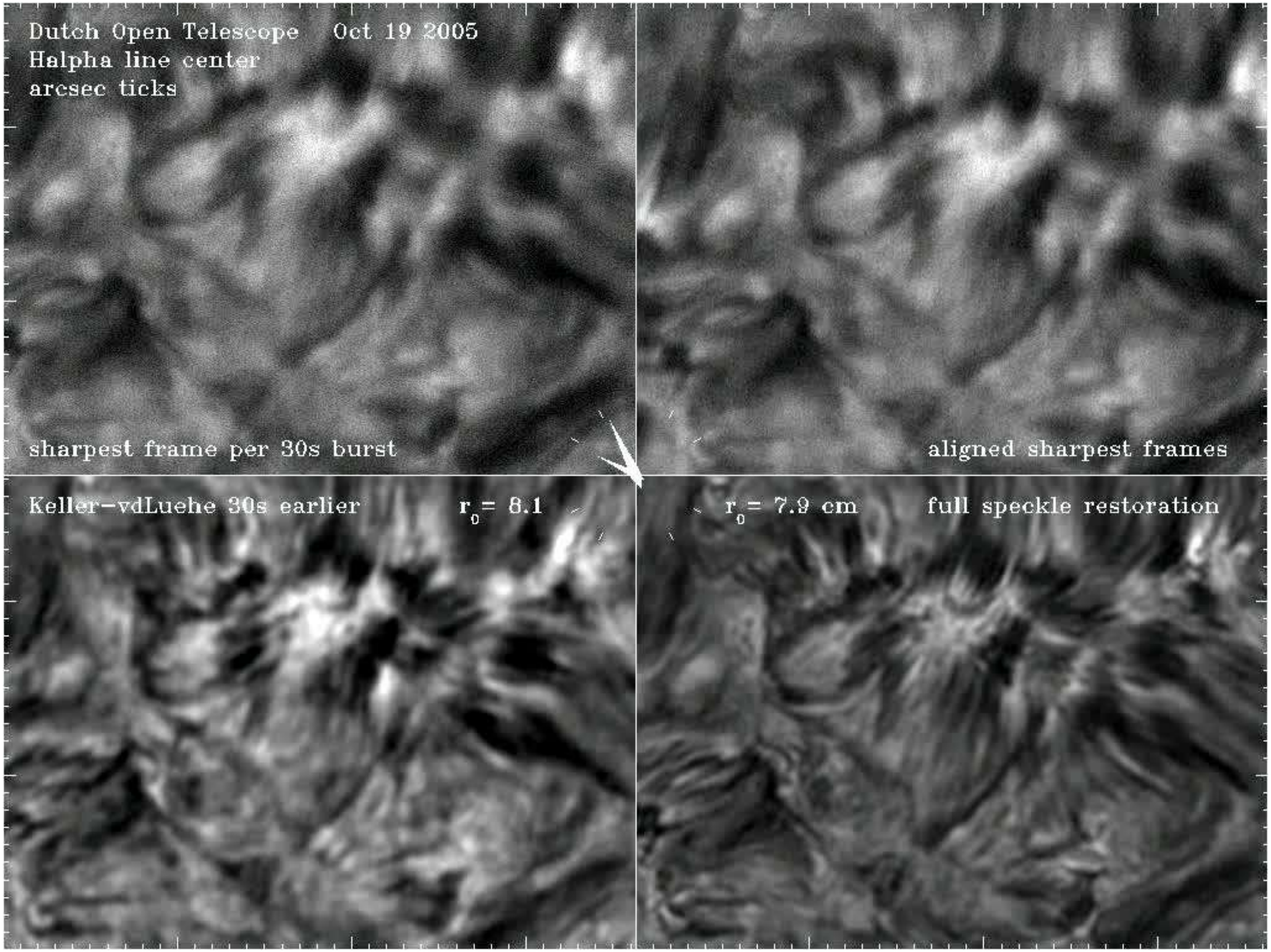

http://dot.astro.uu.nl/DOT_speckle.html

Multispectral tomographic observations

Control room of the Dutch Open Telescope

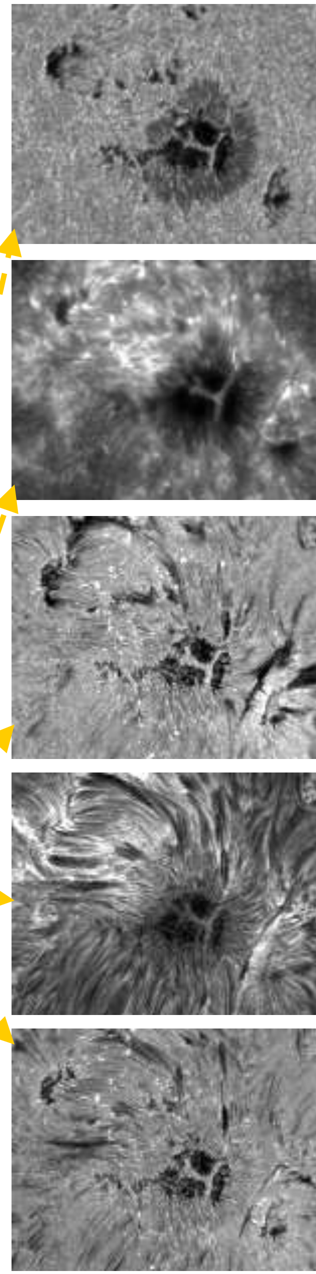

Speckle image reconstruction

$$F(x_1, y_1) = A \iint f(x, y) \times \exp\left\{ \mathrm{i} \frac{k}{2L} \left[(x - x_1)^2 + (y - y_1)^2 \right] \right\} \mathrm{d}x \mathrm{d}y,$$

Speckle code

Computer cluster for fast image reconstruction

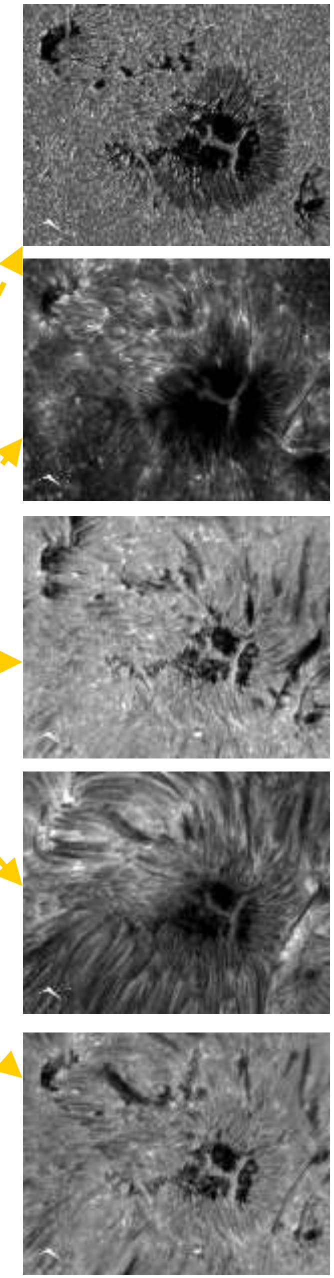

A sunspot in the DOT style

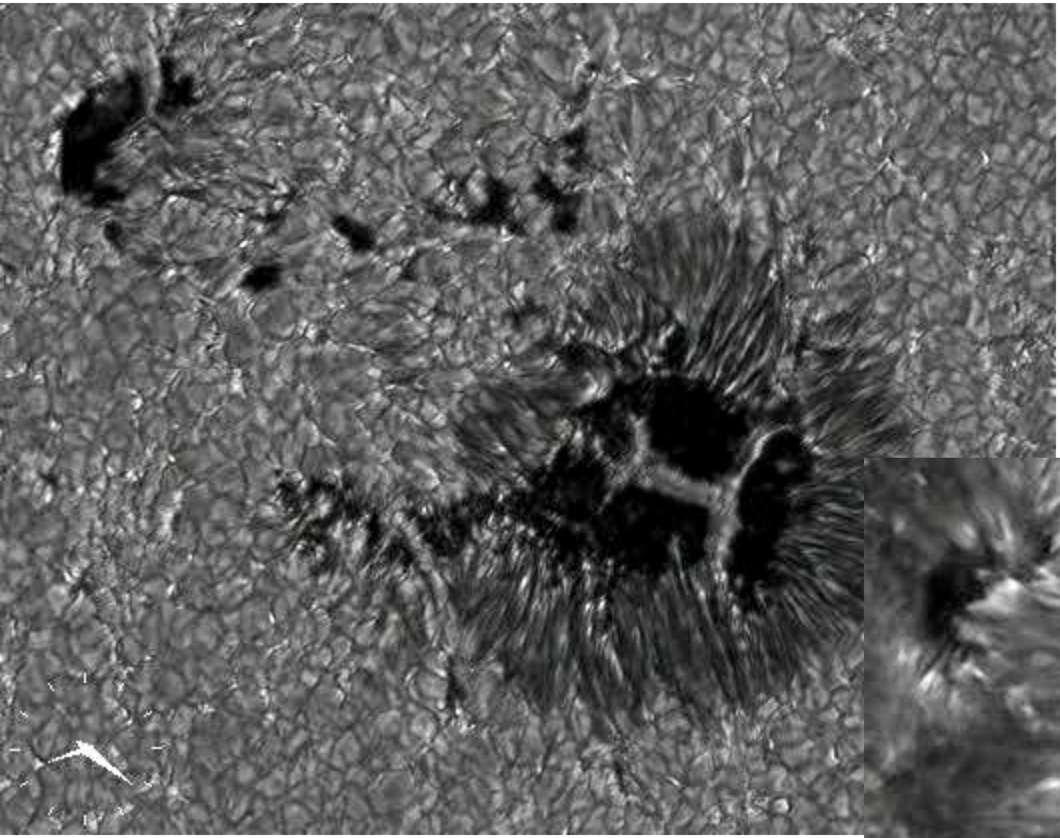

⇐ photosphere in the G band

date: 7 June 2006
duration: 1 hour

upper photosphere
+
lower chromosphere in Ca II H ⇒

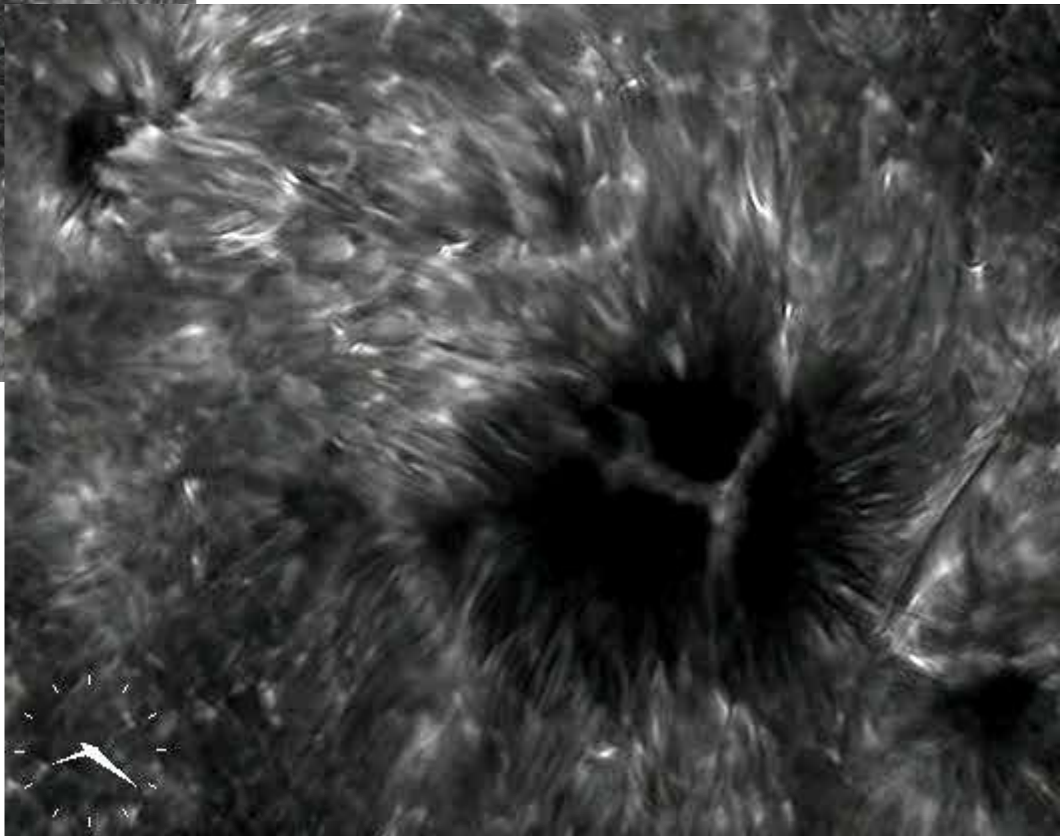

A sunspot in the DOT style

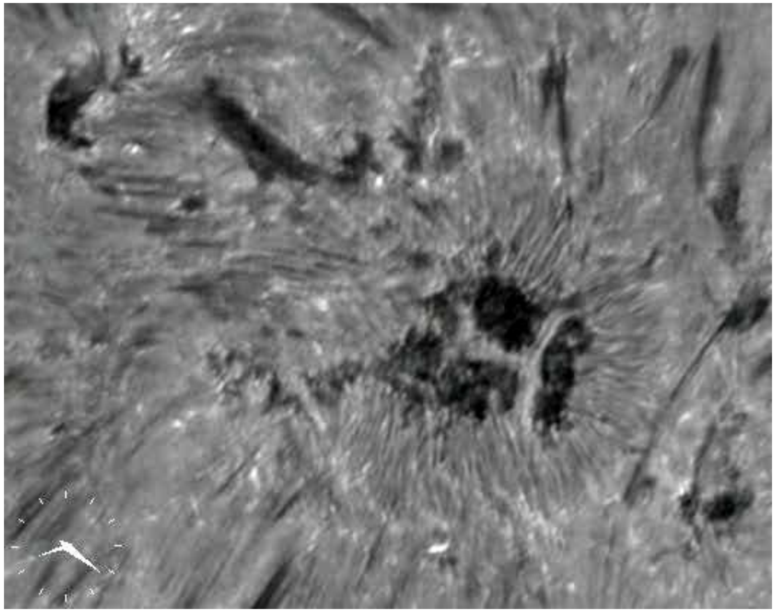

the solar chromosphere in Hα
above a sunspot

blue wing of Hα - 0.7 Å
upward motions

red wing of Hα + 0.7 Å
downward motions

Hα center

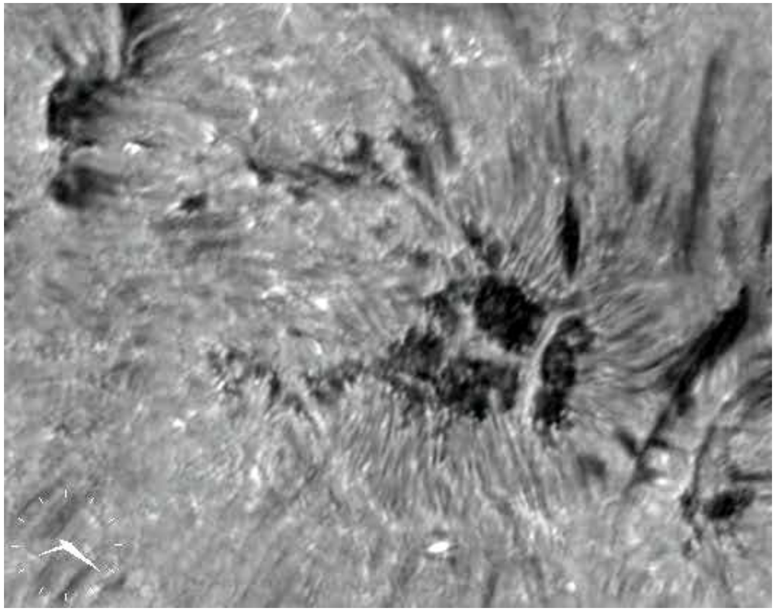

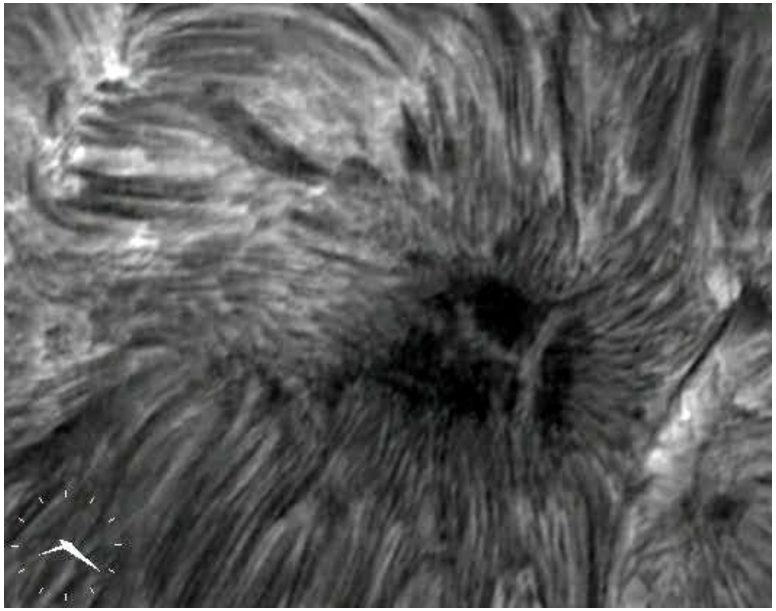

Spectroscopy of dynamic fibrils in Hα and Ca II 8662 Å

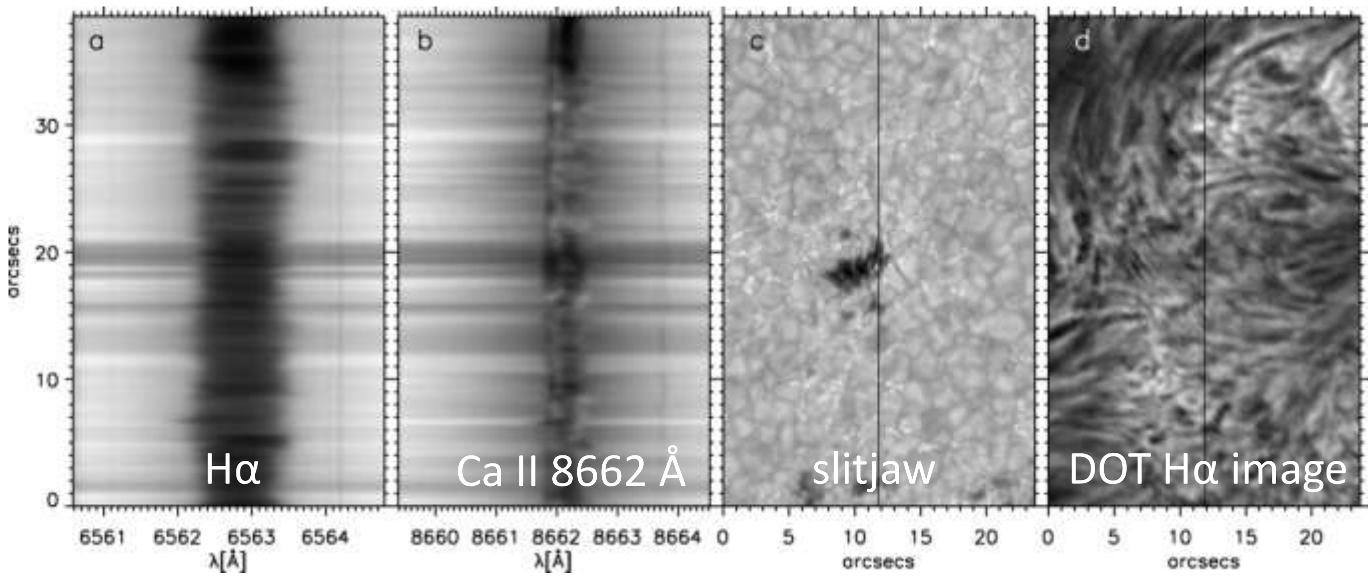

Velocity-time plot for Ca II 8662 Å .

Dynamic fibrils seen as diagonal dark components across the spectral line.

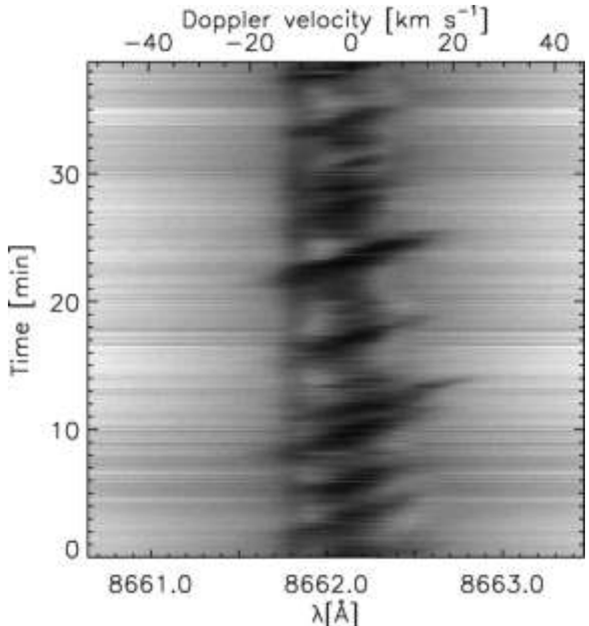

Swedish 1-m Solar Telescope +TRIPPEL spectrograph + Adaptive Optics + Dutch Open Telescope
date: 4 May 2006
duration: 40 min
cadence: 0.5 s

Main result: Extensions and retractions of dynamic fibrils are actual mass motions.

Langangen et al. (2008)

The magnetic field of off-limb spicules

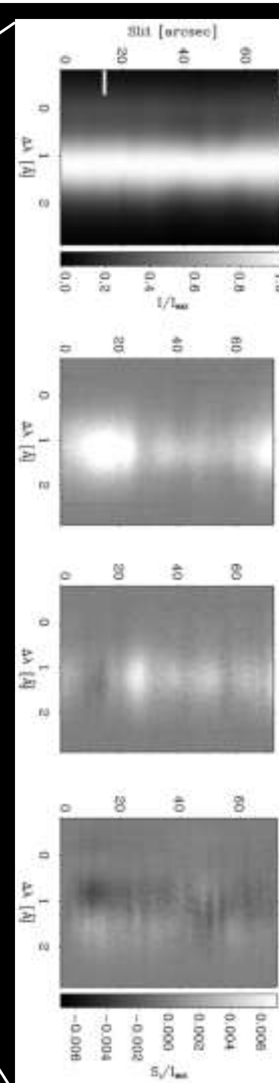

Stokes I

Stokes Q

Stokes U

Stokes V

German VTT + TIP
He I 10 830 Å triplet
17 August 2008

Centeno et al. (2008)

The magnetic field of off-limb spicules

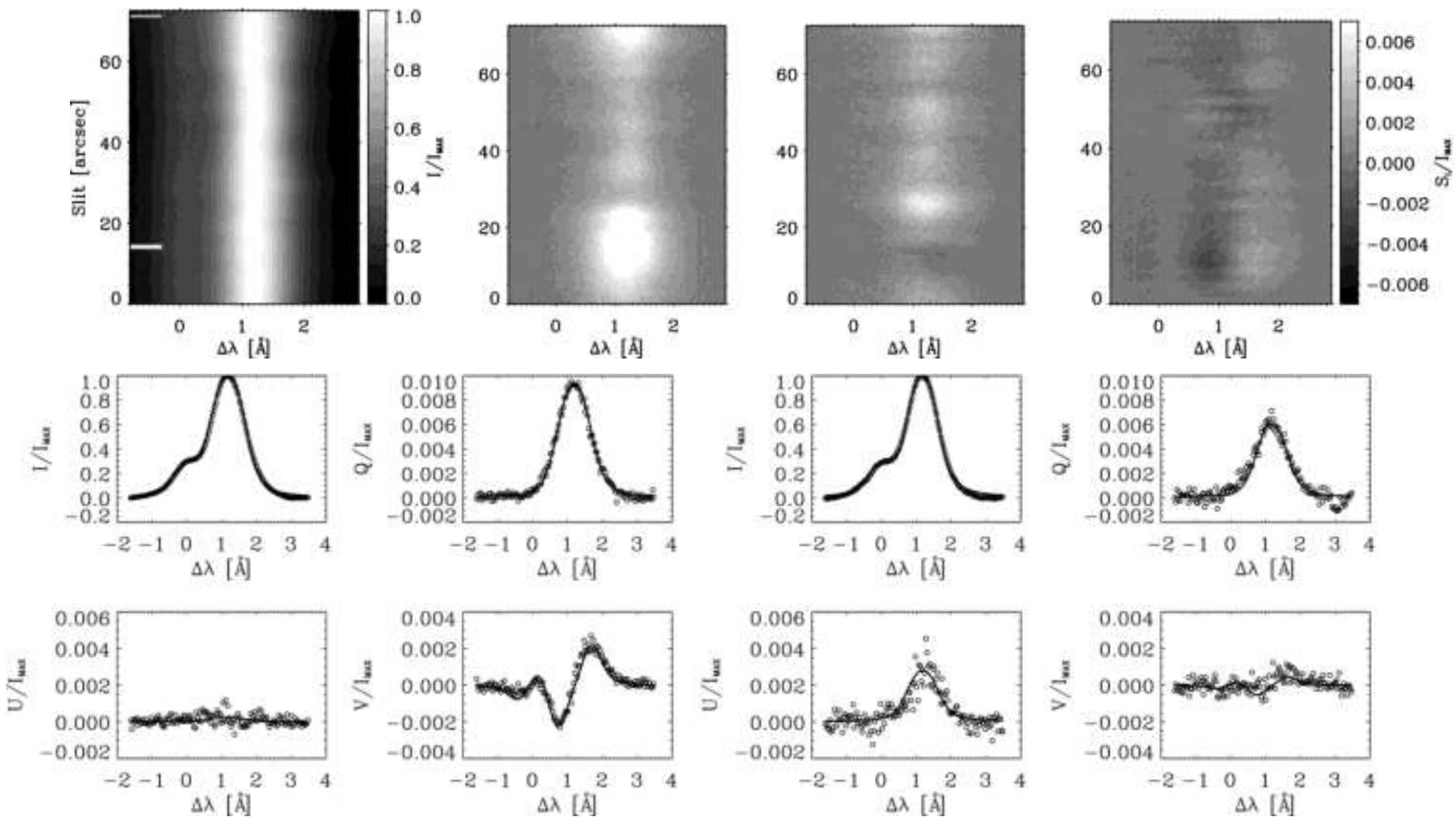

telescope + instrument: German Vacuum Tower Telescope + TIP
date of obseravtion: August 17, 2008
diagnostics: He I 10 830 Å triplet

Main results:

- measurements of magnetic field strengths of spicules
- 48 G (left panels), 9 G (right panels)

Centeno et al. (2010)

The magnetic field of off-limb spicules

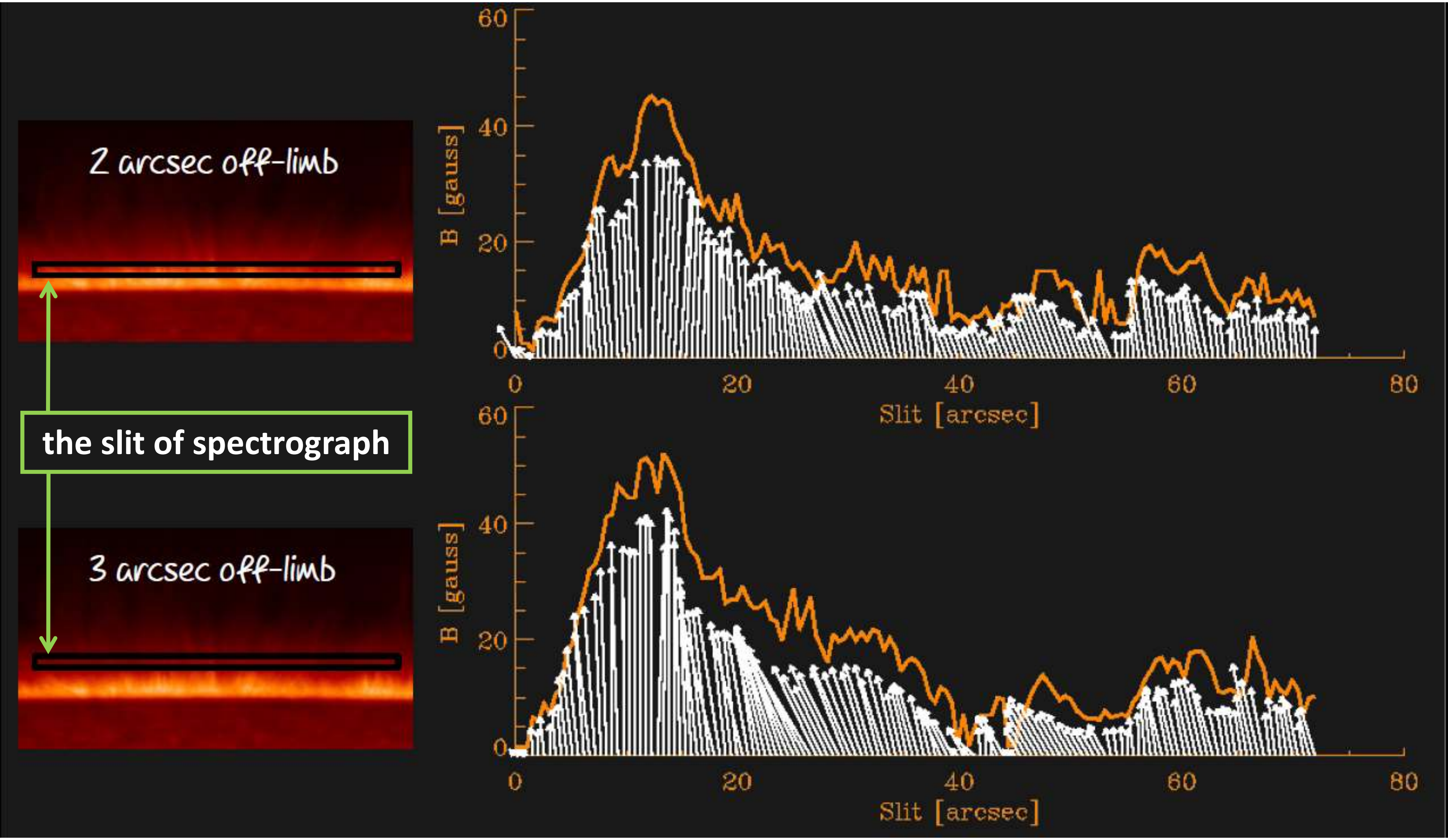

Centeno et al. (2008)

Spicules in the Hinode/SOT style

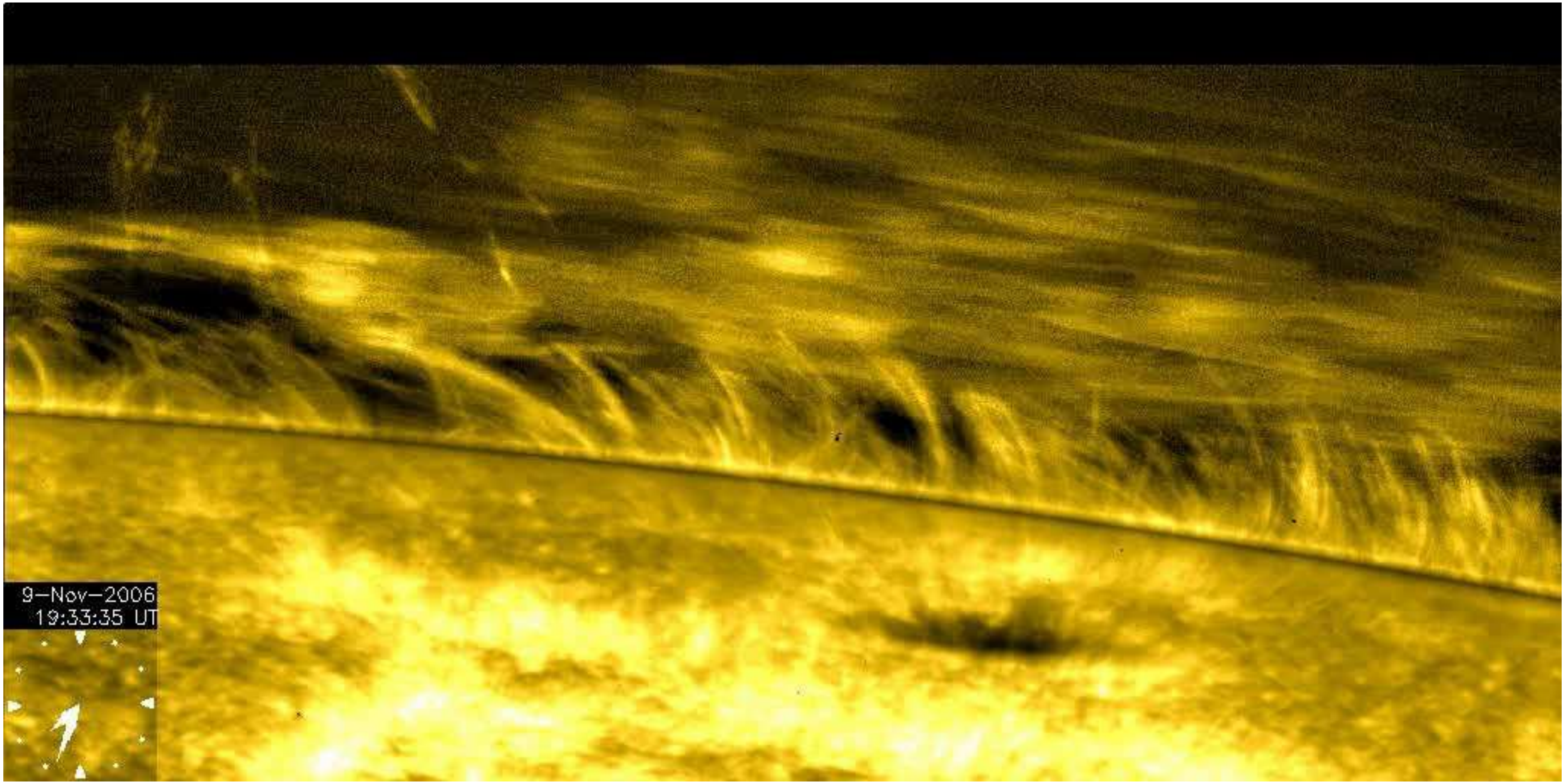

telescope: Solar Optical Telescope (∅ 50 cm)
diagnostics: Ca II H

Main result: discovery of two fundamntally different types of spicules

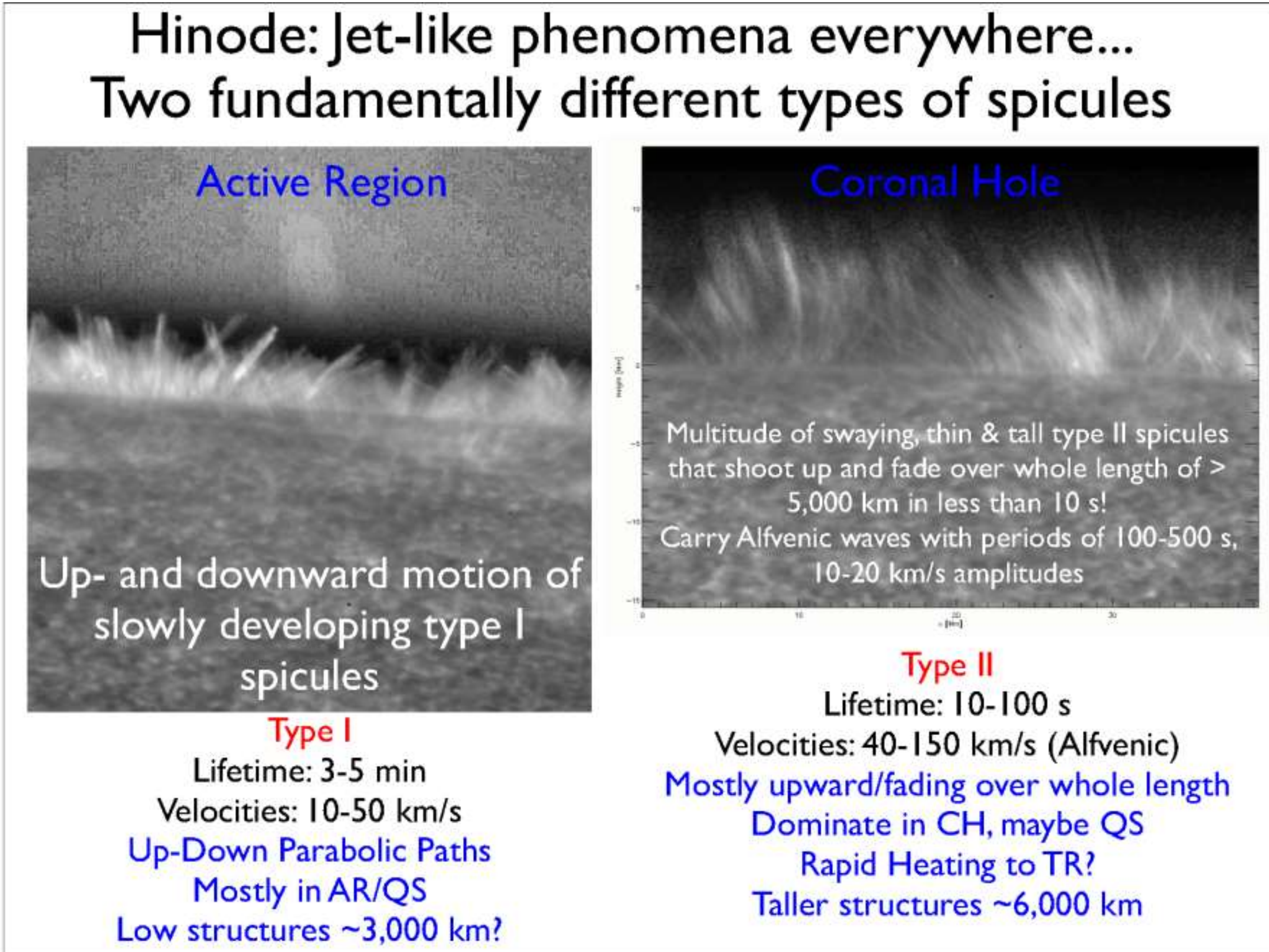

De Pontieu et al. (2008)

Anemone jets in Ca II H by Hinode/SOT

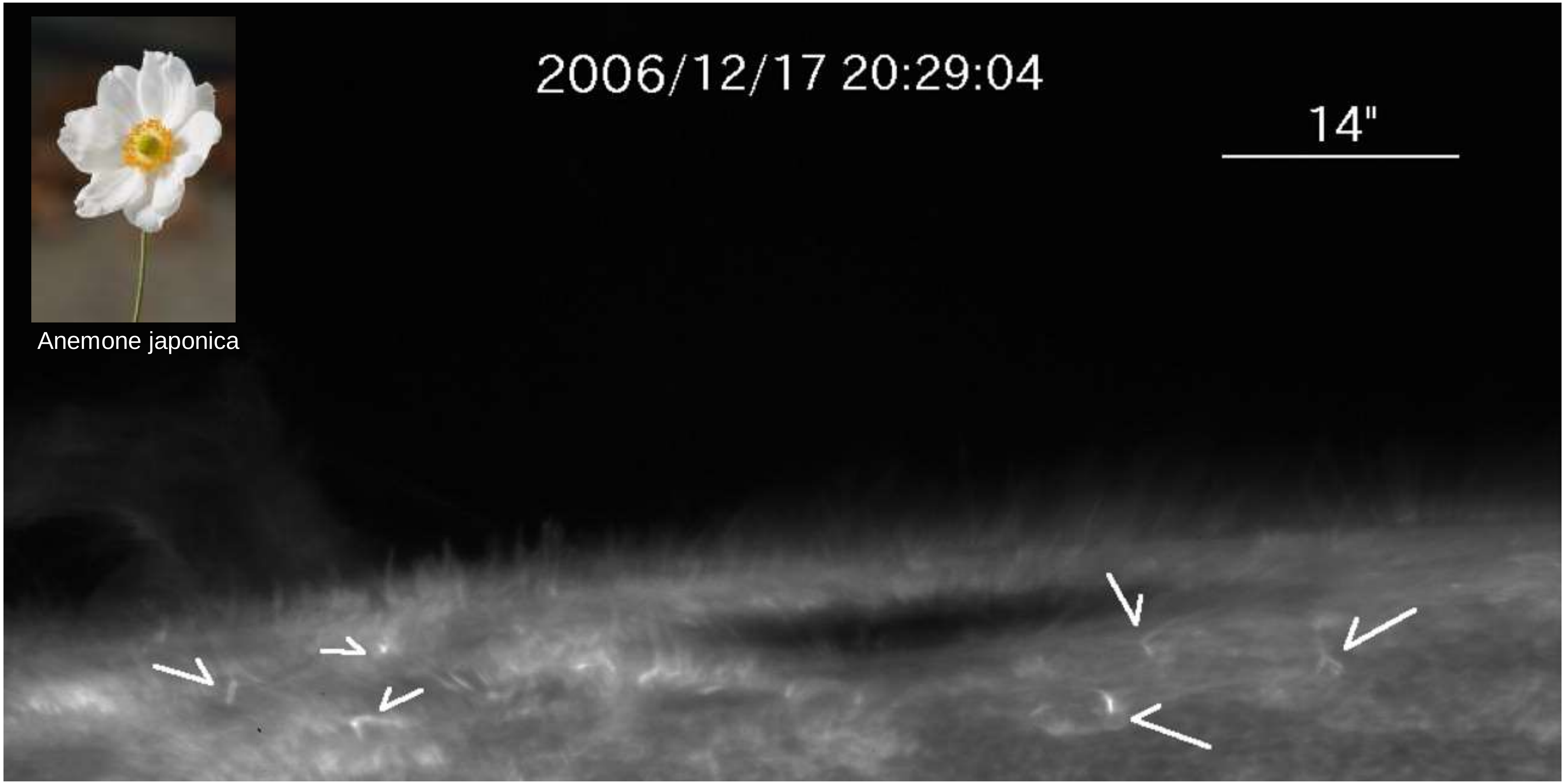

Shibata et al. (2007)

Anemone jets in Ca II H by Hinode/SOT

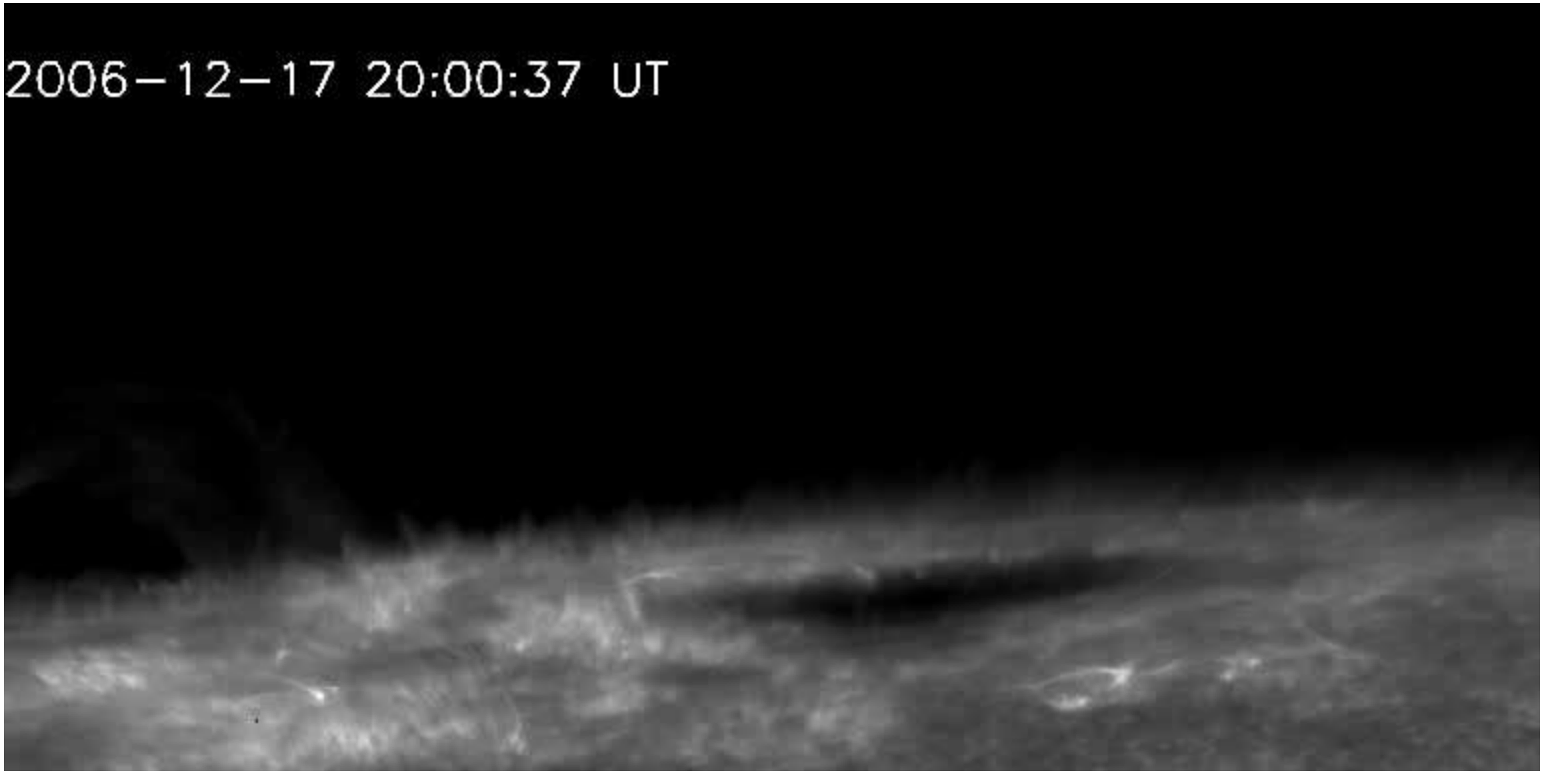

Shibata et al. (2007)

Inverted Y-shape jets implying magnetic reconnection

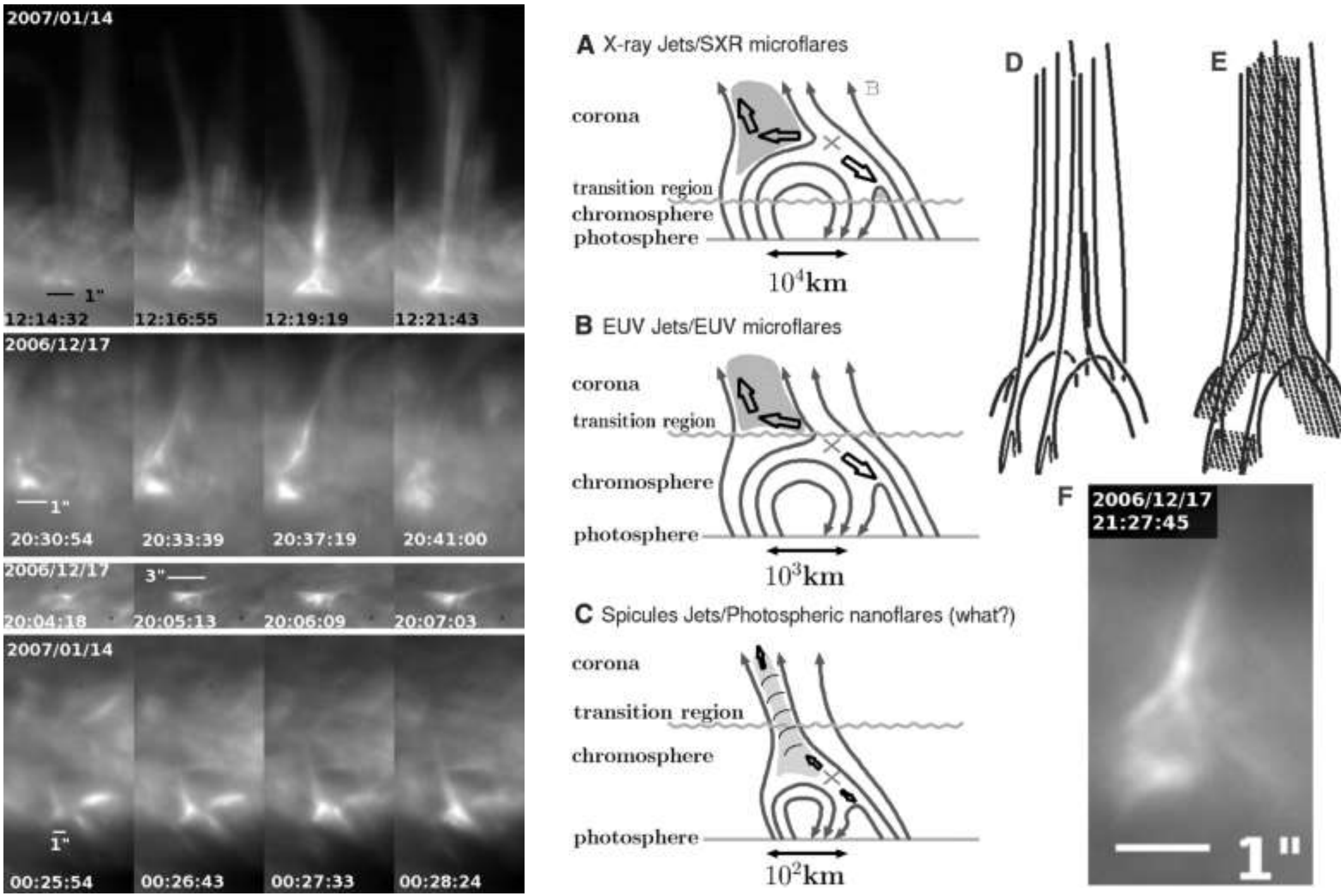

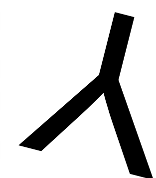

Shibata et al. (2007)

Giant anemone jet in multispectral observations and simulations

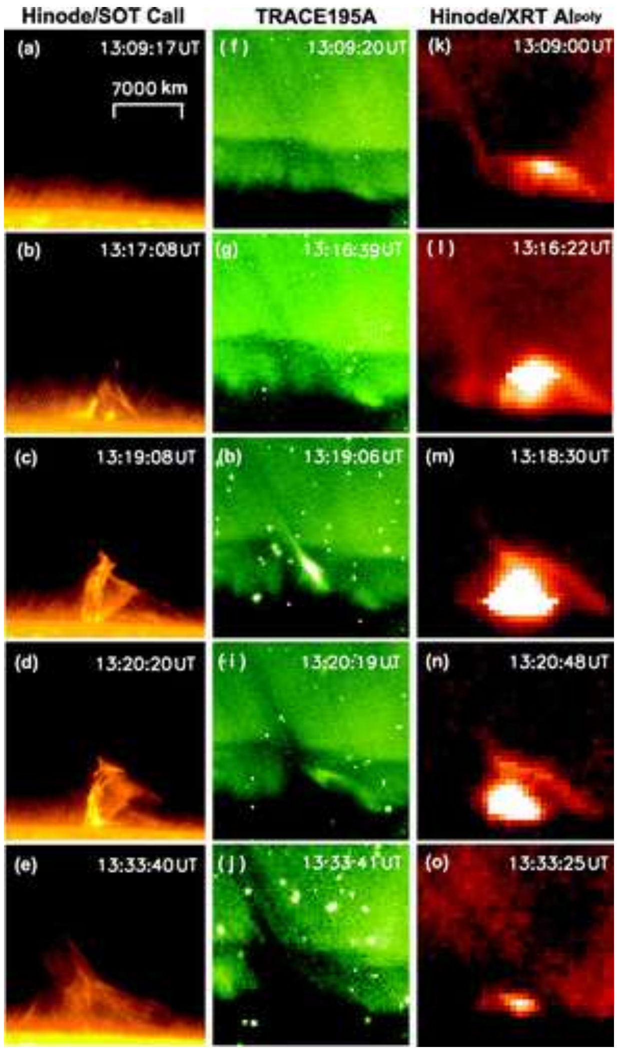

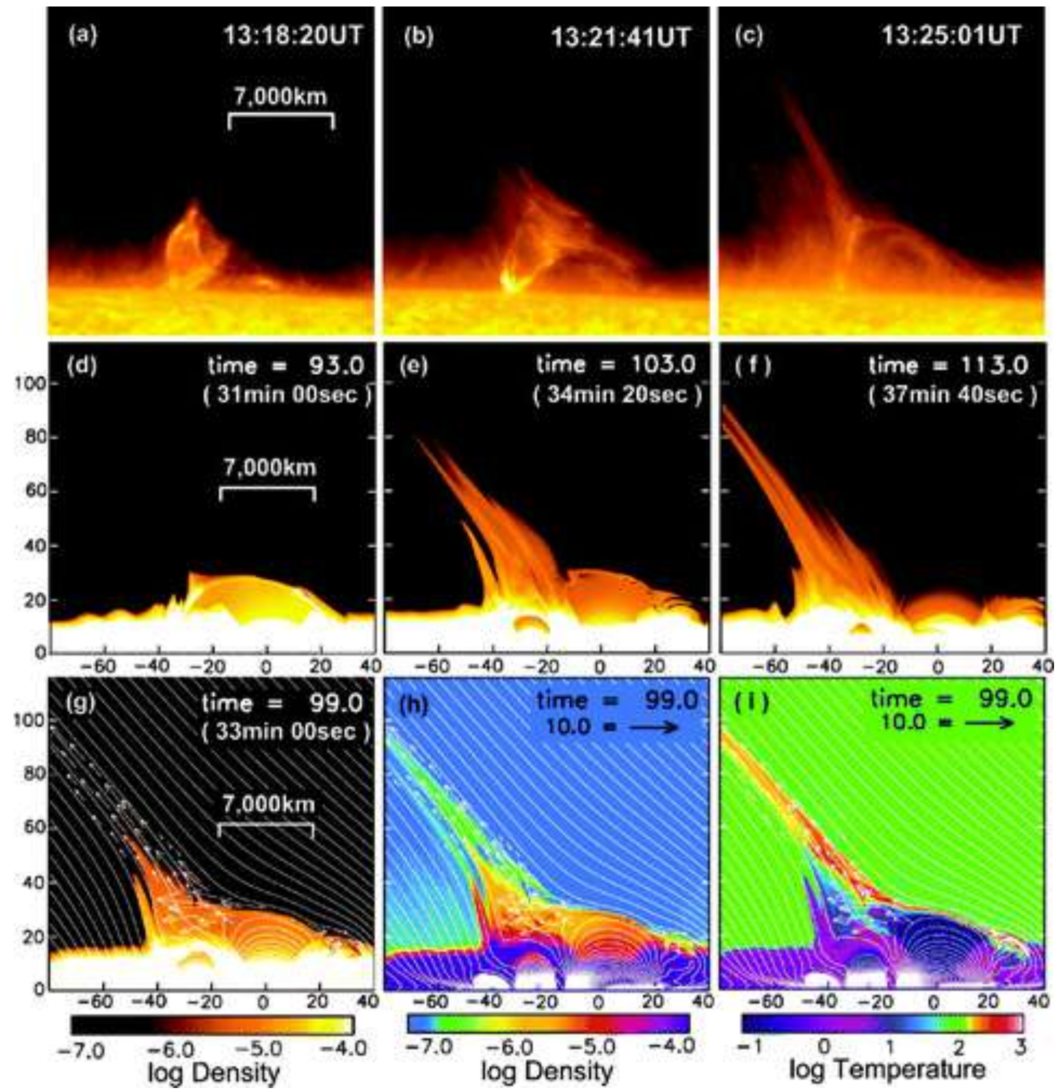

Nishizuka et al. (2008)

Multispectral tomography of the solar atmosphere

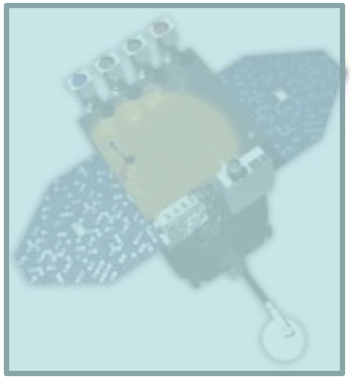

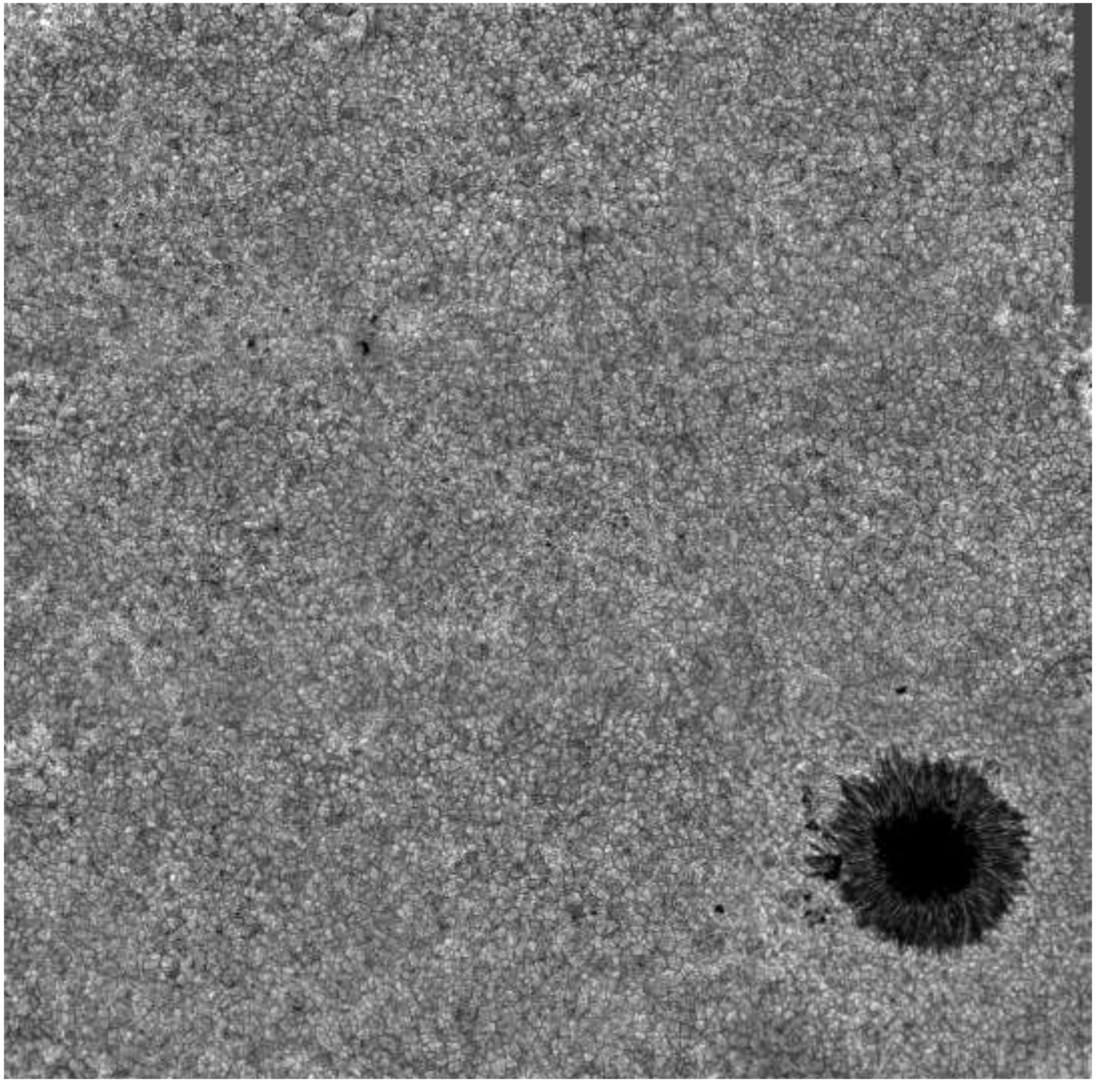

photosphere

DST/IBIS

line wing of Fe I 5434 Å

3 August 2010

Multispectral tomography of the solar atmosphere

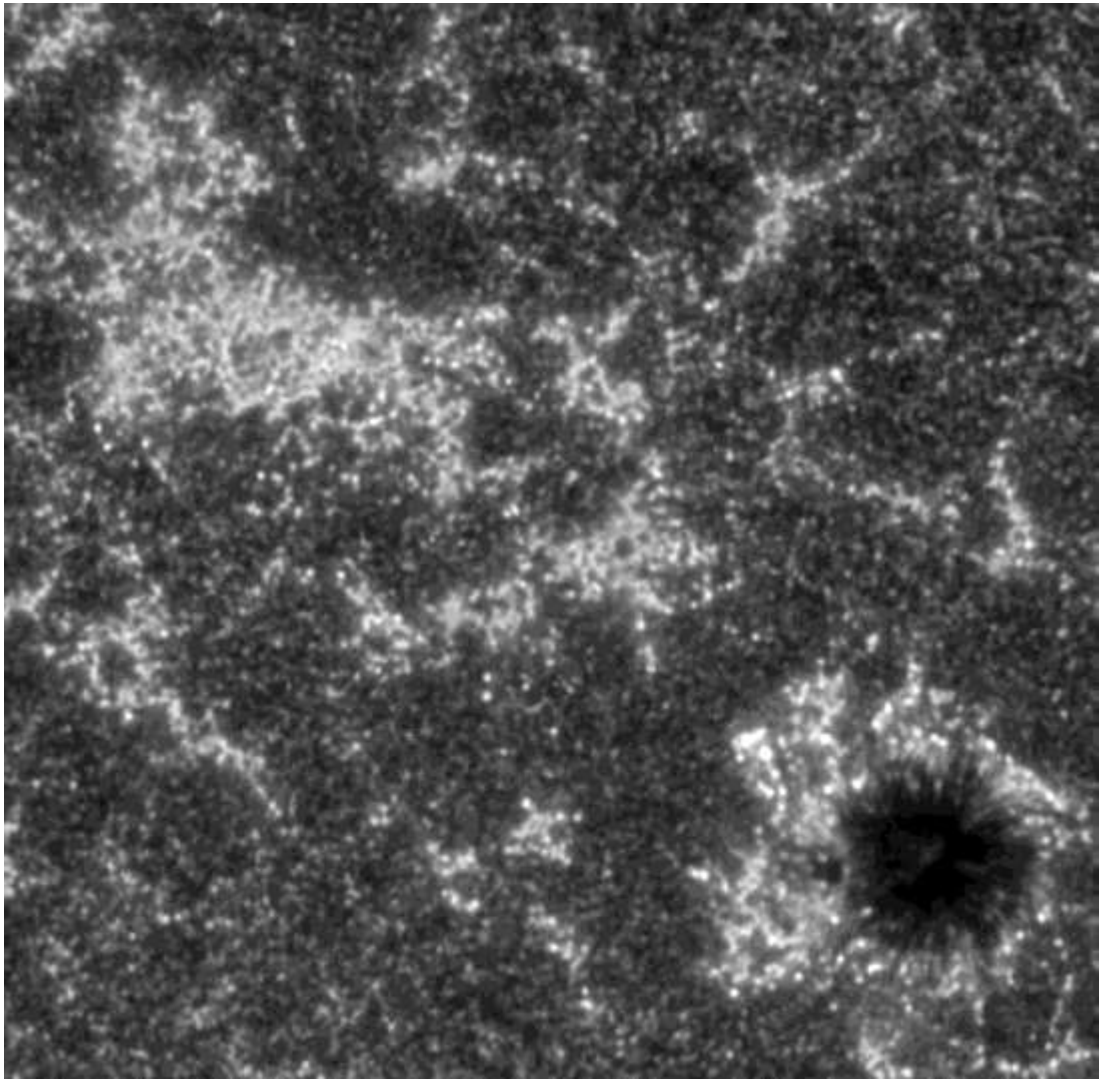

upper photosphere + transition region

SDO/AIA

C IV + continuum 1600 Å

3 August 2010

Multispectral tomography of the solar atmosphere

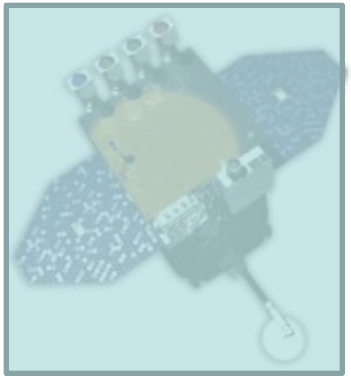

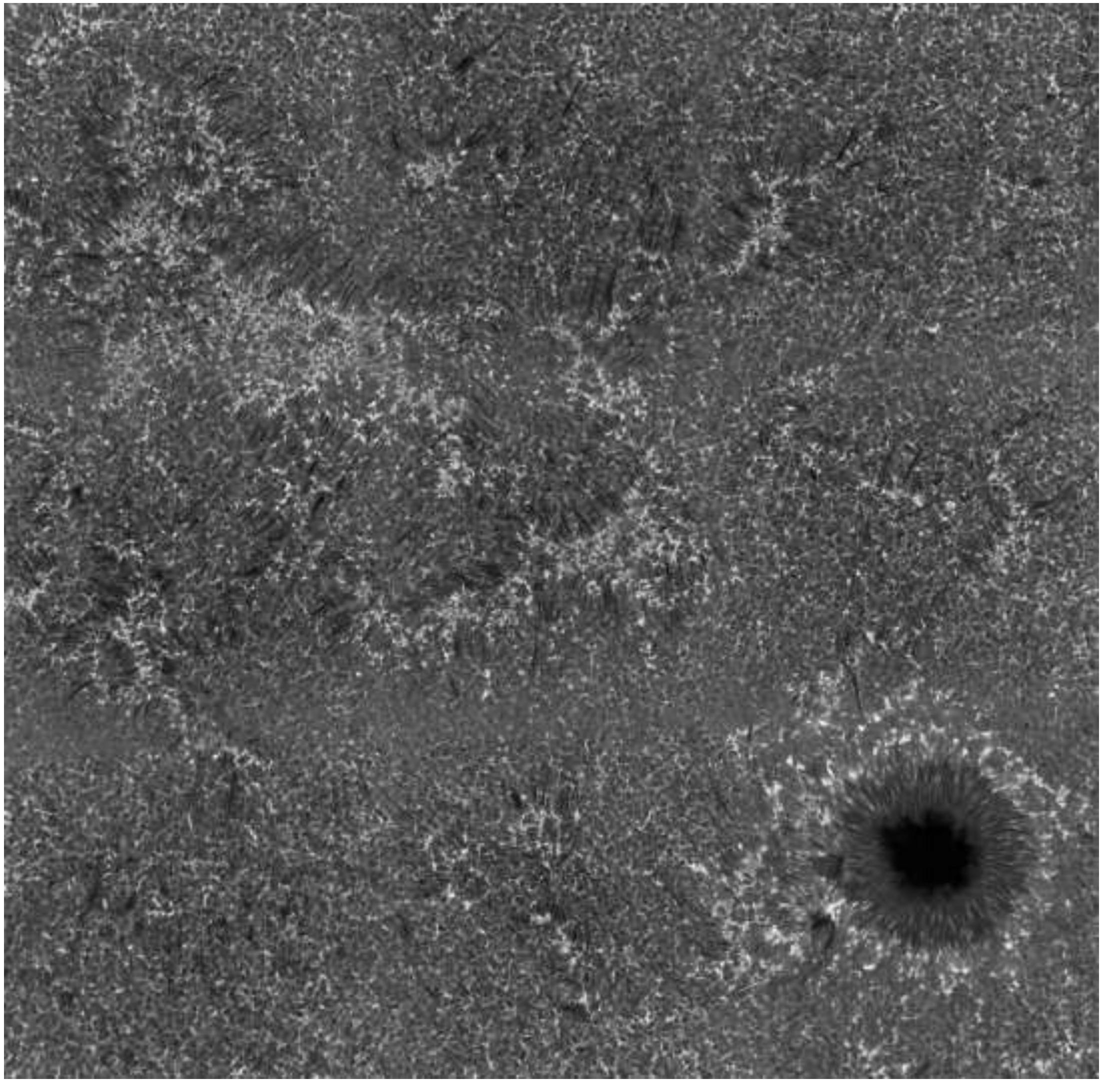

upper
photosphere
+
lower
chromosphere

DST/IBIS

line wing of Ca II 8542 Å

3 August 2010

Multispectral tomography of the solar atmosphere

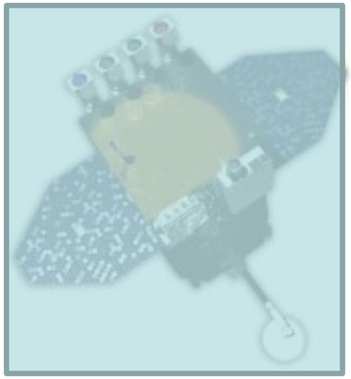

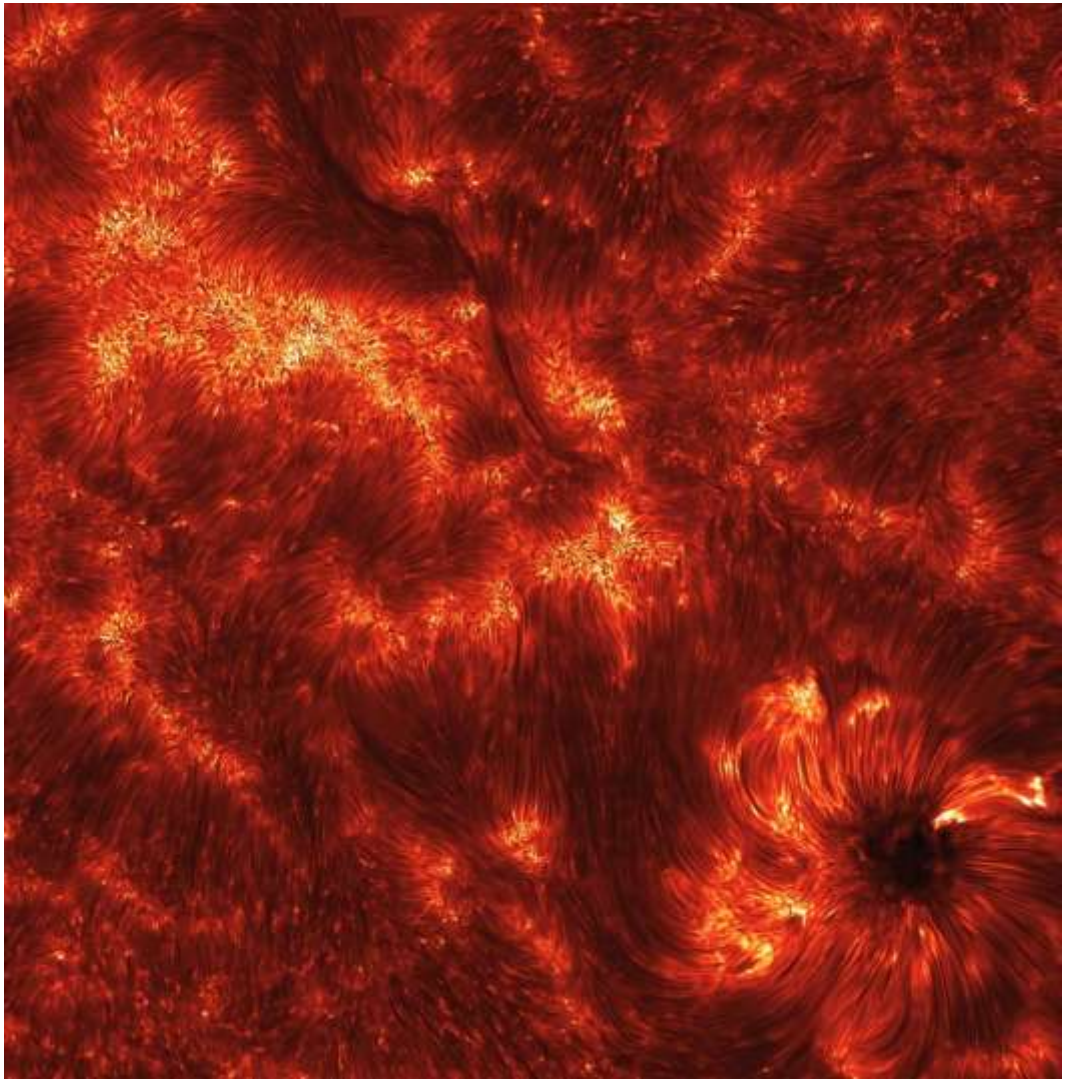

chromosphere

[APOD 2 November 2010]

DST/IBIS

line center of Ca II 8542 Å

3 August 2010

Multispectral tomography of the solar atmosphere

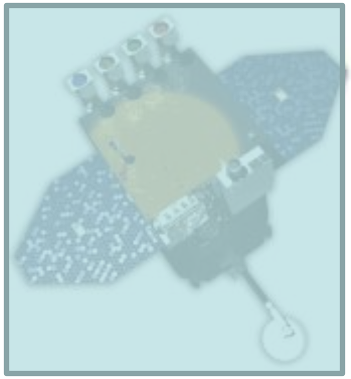

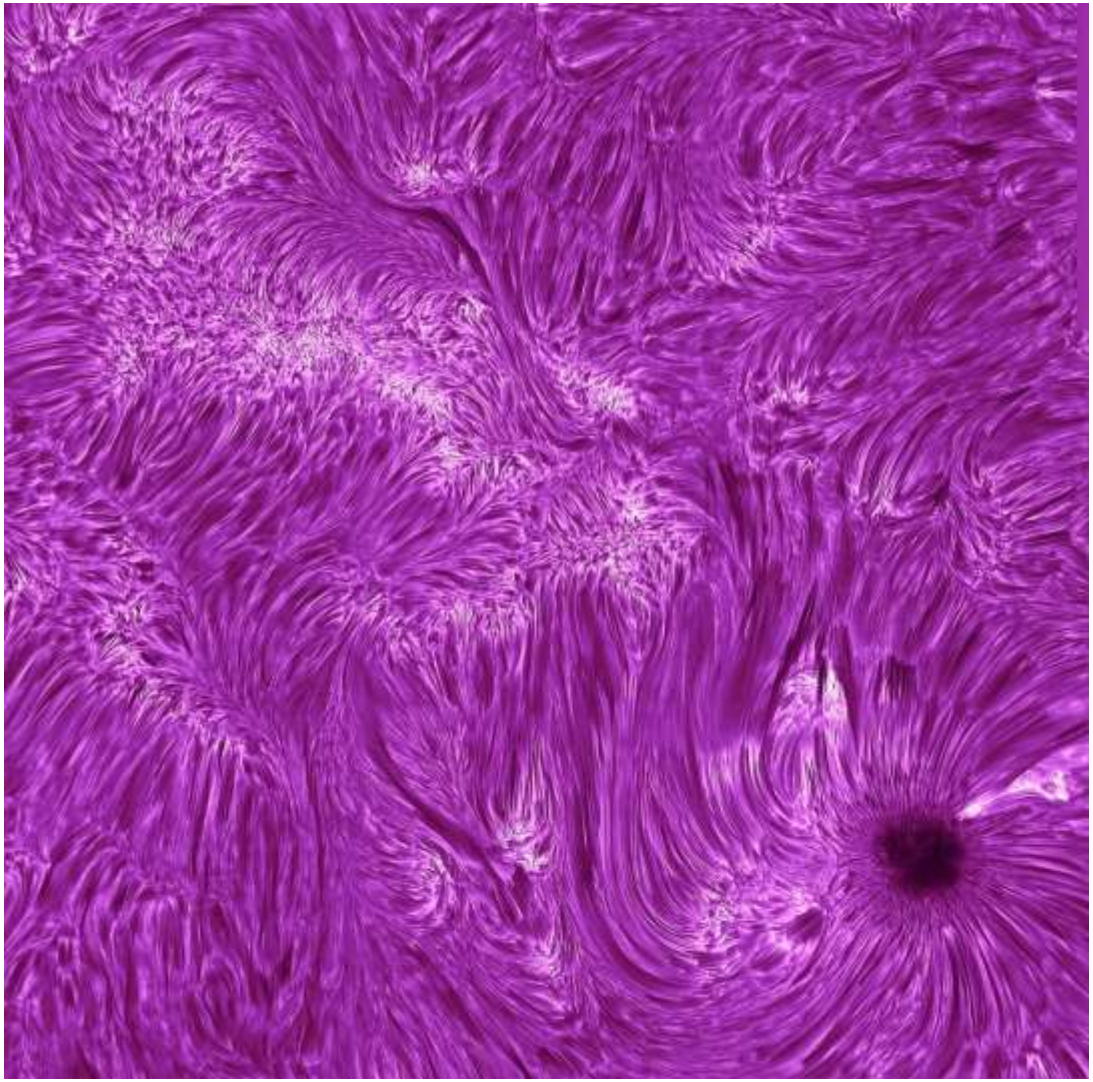

chromosphere

DST/IBIS

line center of Hα 6563 Å

3 August 2010

Multispectral tomography of the solar atmosphere

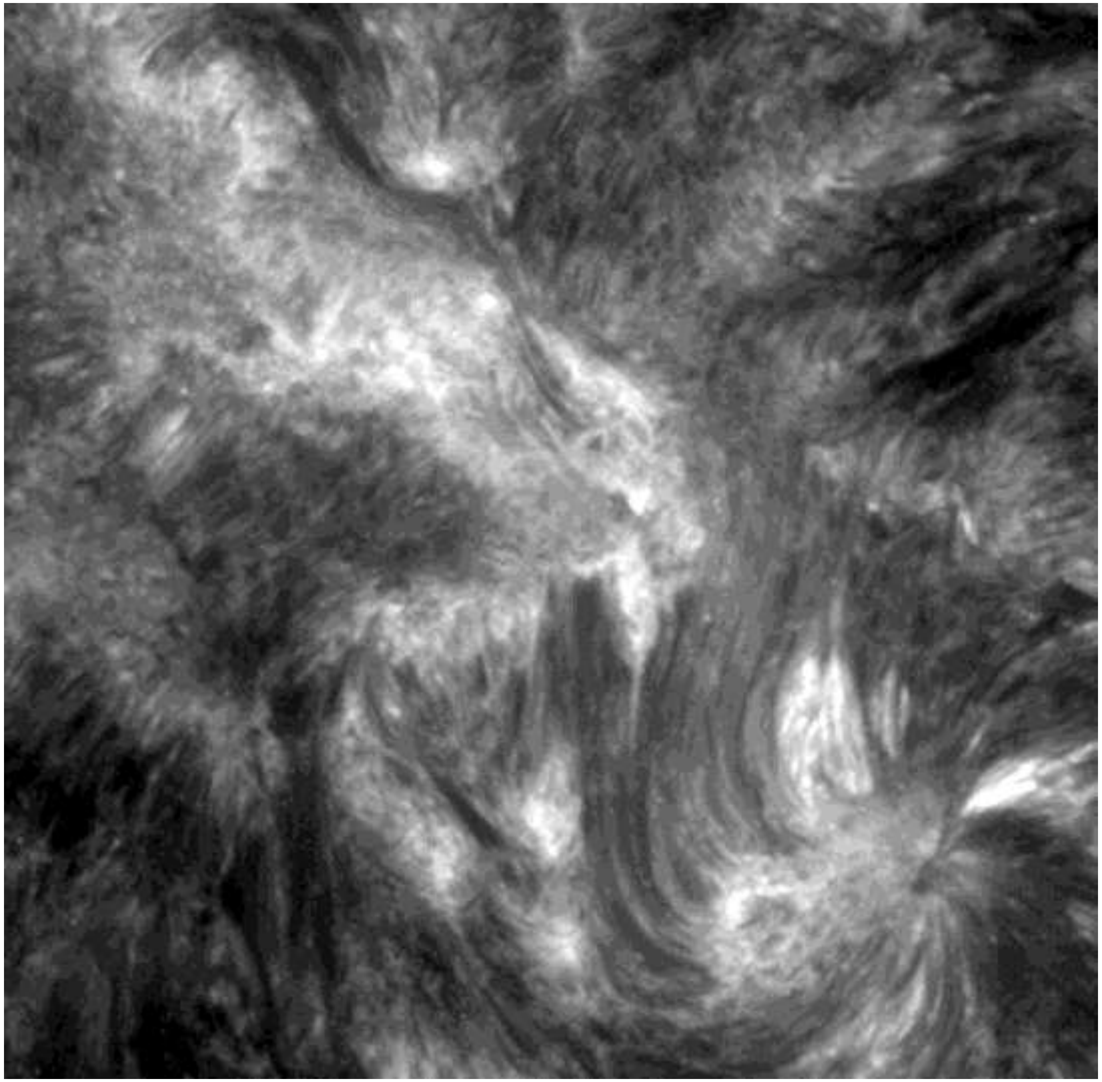

chromosphere
+
transition region

SDO/AIA

He II 304 Å, T = 50 000 K

3 August 2010

Multispectral tomography of the solar atmosphere

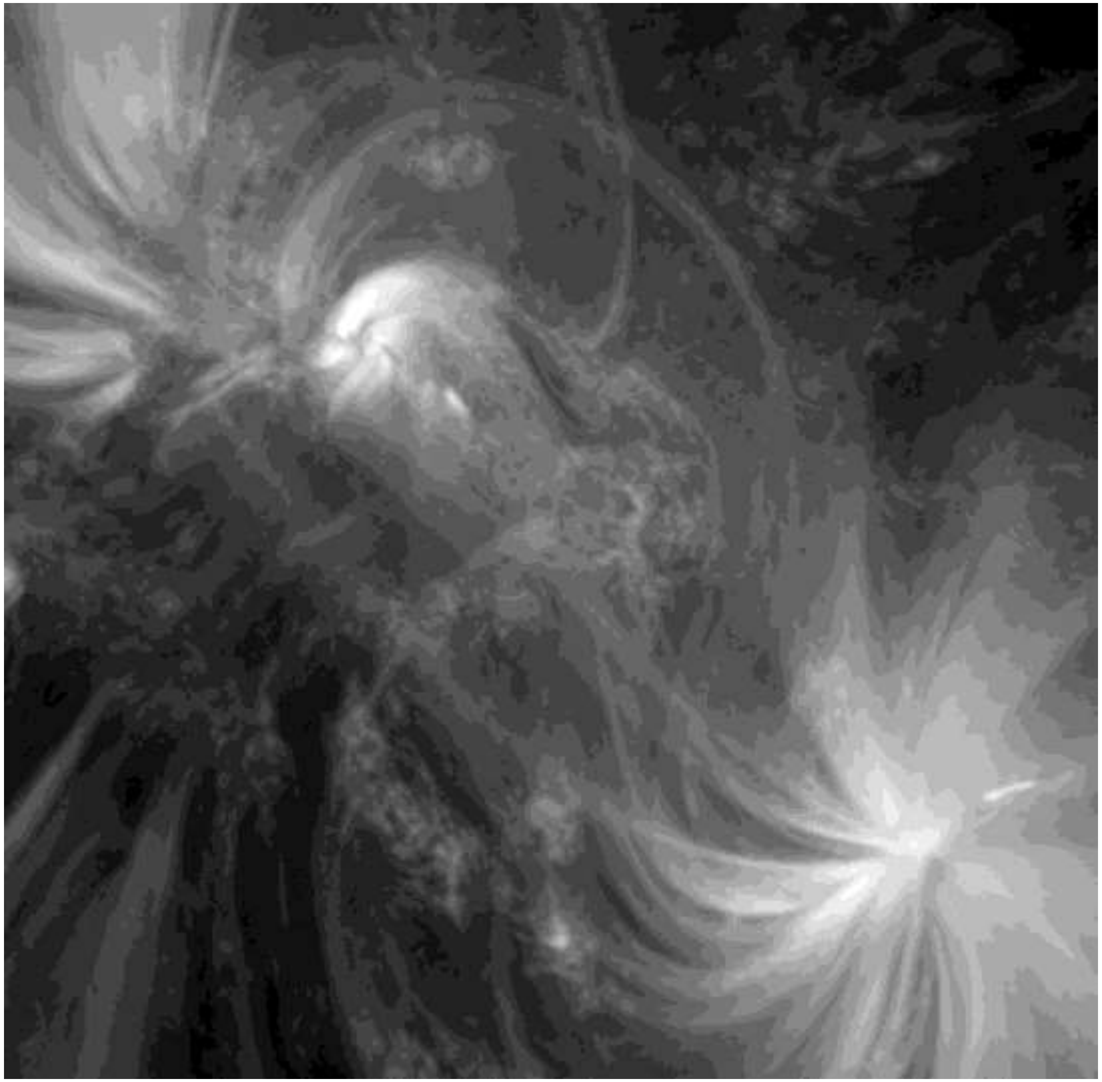

transition region
+
corona

SDO/AIA

Fe IX 171 Å, T = 650 000 K

3 August 2010

Dataspace to live in

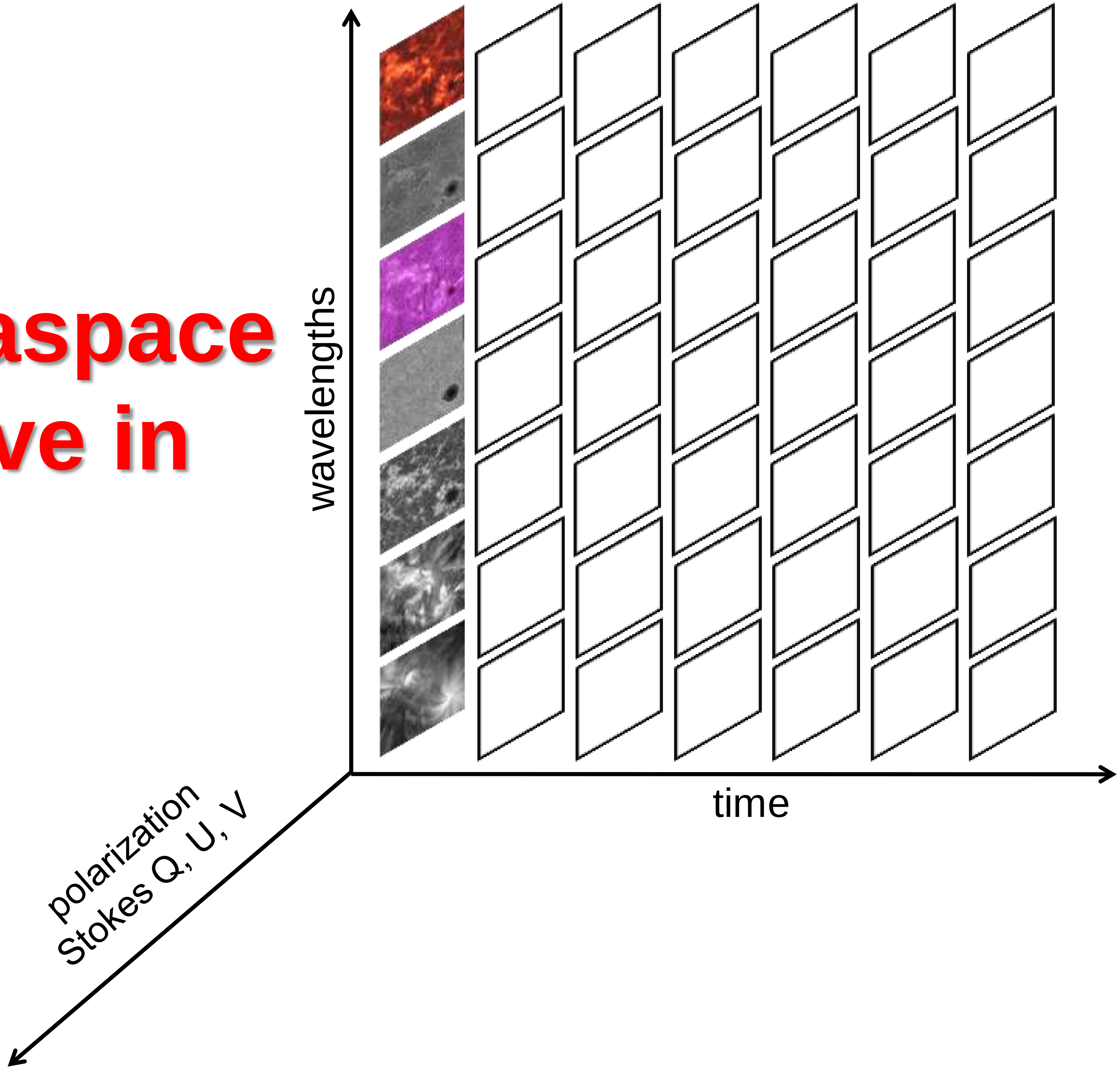

Overview of the talk

1. Observations

a) from the ground
- imaging (SST, DST, DOT)
- spectroscopy (SST)
- spectropolarimetry (VTT)

b) from space
- Hinode

c) simultaneous from the ground and space
- DST + SDO

2. Theory and simulations

- brief hindsight on 1-D simulations
- the latest 2-D simulations
- non-equilibrium time-dependent ionization of hydrogen
- solar atmosphere cartoons

3. The new window into the chromosphere

- Atacama Large Millimeter/submillimeter Array (ALMA)
- simulations of the solar chromosphere at millimeter and submillimeter wavelengths

Equations of 1-D hydrodynamics of spicules

$$\frac{\partial}{\partial t}(\rho A) + \frac{\partial}{\partial z}(\rho v A) = 0 ,$$

$$\frac{\partial}{\partial t}(\rho v A) + \frac{\partial}{\partial z}(\rho v^2 A) = -\rho g A - A\frac{\partial p}{\partial z} + F\rho A h(z,t) ,$$

$$\frac{\partial E}{\partial t} + \frac{1}{A}\frac{\partial}{\partial z}\left[(E+P)vA - \kappa A\frac{\partial T}{\partial z}\right] = -\rho v g - L + S + Eh(z,t)$$

$$E = \frac{1}{2}\rho v^2 + \frac{p}{\gamma - 1} .$$

Sterling (2000)

Numerical spicule models

- strong pulse in the lower atmosphere (the photosphere or low chromosphere)
- weak pulse in the lower atmosphere (rebound shock model)
- pressure-pulse in the middle or upper chromosphere
- Alfén wave models

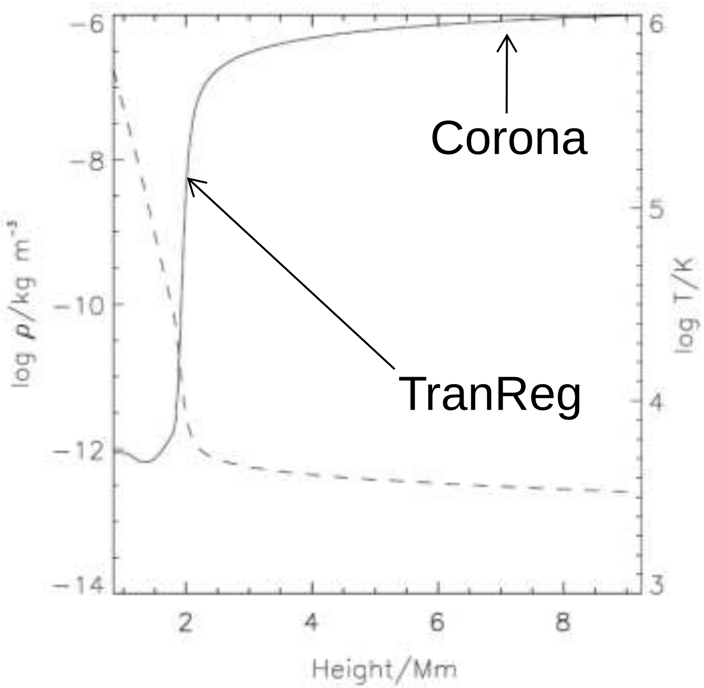

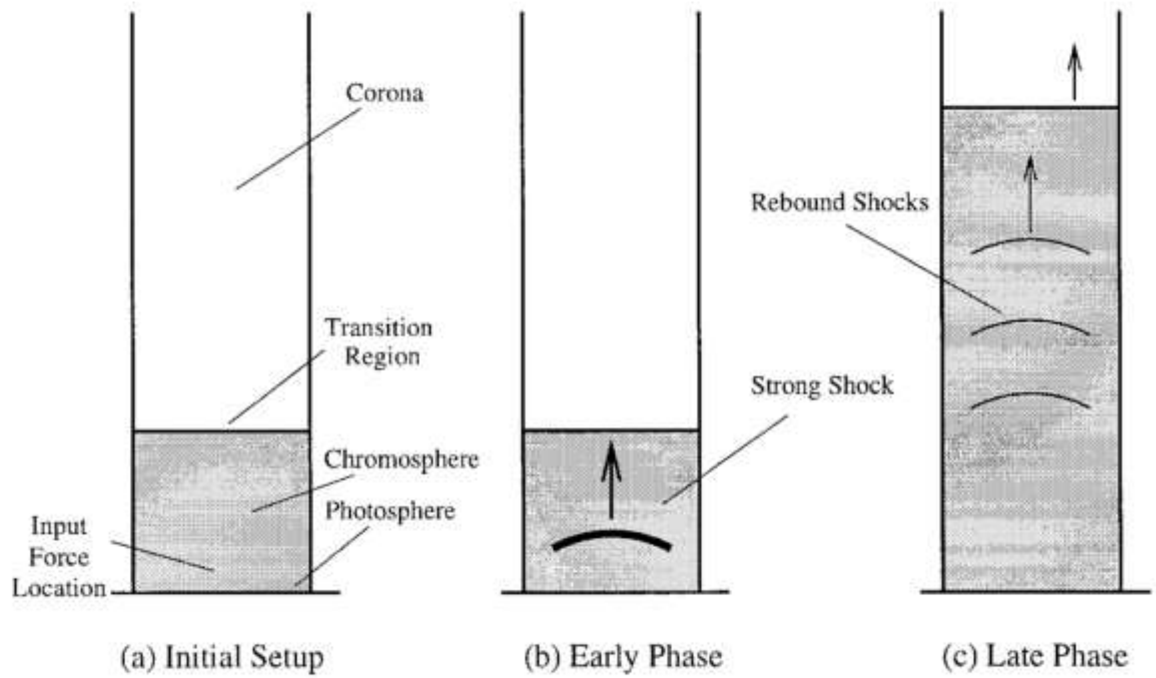

——— initial temperature at t = 0

- - - - - - initial density at t = 0

A model spicule produced by a pressure pulse in the low chromosphere

Sterling (2000)

Numerical hydrodynamics of spicules

Temperature

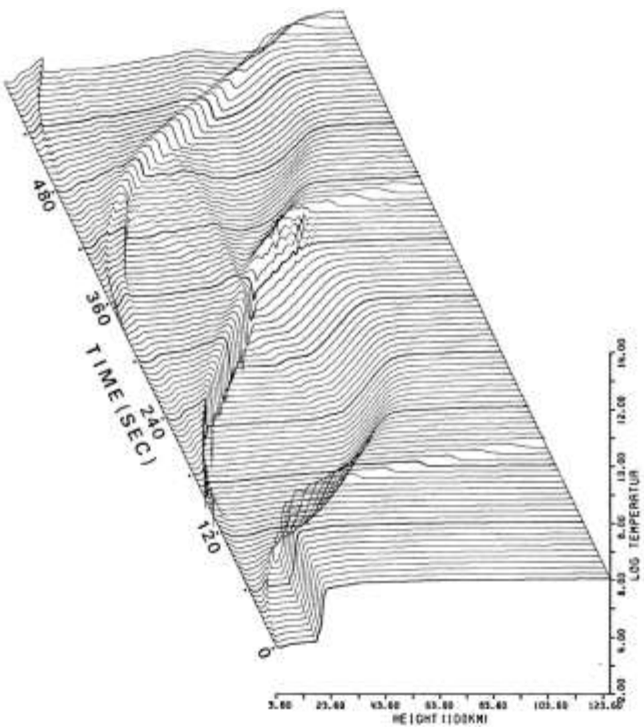

Density

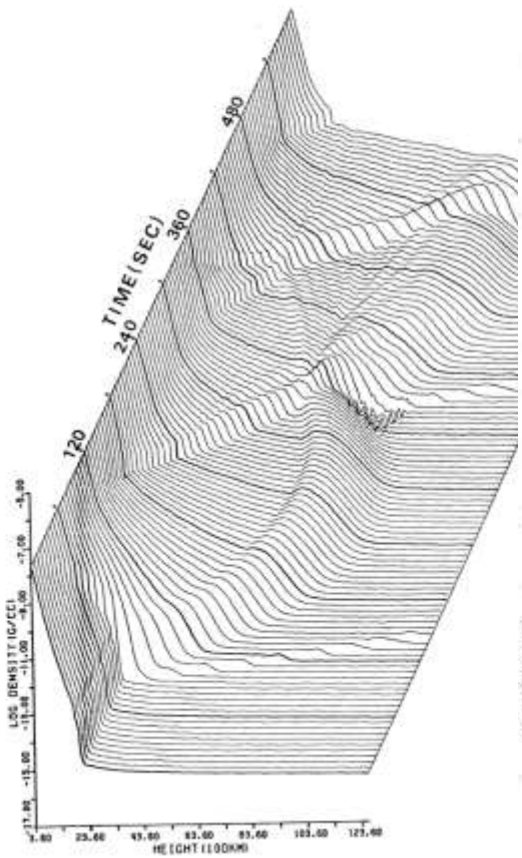

Velocity

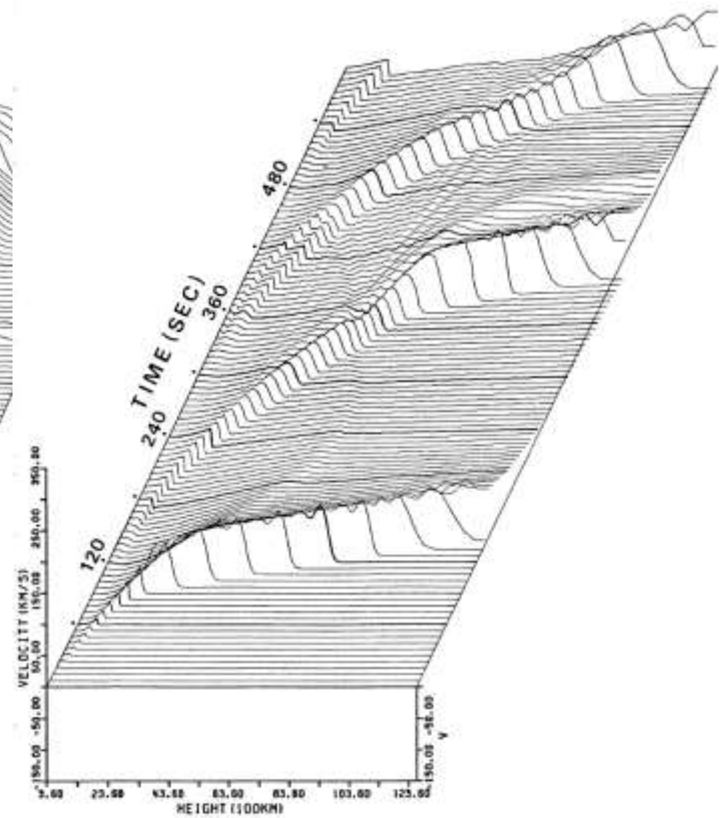

Suematsu et al. 1982: SolPhys, 75, 99.

Numerical hydrodynamics of spicules

Temperature

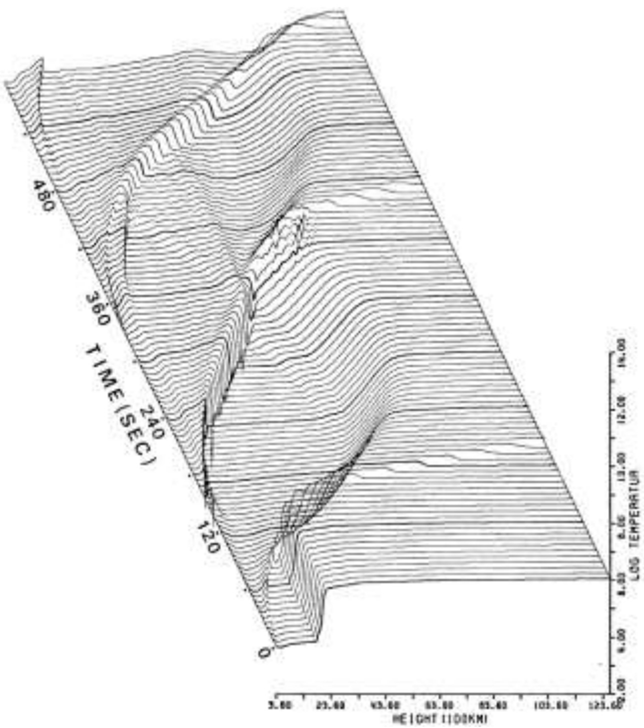

Density

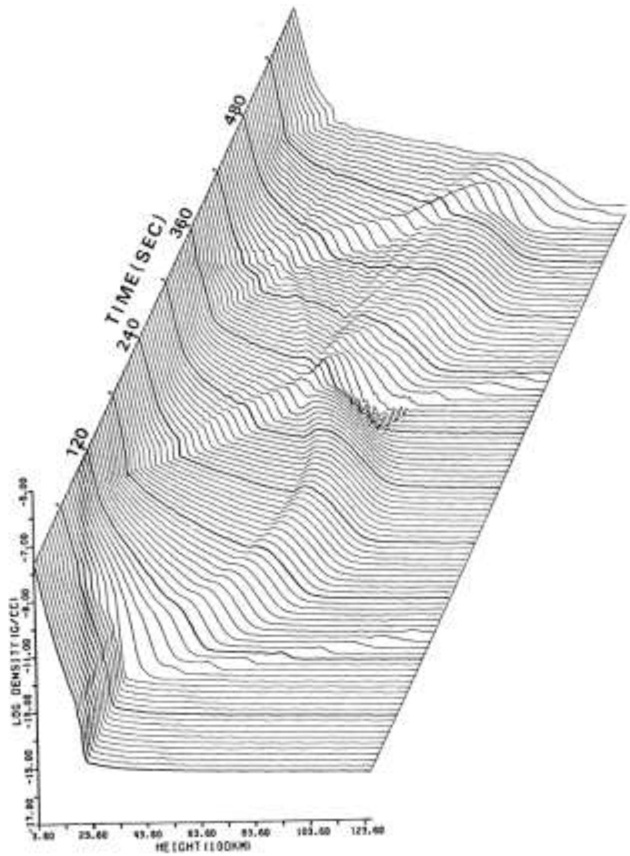

Main results:

- the shock is strong enough to uplift theTransReg – Corona interface
- the matter following behind the interface is identified as a spicule
- the model explains the generation, height and density of spicules

Suematsu et al. (1982)

Alfvén wave model of spicules and coronal heating

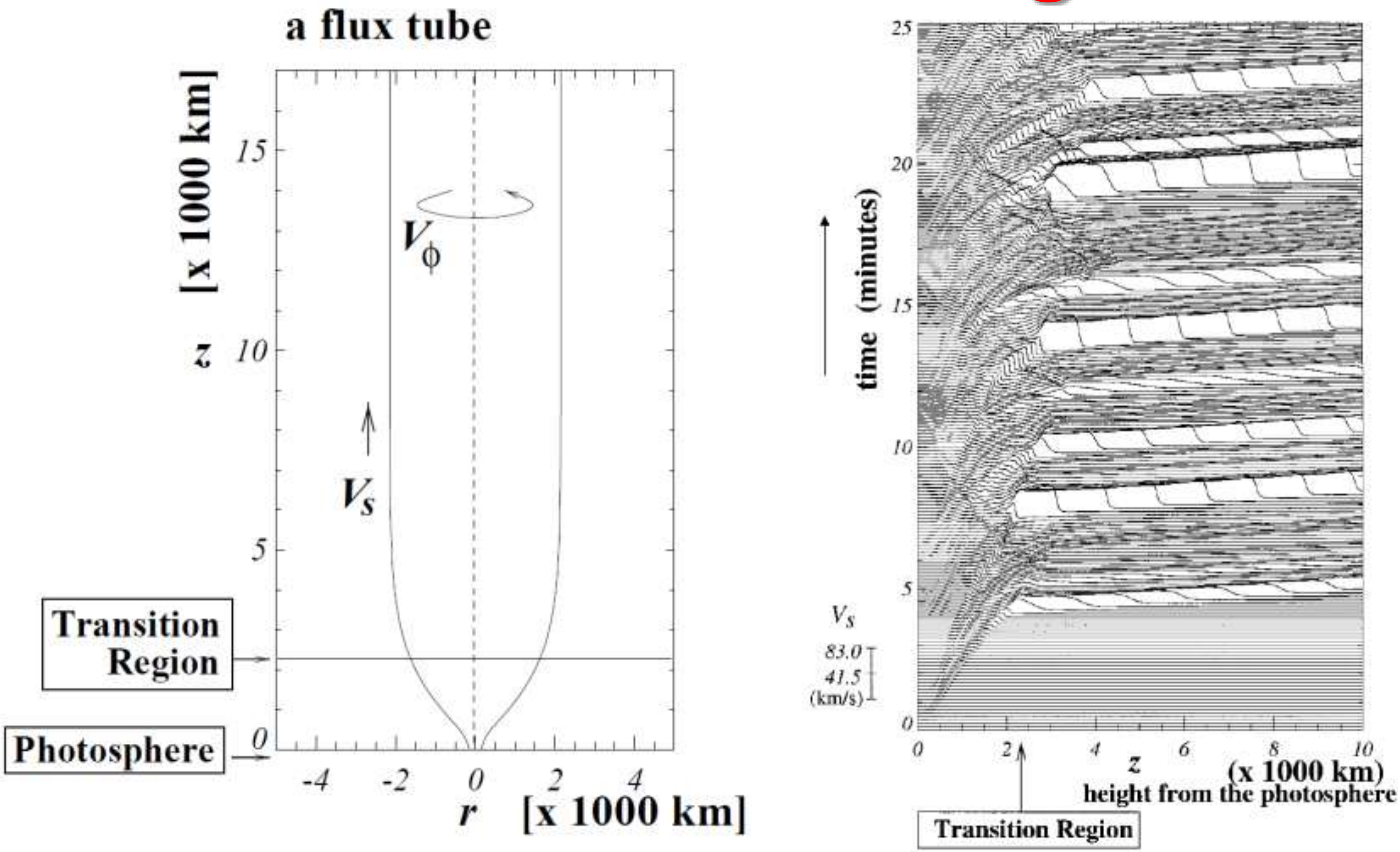

Kudoh & Shibata (1999)

Alfvén wave model of spicules and coronal heating

Density

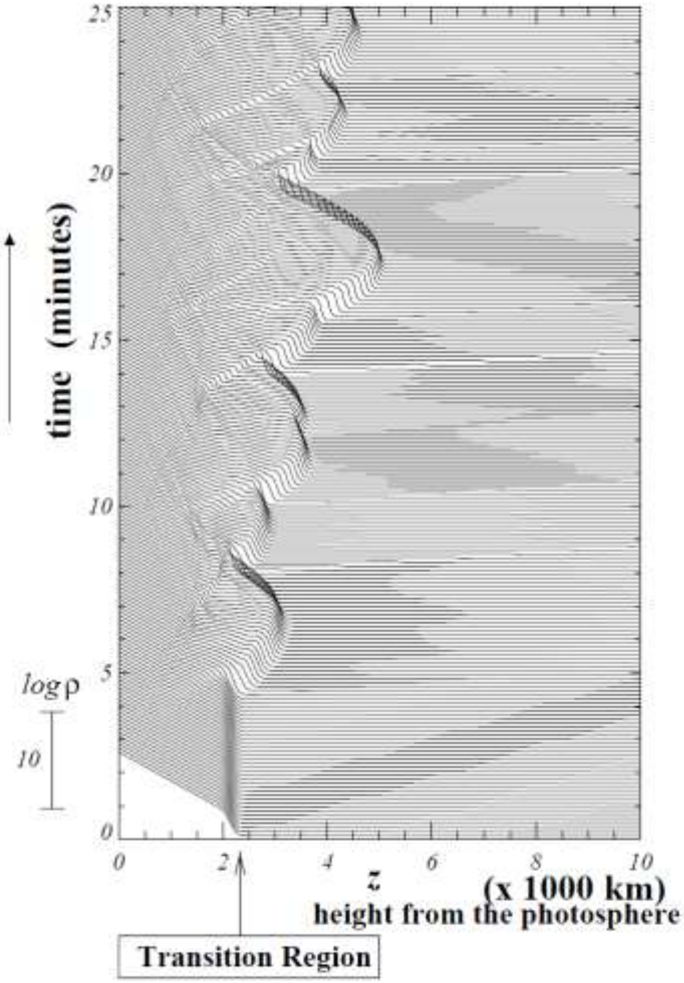

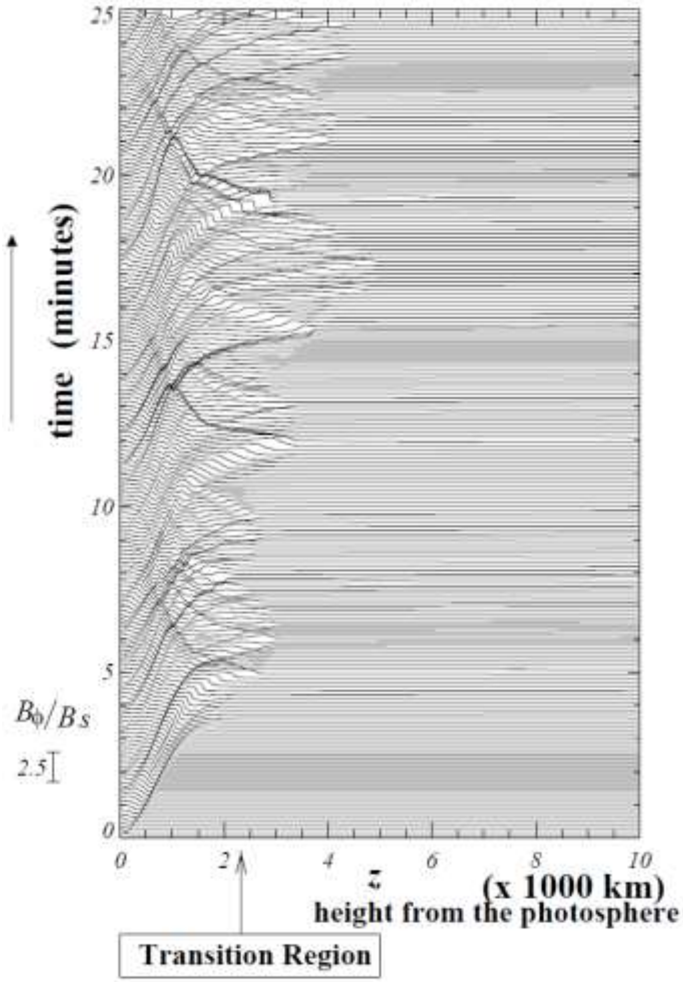

$$\frac{B_\phi}{B_S}$$

Kudoh & Shibata (1999)

Alfvén wave model of spicules and coronal heating

Density

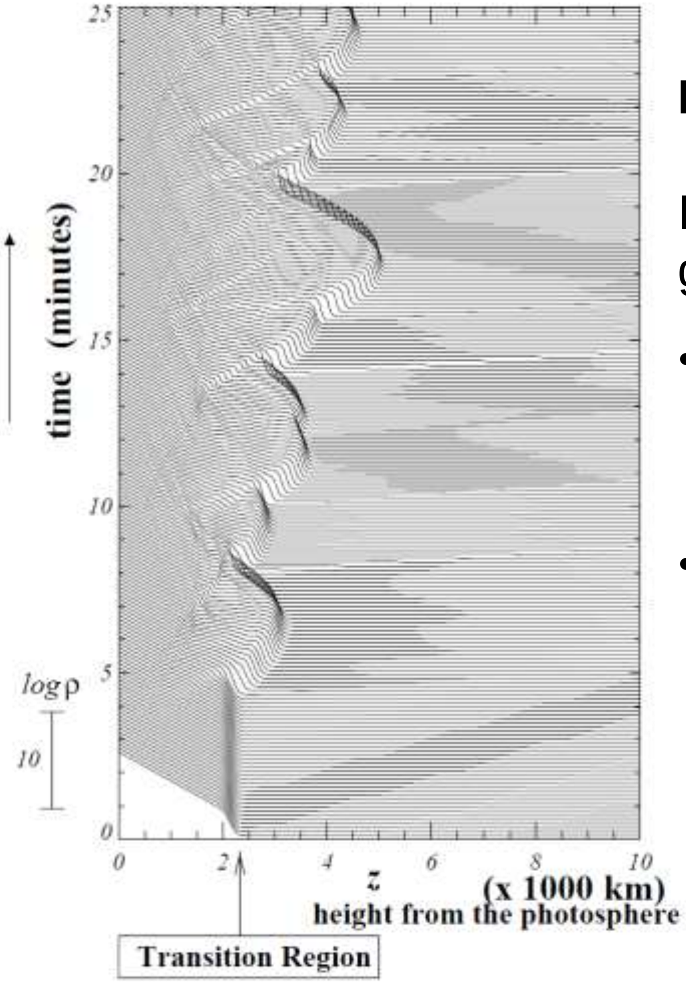

Main results:

If the root mean square of the perturbation is greater than 1 km s^{-1} in the photosphere:

- the transition region is lifted up to more than 5000 km (i.e., the spicule is produced),
- the energy flux enough for heating the quiet corona (3×10^{-5} ergs s^{-1} cm^{-2}) is transported into the corona

Kudoh and Shibata 1999: ApJ, 514, 493.

N-shaped magnetoacoustic shocks

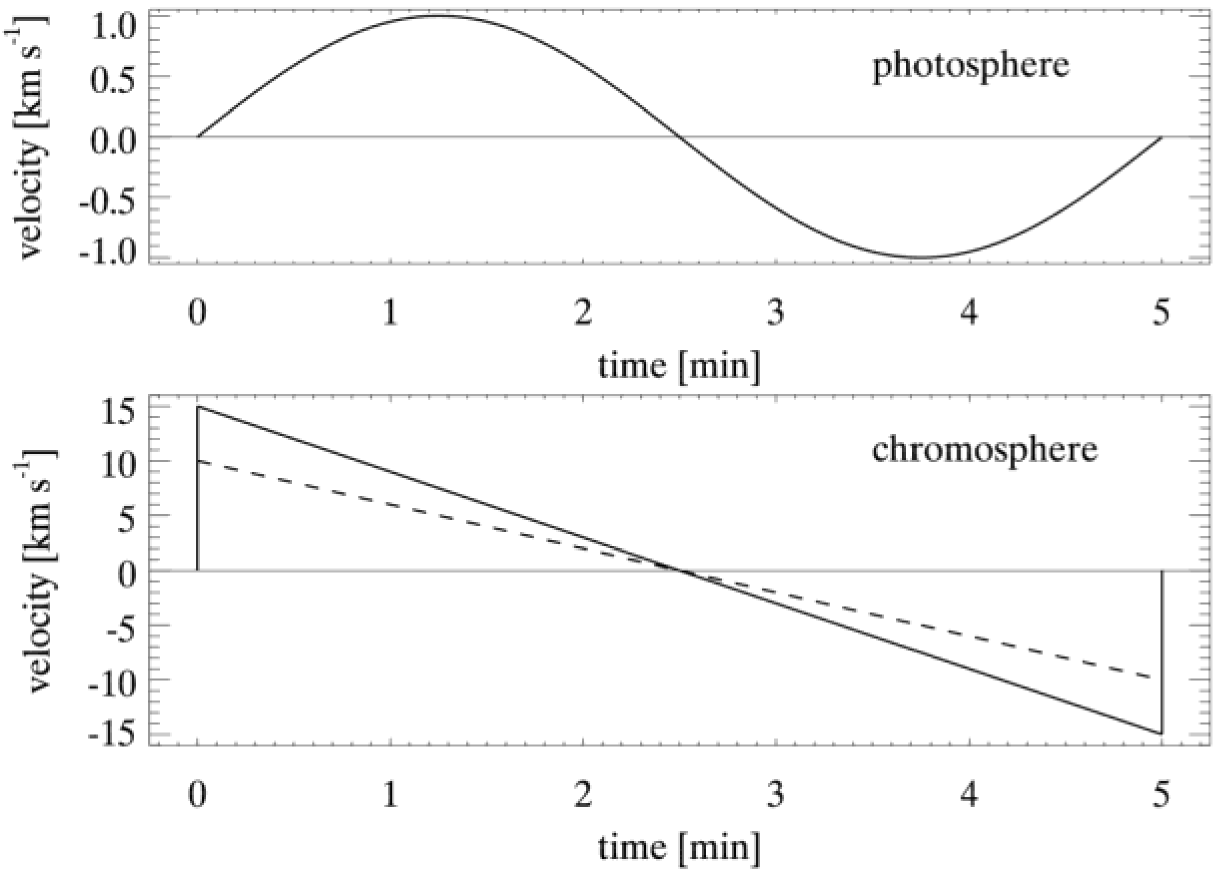

$$P_{\mathrm{ac}} = \frac{4\pi}{g\cos\theta}\sqrt{\frac{RT}{\gamma\mu}}$$

$$E_{kin} = \frac{1}{2}\rho v^2 = const.$$

$$v = v_{\mathrm{max}} - at$$

$$y = y_0 + v_{\mathrm{max}}t - \frac{a}{2}t^2$$

$$v_{\mathrm{max}} = \frac{P}{2}a$$

Reduction of the effective gravity along tilted magnetic channels:

⇨ lowering of cutoff frequency

⇨ propagation of p-modes into the chromosphere as N-shaped shocks

⇨ repetitive lift of chromospheric-transition region interface

Dynamic fibrils in Hα

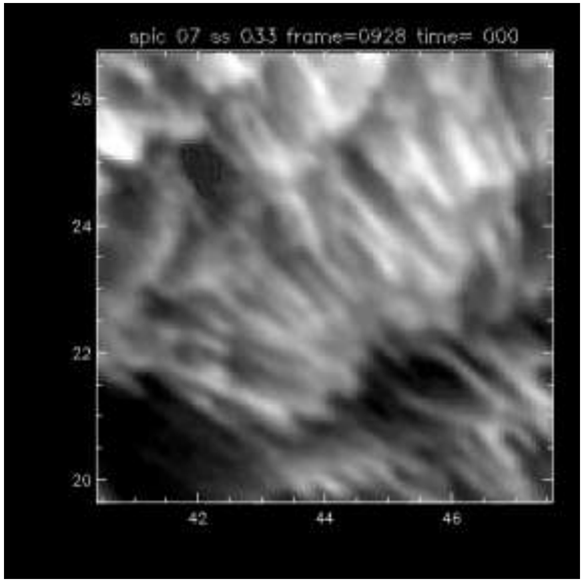

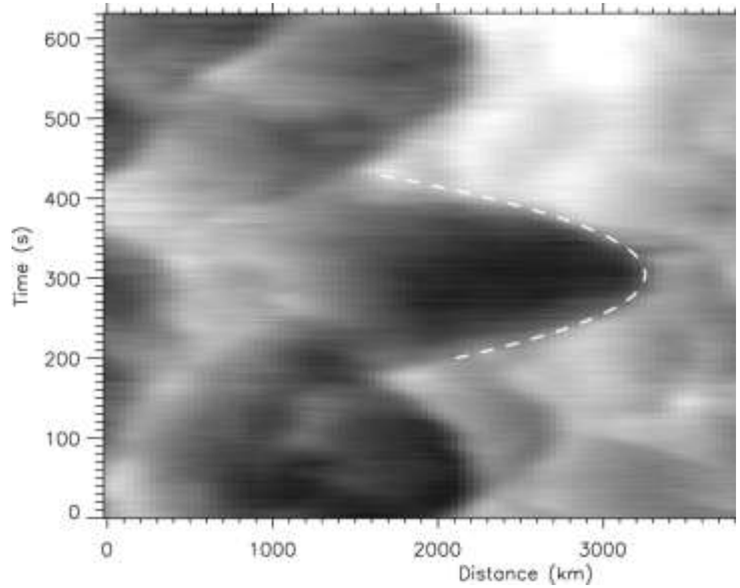

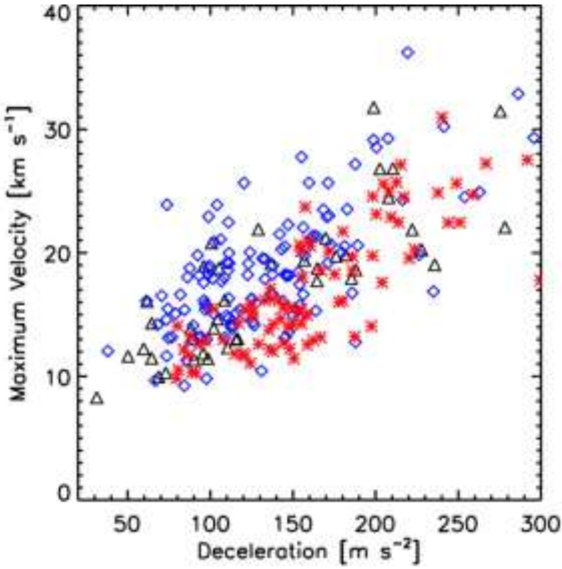

Hansteen et al. (2006)

De Pontieu et al. (2007)

Main results:

- confirmed extensions and retractions
- confirmed parabolic top trajectories
- linear relationship between maximum velocity and deceleration
- Hα dynamic fibrils in a plage co-spatial with areas of increased power of 5-min oscillations
- field-aligned magnetoacoustic shock excitation

Numerical 1-D simulations of shock wave-driven chromospheric jets

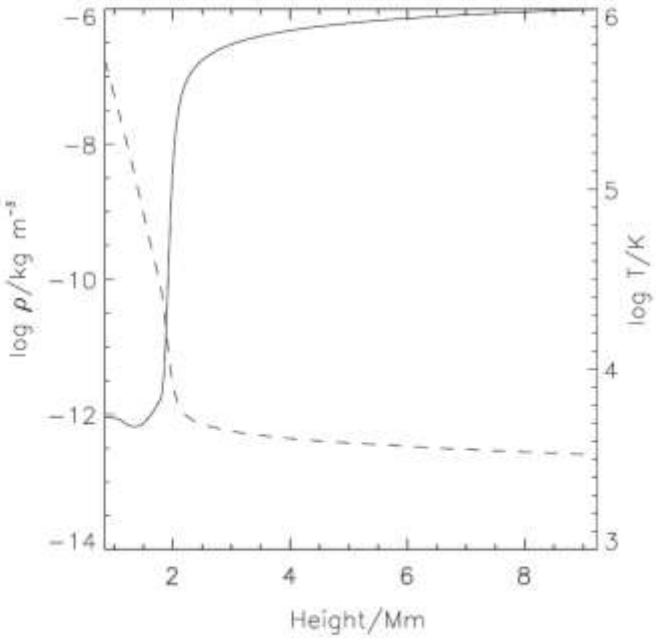

FIG. 1.—Initial density (*dashed line, left axis*) and temperature (*solid line, right axis*) structure of the model.

$$\frac{\partial \varrho}{\partial t} + \nabla \cdot (\varrho \boldsymbol{v}) = 0,$$

$$\frac{\partial \varrho \boldsymbol{v}}{\partial t} + \nabla \cdot \left[\varrho \boldsymbol{v} \otimes \boldsymbol{v} + p_{\rm tot} \underline{\underline{1}} - \frac{\boldsymbol{B} \otimes \boldsymbol{B}}{4\pi} \right] = \varrho \boldsymbol{g} + \nabla \cdot \underline{\underline{\tau}},$$

$$\frac{\partial e}{\partial t} + \nabla \cdot \left[\boldsymbol{v}(e + p_{\rm tot}) - \frac{1}{4\pi} \boldsymbol{B}(\boldsymbol{v} \cdot \boldsymbol{B}) \right] = \varrho(\boldsymbol{g} \cdot \boldsymbol{v})$$

$$+ Q_{\rm rad} + \frac{1}{4\pi} \nabla \cdot (\boldsymbol{B} \times \eta \nabla \times \boldsymbol{B}) + \nabla \cdot (\boldsymbol{v} \cdot \underline{\underline{\tau}}) + \nabla \cdot (K \nabla T)$$

$$\frac{\partial \boldsymbol{B}}{\partial t} + \nabla \cdot [\boldsymbol{v} \otimes \boldsymbol{B} - \boldsymbol{B} \otimes \boldsymbol{v}] = -\nabla \times (\eta \nabla \times \boldsymbol{B}),$$

- 1-D magnetohydrodynamics (MHD) simulations
- choosen magnetic field strength: 60 G (6×10^{-3} T)
- choosen field inclinations: 0°, 30°, 45°, 60°
- choosen piston periods: 180 s, 240 s, 300 s, 360 s
- choosen initial amplitudes: 200 ms^{-1}, 500 ms^{-1}, 800 ms^{-1}, 1100 ms^{-1}

Heggland et al. (2007)

Numerical simulations of shock wave-driven chromospheric jets

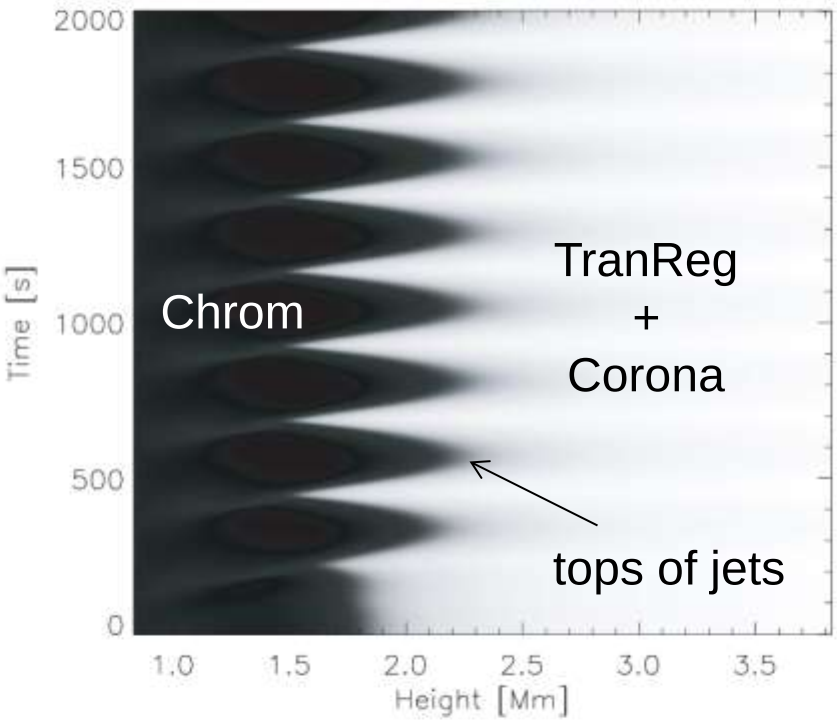

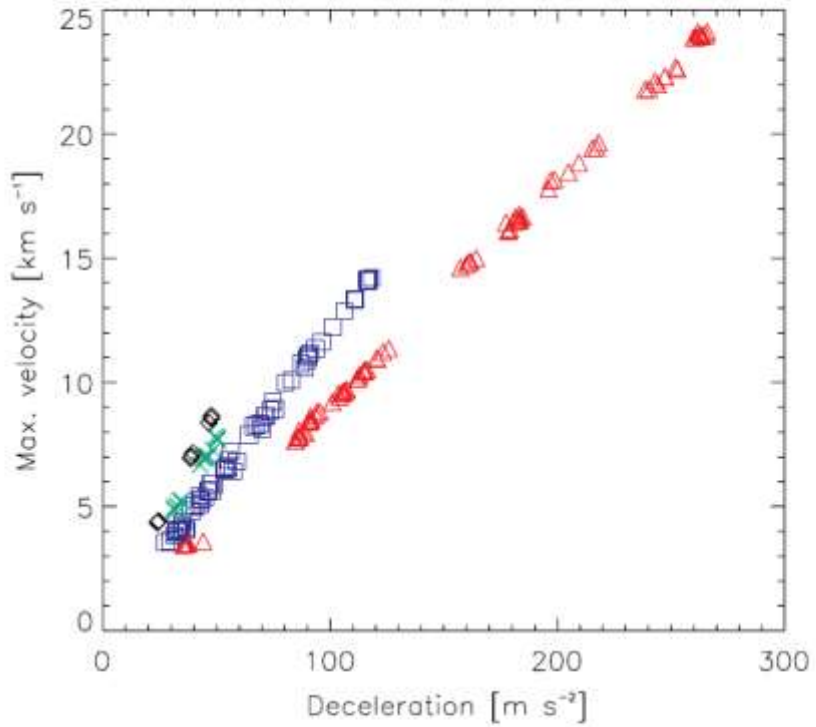

Main results reproduce:

- parabolic shapes of Chrom – TranReg interface
- the range of observed decelerations and roughly max. velocities

This gives strong support that fibrils are driven by magnetoacoustic shocks.

Heggland et al. (2007)

Numerical 2-D MHD simulations of dynamic fibrils

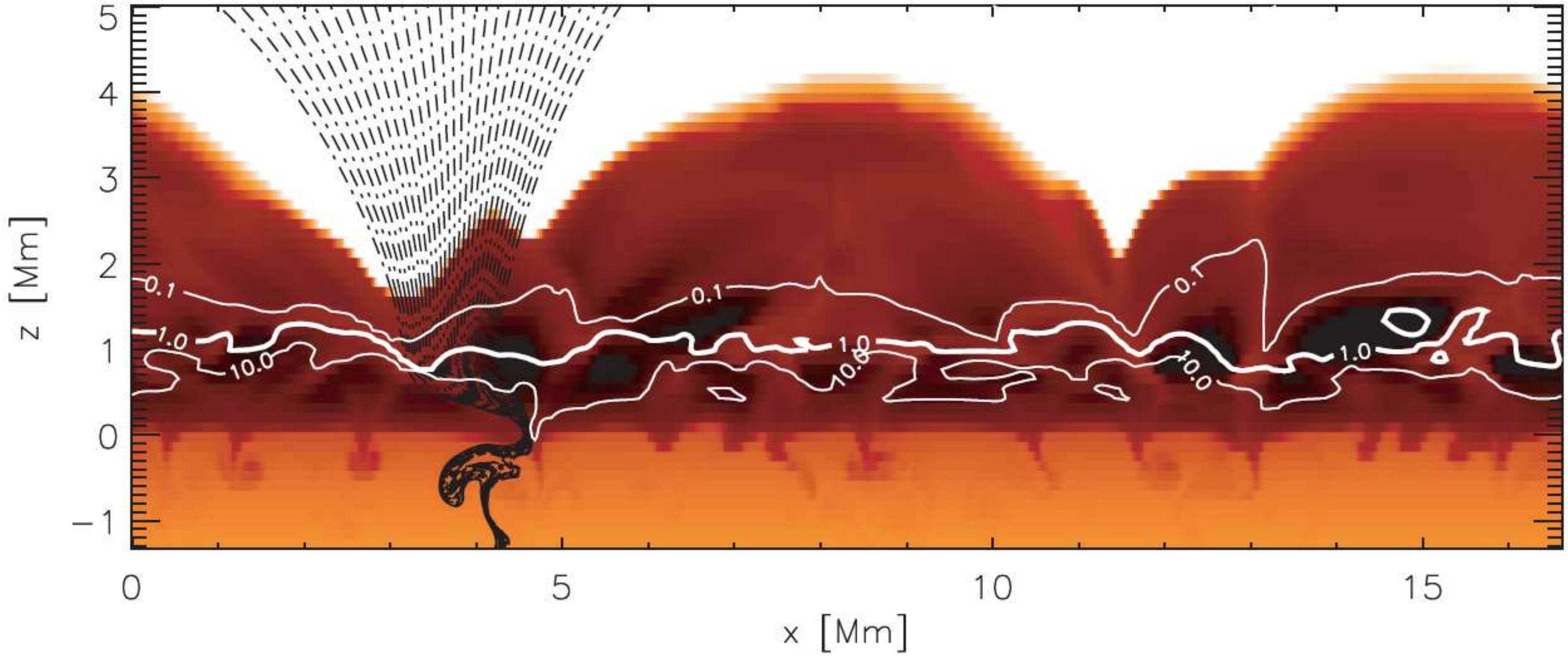

FIG. 15.—Snapshot taken from one of the 2D numerical experiments simulating the generation of a DF. The logarithm of the temperature, T_g, is shown, set to saturate at log $T_g = 4.5$; the minimum temperature is roughly 2000 K (log $T_g = 3.3$). The vertical scale has its origin at the height where $\tau_{500} = 1$. Contours of plasma β are drawn in white where $\beta = 0.1$, 1, and 10, with the $\beta = 1$ contour thicker for clarity. In black are drawn magnetic field lines covering the region where DFs ascend as a result of upwardly propagating shock waves. We find events that resemble observed DFs in this region, as well as in the corresponding opposite polarity region centered on $x = 12$ Mm. Note the highly intermittent nature of the chromospheric temperature structure and the ubiquity of shocks outlined by regions of high T_g. These shock waves seem to preferentially enter the corona where the magnetic field lines also enter the corona. The position of the transition region does not change much in the regions between $x = 5$ and 12 Mm, where the field is more horizontal. [*This figure is available as an mpeg animation in the electronic edition of the Journal.*]

De Pontieu et al. (2007)

Numerical 2-D MHD simulations of dynamic fibrils

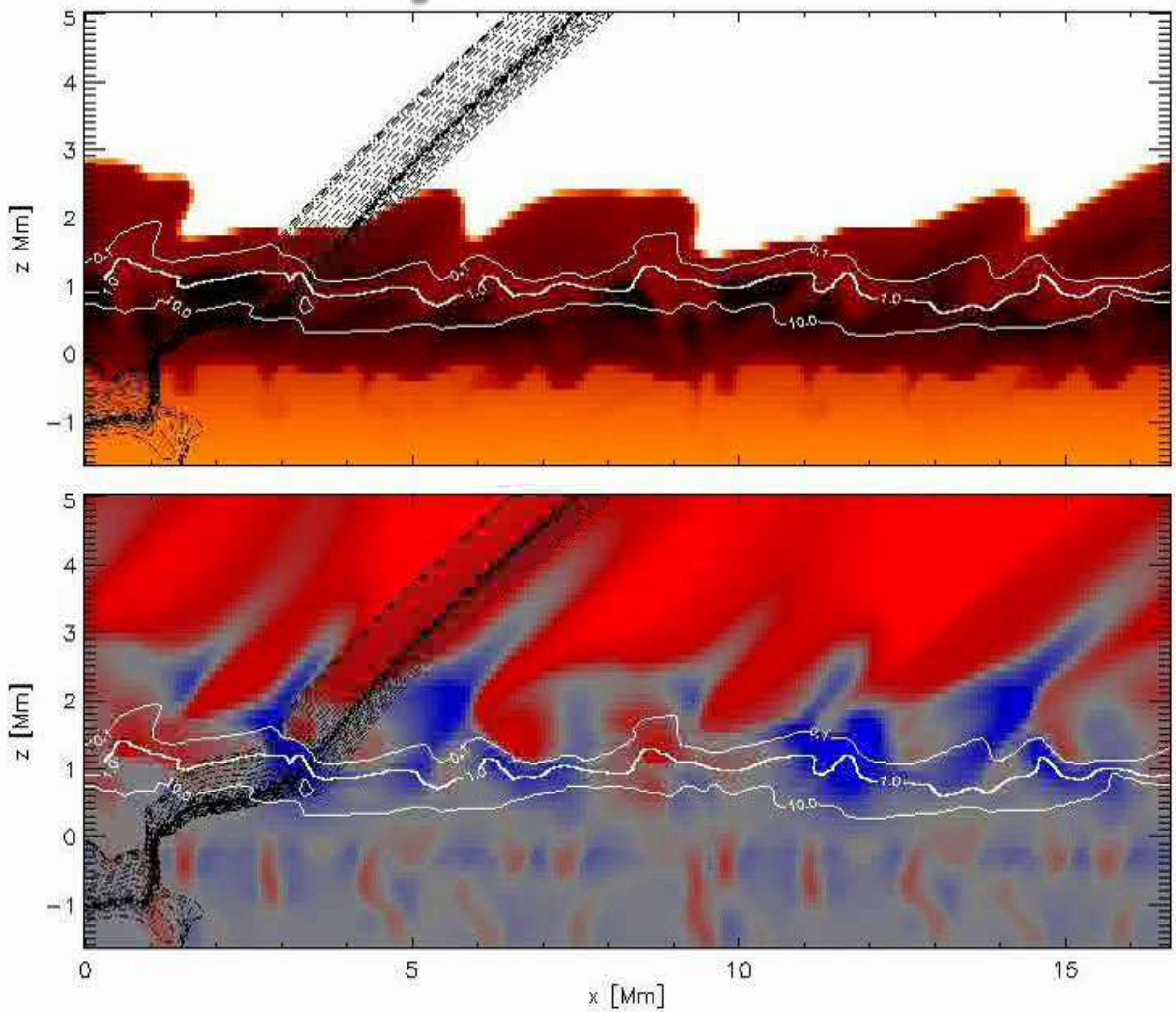

De Pontieu et al. (2007)

Time-slice plot of temperature within dynamic fibril at x = 4 Mm

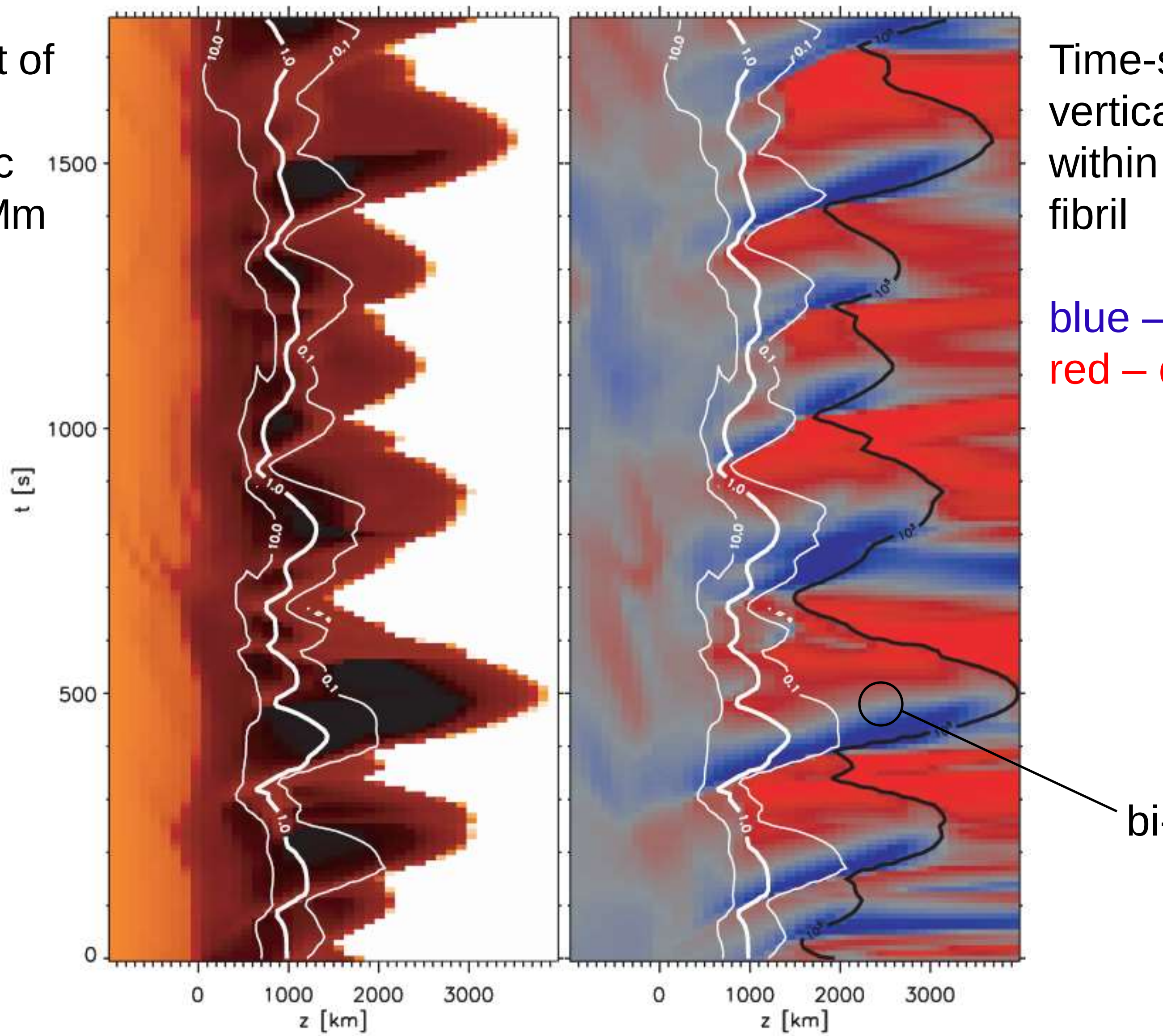

Time-slice plot of vertical velocity within dynamic fibril

blue – upflow
red – downflow

De Pontieu et al. (2007)

Numerical 2-D MHD simulations of dynamic fibrils

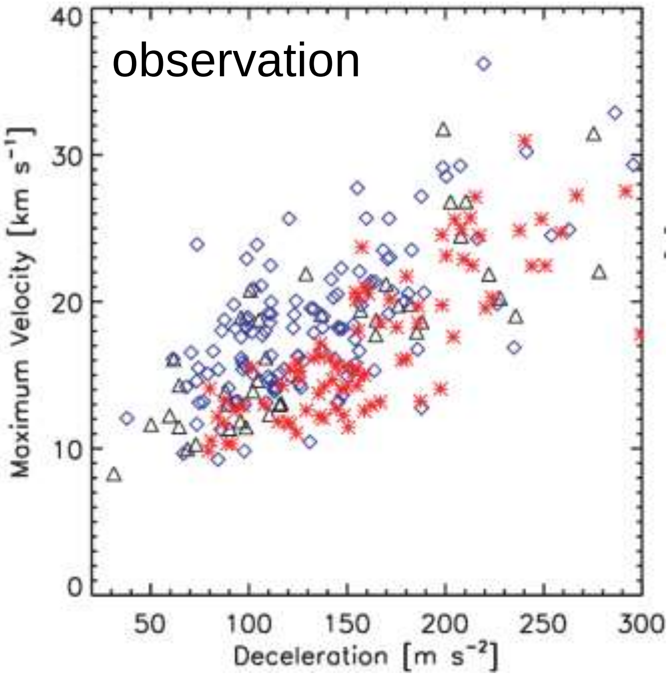

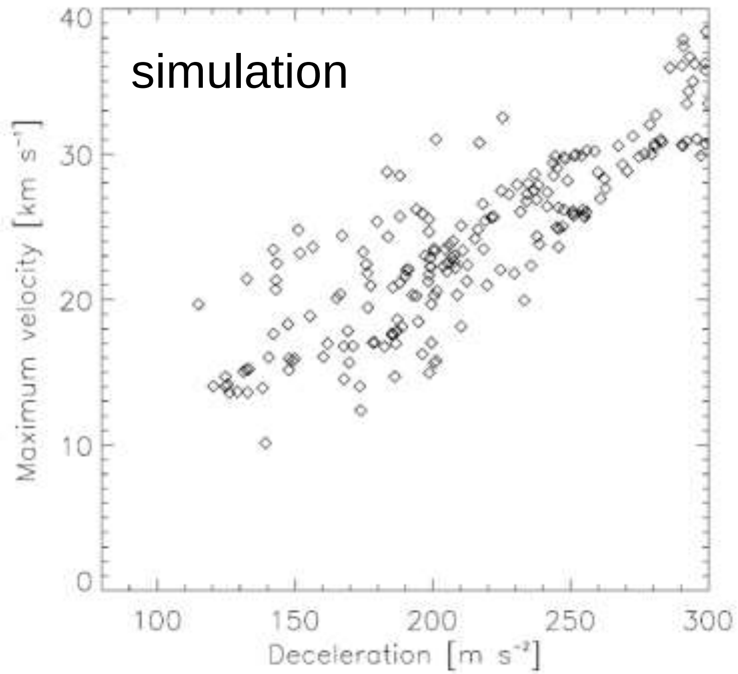

Main results:

- striking similarities of observed and simulated values for deceleration, maximum velocity, maximum length, and duration of dynamic fibrils
- this strongly suggests that dynamic fibrils are formed by upwardly propagating waves generated in the photosphere as a result of p-mode oscillations

De Pontieu et al. (2007)

Non-equilibrium hydrogen ionization in MHD simulations of the solar atmosphere

$$\frac{\partial \varrho}{\partial t} + \nabla \cdot (\varrho \boldsymbol{v}) = 0,$$

$$\frac{\partial \varrho \boldsymbol{v}}{\partial t} + \nabla \cdot \left[\varrho \boldsymbol{v} \otimes \boldsymbol{v} + p_{\text{tot}} \underline{\underline{1}} - \frac{\boldsymbol{B} \otimes \boldsymbol{B}}{4\pi} \right] = \varrho \boldsymbol{g} + \nabla \cdot \underline{\underline{\tau}},$$

$$\frac{\partial e}{\partial t} + \nabla \cdot \left[\boldsymbol{v}(e + p_{\text{tot}}) - \frac{1}{4\pi} \boldsymbol{B}(\boldsymbol{v} \cdot \boldsymbol{B}) \right] = \varrho (\boldsymbol{g} \cdot \boldsymbol{v})$$

$$+ Q_{\text{rad}} + \frac{1}{4\pi} \nabla \cdot (\boldsymbol{B} \times \eta \nabla \times \boldsymbol{B}) + \nabla \cdot (\boldsymbol{v} \cdot \underline{\underline{\tau}}) + \nabla \cdot (K \nabla T)$$

$$\frac{\partial \boldsymbol{B}}{\partial t} + \nabla \cdot [\boldsymbol{v} \otimes \boldsymbol{B} - \boldsymbol{B} \otimes \boldsymbol{v}] = -\nabla \times (\eta \nabla \times \boldsymbol{B}),$$

Radiative heating/cooling:

$$Q_{\text{rad}} = 4\pi \varrho \int_{\nu} \kappa_{\nu} (J_{\nu} - B_{\nu}) \, \mathrm{d}\nu.$$

$$\frac{\partial n_i}{\partial t} + \nabla \cdot (n_i \boldsymbol{v}) = \sum_{j, j \neq i}^{n_l} n_j P_{ji} - n_i \sum_{j, j \neq i}^{n_l} P_{ij}$$

+ equation of chemical equilibrium

+ equations of charge, internal energy, and particle (hydrogen nucleus) conservation

Why non-equilibrium time-dependent hydrogen ionization ?

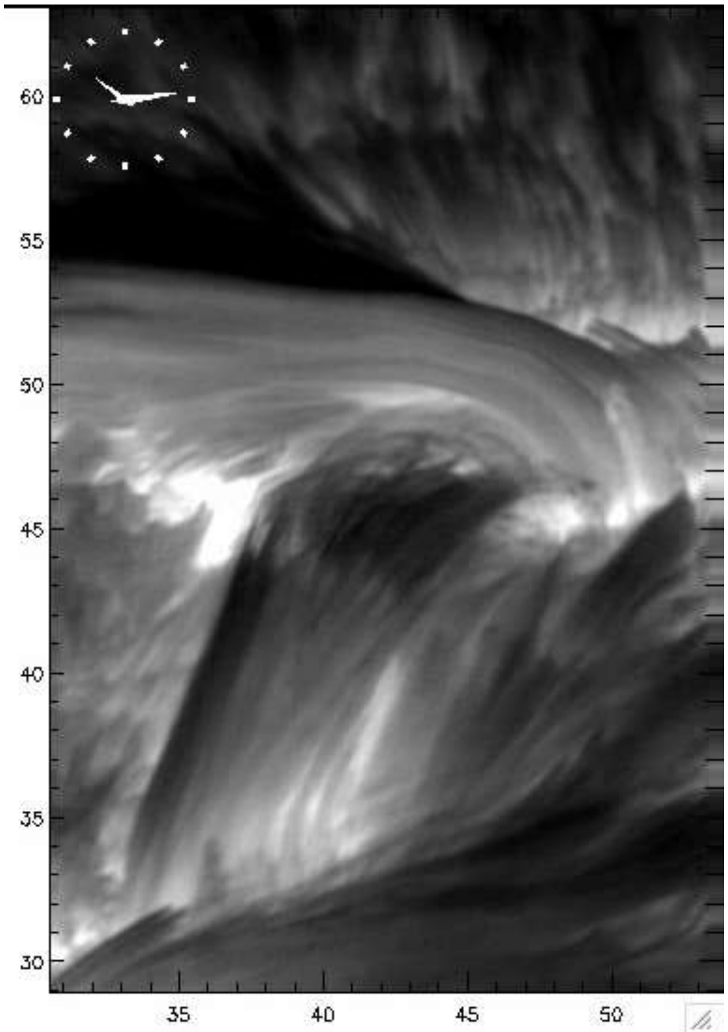

Since characteristic dynamic times of chromospheric fine structures are much shorter than time necessary to establish statistics equilibrium of hydrogen ionization.

In other words, the timescale on which the hydrogen level populations adjust to changes in the atmosphere is too long compared to the timescale on which the atmosphere changes.

Swedish 1-m Solar Telescope

diagnostics: Hα line center
date: October 4, 2005
duration: 72 min

Resolutions - temporal : 3 frames per second
- spatial: ~ 70 – 100 km

van Noort & Rouppe van der Voort (2006)

Non-equilibrium hydrogen ionization in 2-D simulations of the solar atmosphere

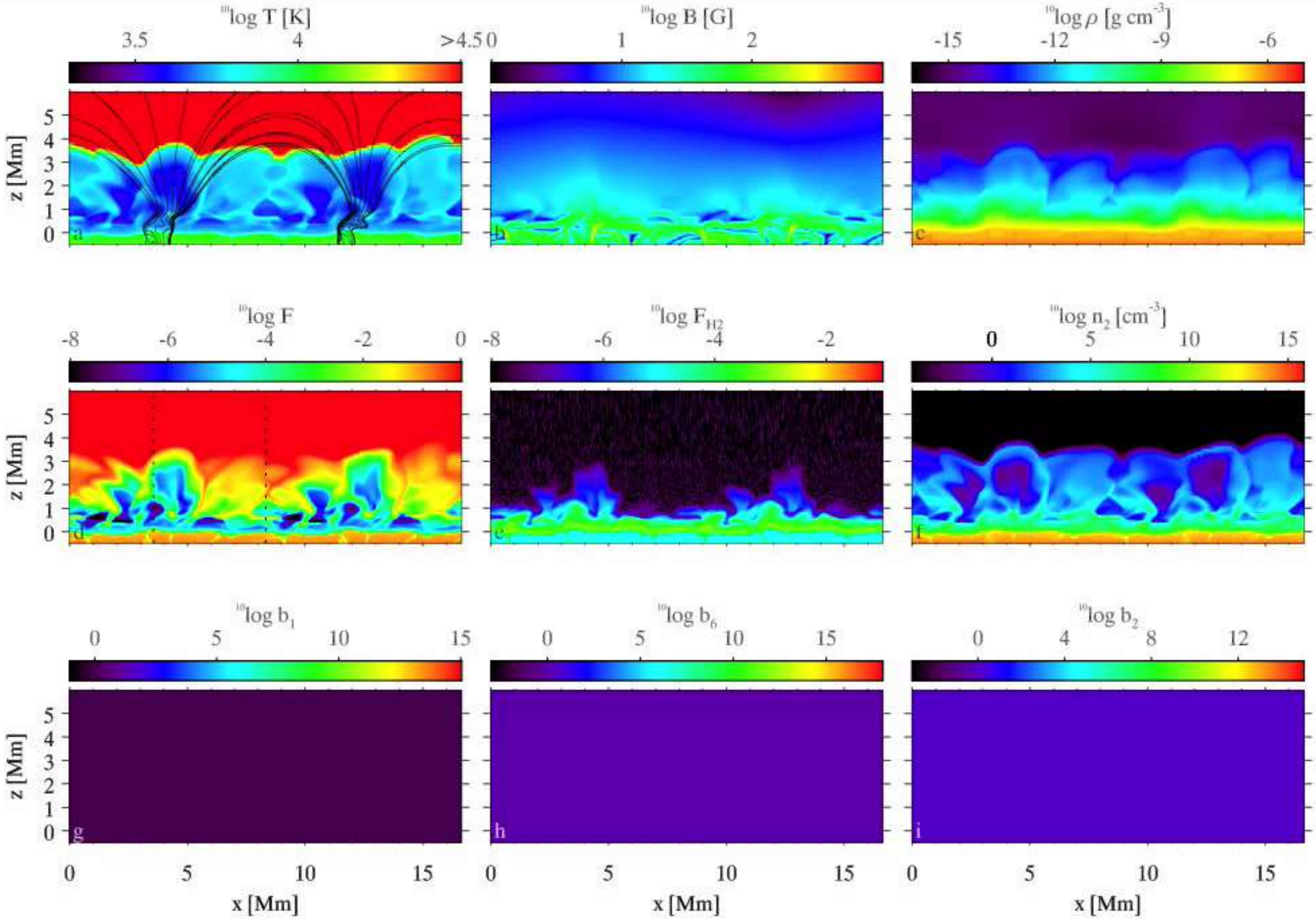

Leenaarts et al. (2007)

Non-equilibrium hydrogen ionization in 2-D simulations of the solar atmosphere

Main results:

- non-equilibrium H ionization is essential in simulations because the resulting temperature structure and hydrogen populations differ dramatically from their LTE values
- the degree of ionization of H in the chromosphere does not follow the local T
- the next step is to compute Hα in detail from this simulation (not yet done)

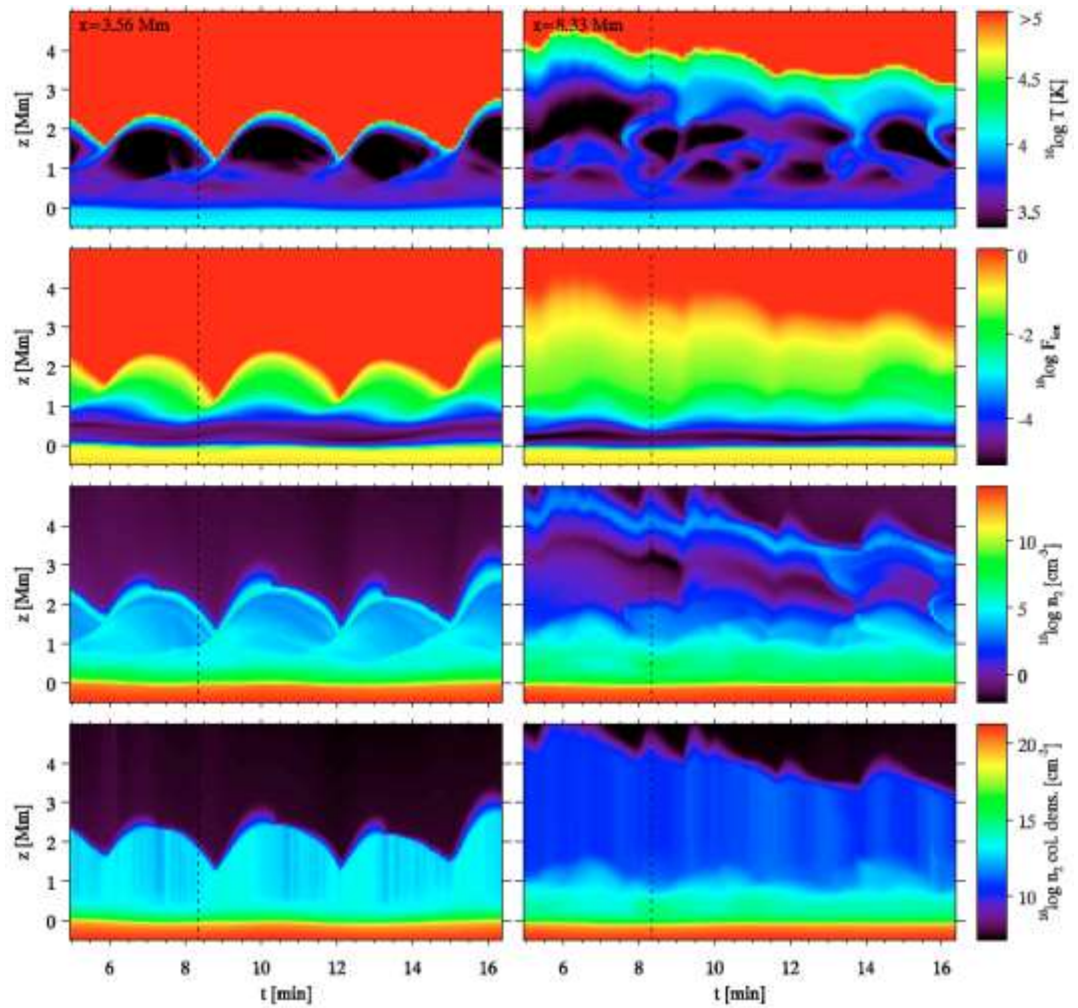

Leenaarts et al. (2007)

Numerical 3-D MHD simulation from the photosphere up to the corona

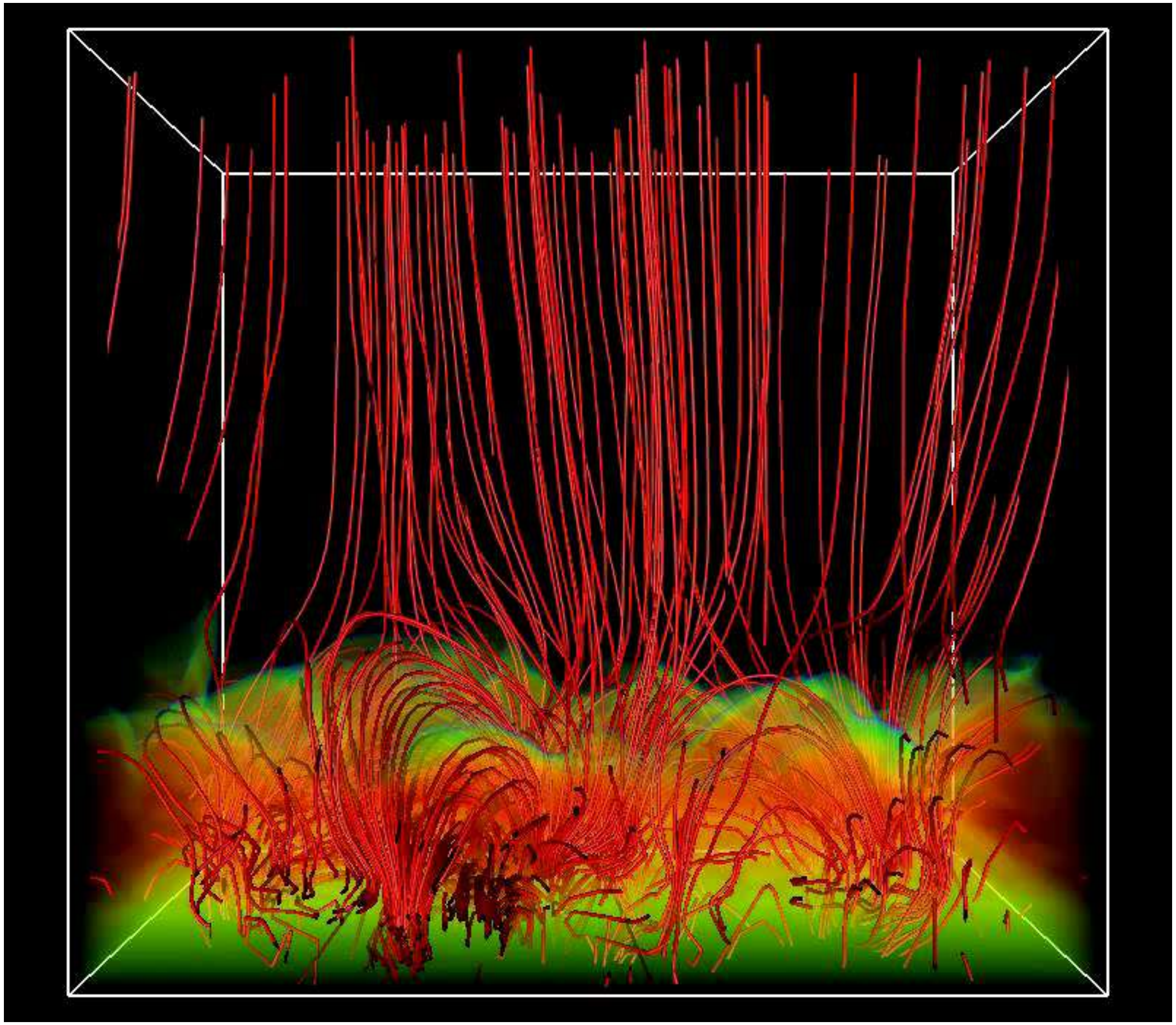

De Pontieu et al.: 2007, Science, 318, 1574.

Next frontier – to reproduce similar Hα images in numerical simulations

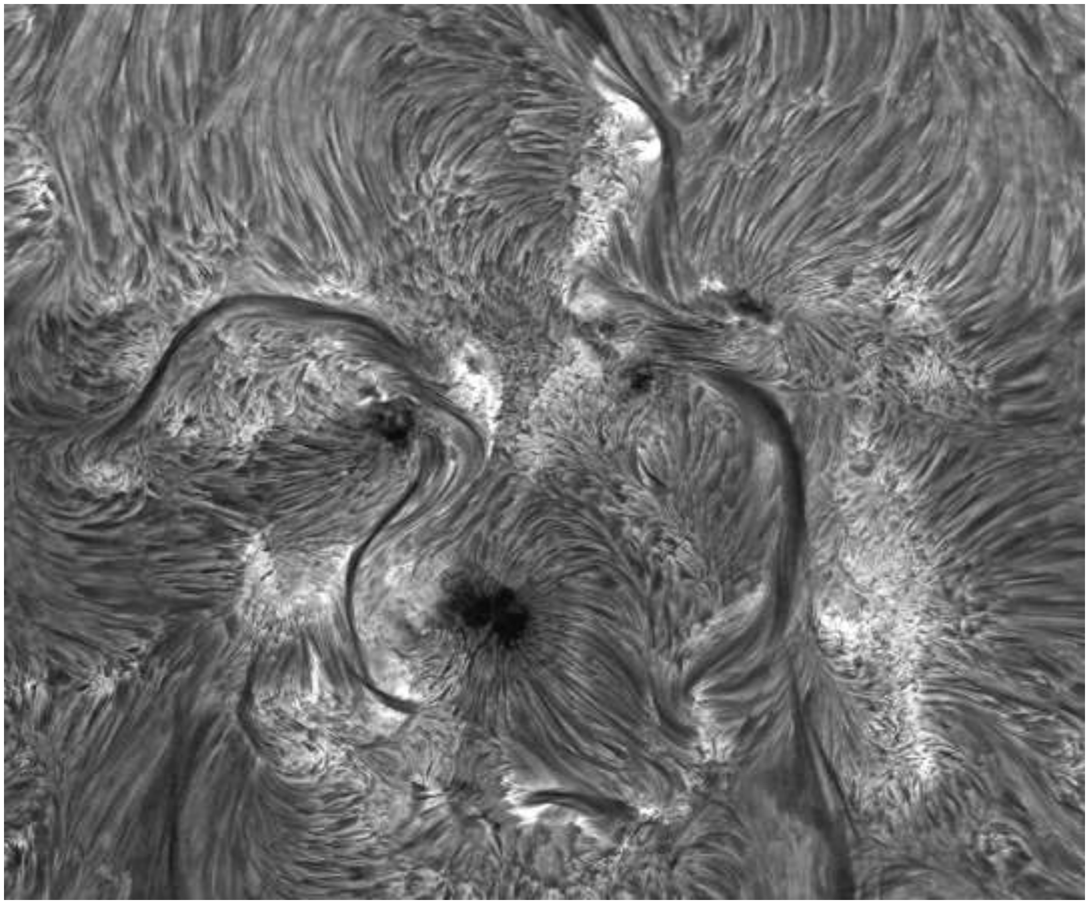

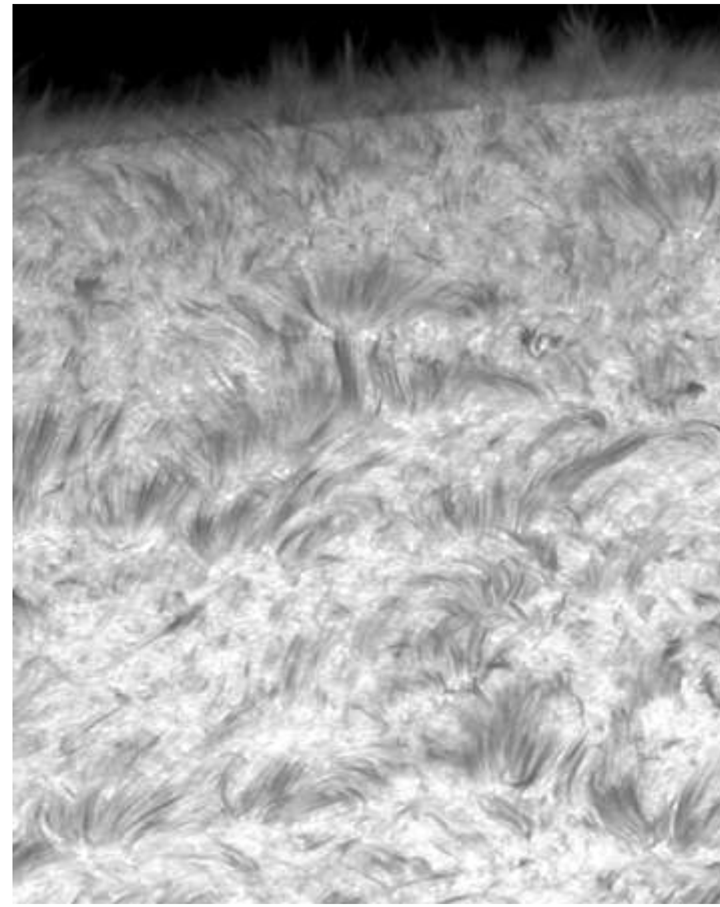

DUTCH OPEN TELESCOPE

Solar atmosphere cartoons in time

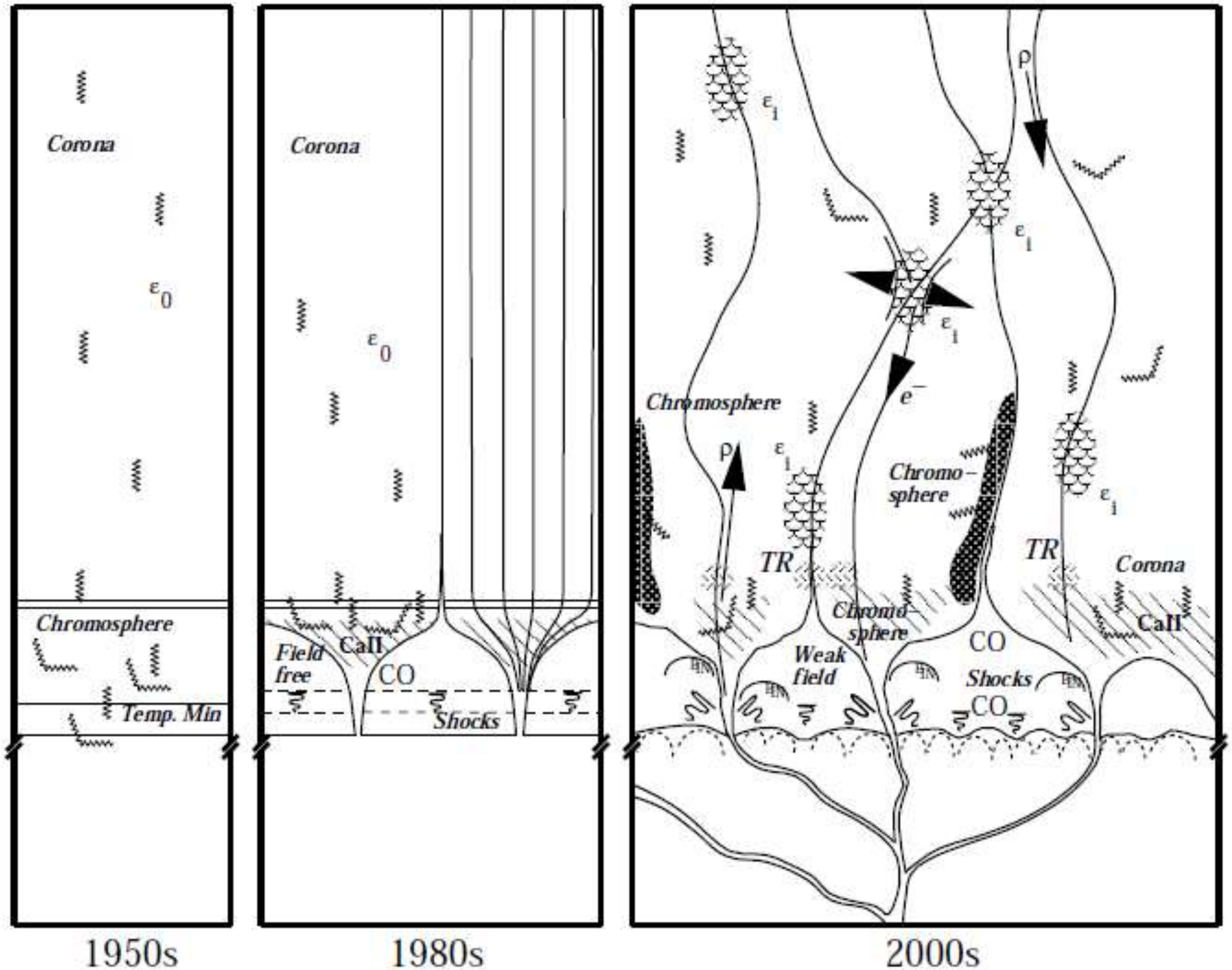

Ayres et al. (2009)

Solar atmosphere cartoons in time

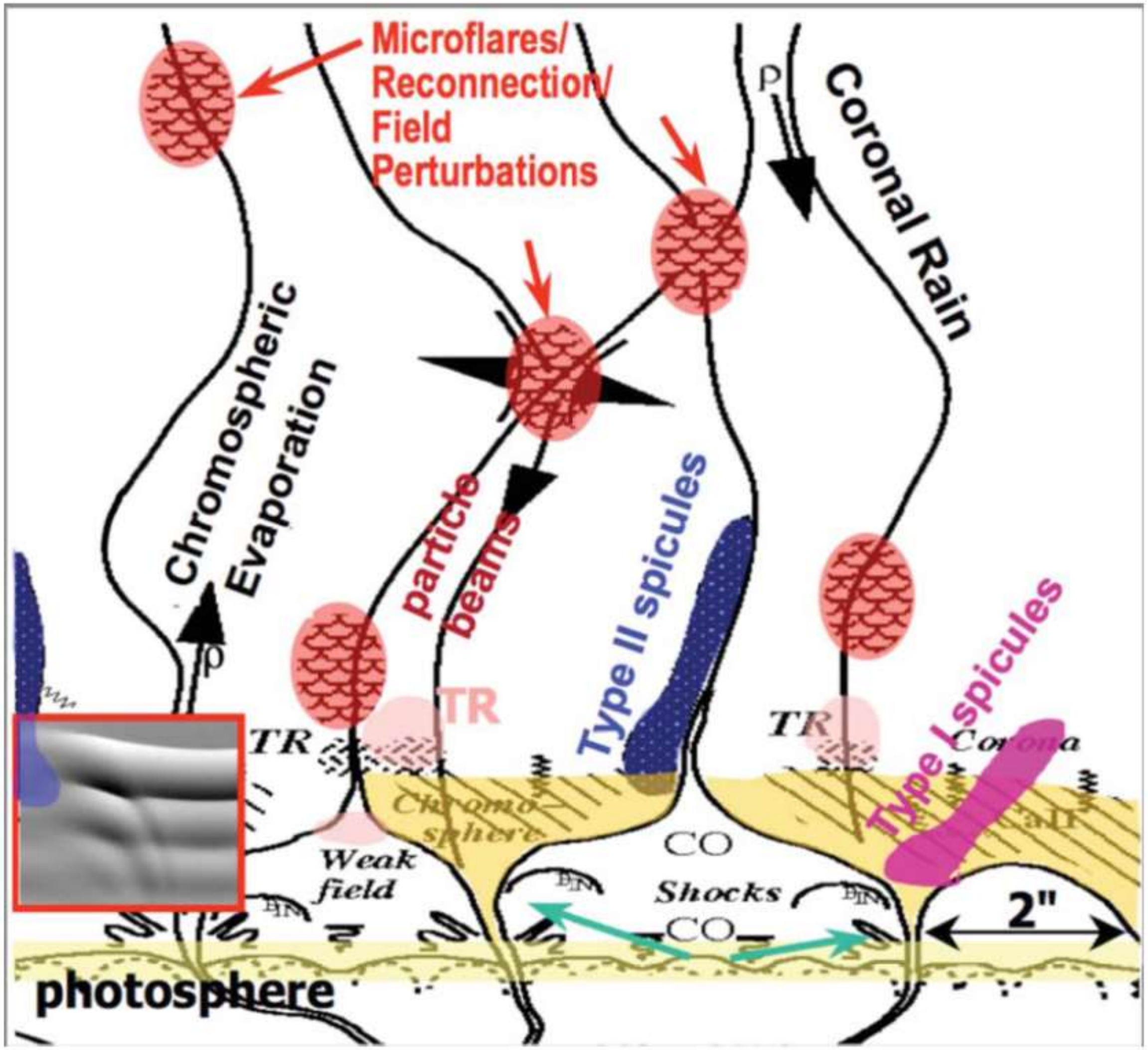

adapted from Rob Rutten

[De Pontieu et al. (2008)]

Overview of the talk

1. Observations

a) from the ground
- imaging (SST, DST, DOT)
- spectroscopy (SST)
- spectropolarimetry (VTT)

b) from space
- Hinode

c) simultaneous from the ground and space
- DST + SDO

2. Theory and simulations

- brief hindsight on 1-D simulations
- the latest 2-D simulations
- non-equilibrium time-dependent ionization of hydrogen
- solar atmosphere cartoons

3. The new window into the chromosphere

- Atacama Large Millimeter/submillimeter Array (ALMA)
- simulations of the solar chromosphere at millimeter and submillimeter wavelengths

Model of the quiet solar atmosphere

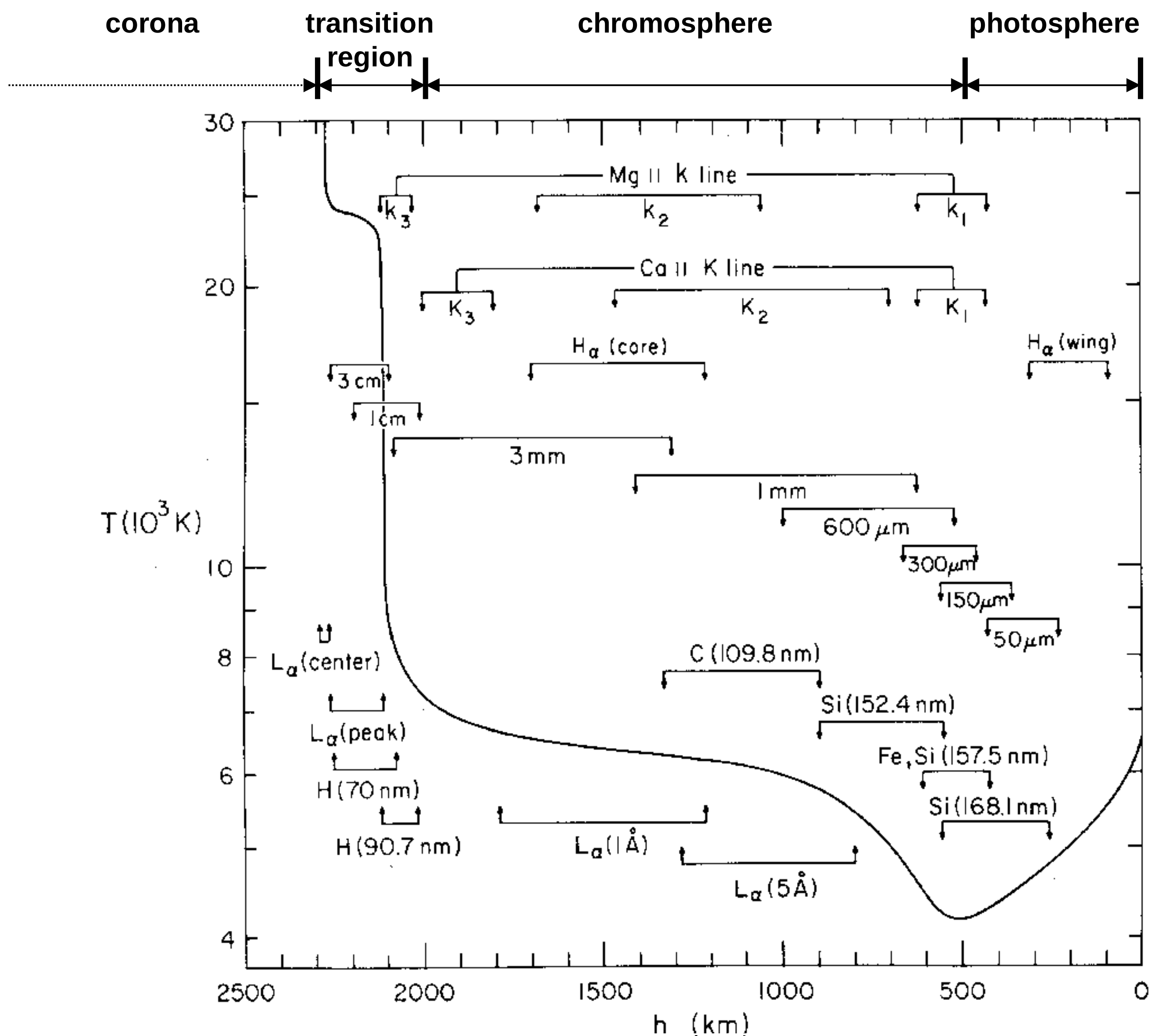

VAL3C

Vernazza et al. (1981)

Model of the quiet solar atmosphere

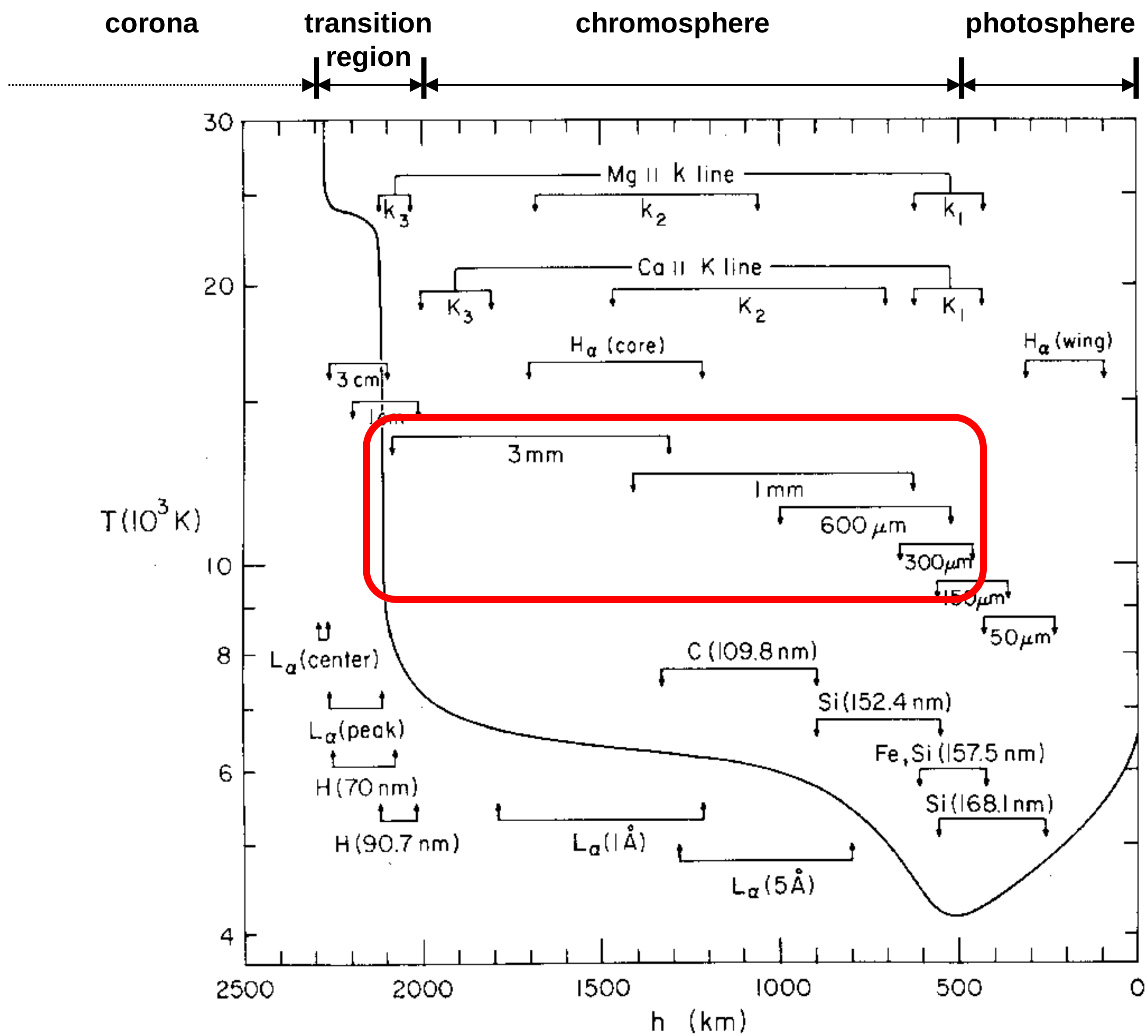

VAL3C

Vernazza et al. (1981)

ALMA – the new window into the solar chromosphere

- ALMA = Atacama Large Millimetre/submillimetre Array
- operated by ESO
- 66 antennas with diameters 12 m and 7 m
- planned full operation in 2012

ALMA – the new window into the solar chromosphere

- main ALMA target - cold universe
- also observations of the solar chromosphere and its fine structures
- expected FoV on the Sun: 21 arcsec at λ = 1 mm
- expected spatial resolution: 1.27 arcsec at λ = 3 mm
  0.42 arcsec at λ = 1 mm
  0.13 arcsec at λ = 0.3 mm

Simulations of inter-network regions of the Sun at millimetre wavelengths

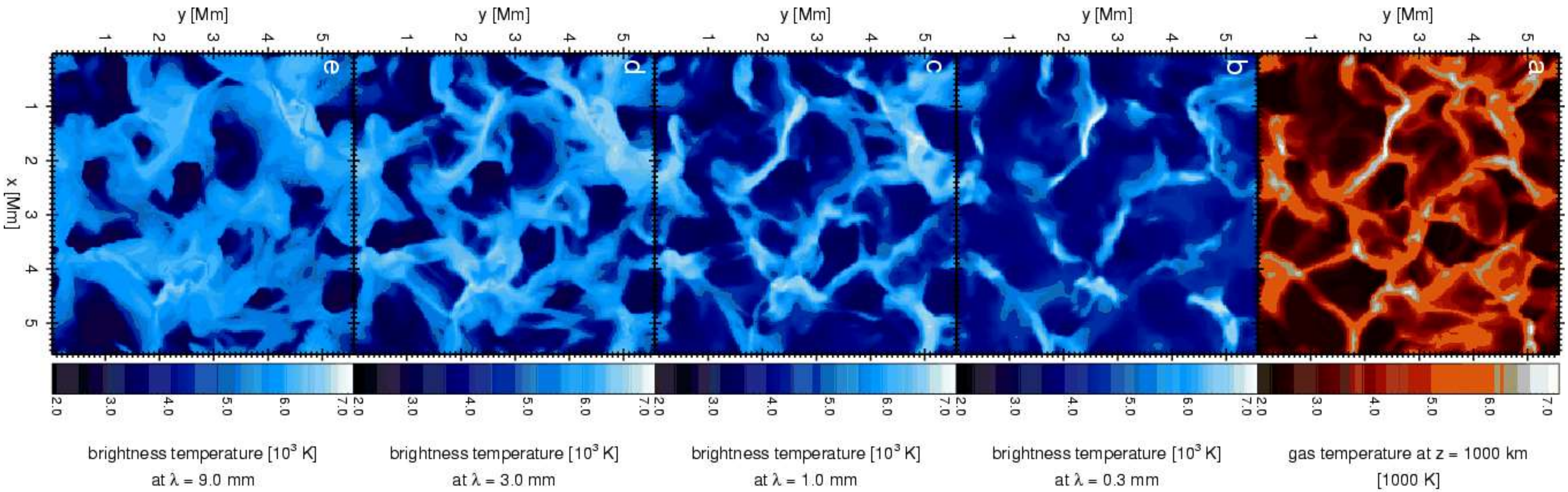

Why is the chromosphere in millimeter wavelengths so atractive ?
Since the source function is Planckian, thus easy LTE (but not opacity).

"ALMA is promising tool for imaging the chromospheric fine-structure at high cadence."

"Application of ALMA is broad and includes the study of the fine-structure of the magnetic network, too."

Wedemeyer-Böhm et al. (2007)